Three dimensional finite element analysis of brittle materials using CDM model

Asad-ur-Rehman Khan

Civil Engineering

June 1994

Abstract

It is well documented that the major part of the nonlinearity in concrete is attributed to the development of microcracks and microvoids which tend to destroy the interface of bond between the cement matrix and aggregate and/or destroy the material grains and thus affecting the elastic properties.

In the past two decades, the damage mechanics approach has emerged as a viable framework for the description of the observed phenomenological behavior of concrete such as material stiffness degradation, microcrack initiation and the strong directionality of DAMAGE.

It is the objective of this thesis to incorporate a continuum damage model into a three dimensional finite element code (DAMAG3D) to predict the ultimate capacity and the overall response of structures made up of britle materials. The model is verified through the well-known Brazilian test, uniaxial compression test and plain concrete prism under strip loading. Numerical predictions are compared with the experimental results and the results predicted by other models.

Three Dimensional Finite Element Analysis of Brittle Materials Using CDM Model

by

Asad-ur-Rehman Khan

A Thesis Presented to the

FACULTY OF THE COLLEGE OF GRADUATE STUDIES

KING FAHD UNIVERSITY OF PETROLEUM & MINERALS

DHAHRAN, SAUDI ARABIA

In Partial Fulfillment of the
Requirements for the Degree of

MASTER OF SCIENCE

In

CIVIL ENGINEERING

June, 1994

INFORMATION TO USERS

This manuscript has been reproduced from the microfilm master. UMI films the text directly from the original or copy submitted. Thus, some thesis and dissertation copies are in typewriter face, while others may be from any type of computer printer.

The quality of this reproduction is dependent upon the quality of the copy submitted. Broken or indistinct print, colored or poor quality illustrations and photographs, print bleedthrough, substandard margins, and improper alignment can adversely affect reproduction.

In the unlikely event that the author did not send UMI a complete manuscript and there are missing pages, these will be noted. Also, if unauthorized copyright material had to be removed, a note will indicate the deletion.

Oversize materials (e.g., maps, drawings, charts) are reproduced by sectioning the original, beginning at the upper left-hand corner and continuing from left to right in equal sections with small overlaps. Each original is also photographed in one exposure and is included in reduced form at the back of the book.

Photographs included in the original manuscript have been reproduced xerographically in this copy. Higher quality 6" x 9" black and white photographic prints are available for any photographs or illustrations appearing in this copy for an additional charge. Contact UMI directly to order.

UMI

A Bell & Howell Information Company
300 North Zeeb Road, Ann Arbor, MI 48106-1346 USA
313/761-4700 800/521-0600

THREE DIMENSIONAL FINITE ELEMENT ANALYSIS OF BRITTLE MATERIALS USING CDM MODEL

BY

ASAD-UR-REHMAN KHAN

A Thesis Presented to the

FACULTY OF THE COLLEGE OF GRADUATE STUDIES

KING FAHD UNIVERSITY OF PETROLEUM & MINERALS

DHAHRAN, SAUDI ARABIA

In Partial Fulfillment of the
Requirements for the Degree of

MASTER OF SCIENCE

In

CIVIL ENGINEERING

JUNE 1994

UMI Number: 1361067

UMI Microform Edition 1361067
Copyright 1995, by UMI Company. All rights reserved.

This microform edition is protected against unauthorized copying under Title 17, United States Code.

UMI

300 North Zeeb Road
Ann Arbor, MI 48103

THREE DIMENSIONAL FINITE ELEMENT ANALYSIS OF BRITTLE MATERIALS USING CDM MODEL

by

ASAD-UR-REHMAN KHAN

Civil Engineering Department
KFUPM, Dhahran,

KING FAHD UNIVERSITY OF PETROLEUM AND MINERALS

DHAHRAN, SAUDI ARABIA

This thesis, written by

Asad-ur-Rehman Khan

under the direction of his Thesis Advisor, and approved by his Thesis committee, has been presented to and accepted by the Dean, College of Graduate Studies, in partial fulfillment of the requirements for the degree of

MASTER OF SCIENCE IN CIVIL ENGINEERING

Thesis Committee:

Chairman (Dr. A. H. Al-Gadhib)

Member (Dr. M. H. Baluch)

Member (Dr. A. A. Khathalan)

Member (Dr. A. K. Al-Musallam)

Dr. Alfarabi Sharif
Department Chairman

Dr. Ala H. Rabeh
Dean, College of Graduate Studies

Date: 4.1.94

23-7

dedicated to

my Parents,

Wife and Son

23-7

ACKNOWLEDGEMENTS

Firstly,I thank ALLAH, All the praise is for Him, The All Kind and Merciful, Who bestowed me with the strength to complete the work.Then acknowledgment is due to King Fahd University of Petroleum and Minerals for supporting this research work.

I acknowledge my deep gratitude to my major advisor Dr.Ali Al-Gadhib for providing me with inspiration,encouragement and continuous guidance all the way. I am also grateful to the other committee members Dr.M.H.Baluch, Dr.A.A.Al-Khathlan and Dr.A.A.Al-Musallam for their valuable suggestions and commentsthey made to improve the work.

I must acknowledge the support offered by Data Processing Centre of KFUPM that made the research work possible.

I would also like to thank my friends who lent me help at different stages of the work.

Finally,I thank my parents and my wife who, through their moral support have permitted me to indulge my passion for the long task of completing this work.

CONTENTS

Chapter I: INTRODUCTION 1

BACKGROUND TO THE PROBLEM 1
SCOPE AND OBJECTIVES 3
LITERATURE REVIEW 4
ORGANIZATION OF THESIS 9

Chapter II: MATERIAL MODELLING 10

INTRODUCTION 10
CONTINUUM DAMAGE MECHANICS 10
Isotropic Damage 14
Orthotropic Damage 15
BEHAVIOR OF CONCRETE 19
REVIEW OF SOME EXISTING DAMAGE MODELS OF CONCRETE 23
Theoretical Preliminaries 23
Scalar Damage Model (Mazars) 26
Unilateral Damage Model (Ladeveze ; Mazars) 28
Damage Model with Permanent Strains and Induced Anisotropy 30
Constitutive Model for Concrete in Cyclic Compression (Chen) 31
Damage Model for Cyclic Loading of Concrete (Suaris) 37
Physical interpretation of Rc 44
Damage Model for Concrete using Bounding Surface Concept 45
WHY SUARIS DAMAGE MODEL 49
Inversion of Constitutive Relations 50
Equations for the Evolution of Damage 51

Chapter III: FINITE ELEMENT MODEL 53

INTRODUCTION 53
FINITE ELEMENT FORMULATION 53
Total Potential Energy of the System 54
Element Stiffness Matrix 55
Finite Element Discretization 57

23-7

Element Geometry 57
Displacement Field 59
20- Node Hexahedral Element 60
Strain Displacement Relationship 62
CONSISTENT NODAL FORCES DUE TO DISTRIBUTED SURFACE LOADING 67

Chapter IV: FINITE ELEMENT IMPLEMENTATION 70

INTRODUCTION 70
PROGRAM DAMAG3D PARAMETERS 70
FLOW OF OPERATIONS 72
METHODOLOGY 72
DESCRIPTION OF SUBROUTINES 75
Dynamic Dimensioning 75
Input and Output Module 75
Stiffness and Solution Module 76
SUBROUTINE RESIDU 77

Chapter V: RESULTS 79

. PARAMETRIC STUDY 79
Effect of Beta on Uniaxial Tensile Test Results 80
Effect of Alpha on Uniaxial Compressive Test Results 80
GEOMETRY AND MATERIAL PROPERTIES 83
Uniaxial Compression Test 83
Plane Concrete Prism Under Strip Loading 83
Brazilian Test 83
RESULTS 87
Failure Loads 88
Stress-Strain Curves 89
Contours of Damage Distribution 95

Chapter VI: CONCLUSIONS 104

CONCLUSIONS 104
RECOMMENDATIONS 105

Appendix A: INSTRUCTIONS FOR PREPARING DATA FOR PROGRAM DAMAG3D 106

Appendix B: SAMPLE INPUT DATA AND OUPUT FILES FOR PROGRAM DAMAG3D 110

DATA FILE 111

23-7

OUTPUT FILES 113

Appendix C: DETAILED EXPRESSIONS FOR D MATRICES . . . 125

REFERENCES **136**

23-7

FIGURES

1. Volume Element from a Damaged Body 13
2. Distribution of Cracks in Three Principal Directions. 17
3. Bounding Surface in Principal Stress Space 33
4. Illustration of Bounding, Loading and Limit Fracture Surfaces 39
5. Definition of Normalized Distance in Deviatoric Plane 42
6. 20- Noded Isoparametric Element 58
7. Arrangement of Nodes in 20-Noded Hexahedral 61
8. Surface Loaded with Distributed Loading 68
9. Flow of Operations 73
10. Flow Chart for Iteration within each Iteration 78
11. Effect of Beta on Uniaxial Tensile Test Results 81
12. Effect of Alpha on Uniaxial Compressive Test Results 82
13. Finite Element Mesh of Cylinder for Uniaxial Compression Test 84
14. Finite Element Mesh of Plain Concrete Prism 85
15. Finite Element Mesh of Cylinder for Brazilian Test 86
16. Stress-Strain Curve for Uniaxial Compression Test. 91
17. Modified Stress-Strain Curve for Uniaxial Compression Test. 92
18. Stress-Strain Curve for PC Prism under Strip Loading. 93
19. Stress-Strain Curve for Brazilian Test. 94
20. % of Maximum Damage at Different Load Levels. 97
21. Distribution of Damage for PC Prism under Strip Loading. . . 98
22. Distribution of Damage for PC Prism under Patch Load. 99

23-7

23. Damage Distribution for Brazilian Test 100

24. Damage Distribution for Brazilian Test (Resende) 101

25. Damage Surface for Brazilian Test 102

26. Damage Surface for Brazilian Test over the Length 103

23-7

TABLES

1. Specimen Geometry and Material Properties 87

2. Comparison of Failure Loads 89

3. % of Maximum Damage at Different Stages 95

23-7

Abstract

Name: Asad-ur-Rehman Khan

Title: Three Dimensional Finite Element Analysis of Brittle Materials Using CDM Model

Major Field: Civil Engineering

Date of Degree: June 1994

It is well documented that the major part of the nonlinearity in concrete is attributed to the development of microcracks and microvoids which tend to destroy the interface of bond between the cement matrix and aggregate and/or destroy the material grains and thus affecting the elastic properties.

In the past two decades, the damage mechanics approach has emerged as a viable framework for the description of the observed phenomenological behavior of concrete such as material stiffness degradation, microcrack initiation and the strong directionality of damage.

It is the objective of this thesis to incorporate a continuum damage model into a three dimensional finite element code (DAMAG3D) to predict the ultimate capacity and the overall response of structures made up of brittle materials. The model is verified through the well-known Brazilian test, uniaxial compression test and plain concrete prism under strip loading. Numerical predictions are compared with the experimental results and the results predicted by other models.

Master of Science Degree

King Fahd University of Petroleum and Minerals

Dhahran, Saudi Arabia

June 1994

23-7

ملخص

ألأسم : أسد ألرحمان خان
ألعنوان : تحليل ألمواد الغير مرنه باستخدام نلأ من نموذج العناصر المحدودة ذات الأبعاد الثلاثة و نموذج الضرر المستمر
التخصص : الهندسة المدنية
تاريخ التخرج : يونيه 1994م

لقد وثق بشنل جيد أن الجزء الأنبر للتصرف اللأخطى فى الخرسانة سببه الريسىء وجود او حدوث شروخ وفجوات تؤدى الى تدمير السطح المشترئ و الرابط بين الأسمنت و الحصى والى تفنيئ الجزيأت المنونة للمادة و ينعنس ذلئ له تاثير خواص المرونة للمادة.

لقد تكونت الطريقة المتبعة لدراسة ميناننلية التضرر فى العقدين الماضيين نتيجة لوصف او ملأحظة التصرف الظاهرى للخرسانة نتدهور الصلأبة و تنوين الشروخ و معرفة الأتجاه الأمثل للضرر.

هدف هذه الأطروحة هو ادخال او استخدام نموذج الضرر المستمر فى برنامج العناصر المحدودة ذوالأبعاد الثلاثة فى تقدير الطاقة القصوى والأستجابة للمنشأ بشنل عام فيم هذا النسوذج من خلال تجربة برازيلين و الضغط على الأ سطونة و مضلع مصنعوين من الخرسانة لقد قورينت القيم الرقمية للنموذج بالنتائج التجربية و ايضا مع نتائج نماذج اخرى

درجة الماجستير فى العلوم الهندسية
جامعة الملك فهد للبترول والمعادن
الظهران المملكة العربية السعودية
يونية 1994 م

23-7

Chapter I
INTRODUCTION

1.1 BACKGROUND TO THE PROBLEM

All structures are three dimensional, but when it comes for the analysis of these structures, the usual practice is to idealize them as two dimensional structures with either plane stress or plane strain conditions being assumed.For the analysis of structures which have complex geometries, varying material properties and/or subjected to intricate loading together with non-linear behavior of material, numerical methods are gaining popularity, and the approach to turn to. The finite element method (FEM) is one of the numerical technique which is now firmly accepted as a most powerful method for the solution of a variety of problems encountered in engineering.For linear analysis, the technique is widely employed with confidence. Since tendency nowadays is to go for ultimate design, therefore, non-linear finite element analysis should be applied keeping in mind the accessibility of two major factors. Firstly, considerable computing power is required, keeping in view the increased numerical operations associated with non-linear problems. Secondly, the accuracy of any proposed solution technique must be proven. Developments in the last decade or so have ensured that high-speed digital computers fulfilling this need are now available, also the devel-

opment of improved element characteristics and more efficient non-linear solution algorithms have ensured that non-linear finite element analysis can be performed with confidence. With the rapid increase in PC's and mainframe CPU and memory capacities, fully three-dimensional finite element analysis is becoming possible, which is definitely more accurate than the two dimensional analysis.

With the advancement of finite element technique and availability of high speed computers, there has been a demand for refined and sophisticated models in order to trace the response of brittle materials in the non-linear post-cracking and post-yield range, since they cannot be treated as ductile materials due to their different behavior in tension and compression, initiation and propagation of cracks etc. The behavior of brittle materials under compressive and tensile states of stress has the following essential features:

1. The 'softening' of the specimen (i.e., negative slope of the stress-strain curve) in the post failure domain.
2. Positive dilatancy (volumetric strain) in the later stages of the compression test.
3. The gradual degradation of material strength characterized by the change in the elastic properties (mainly elastic modulus) in subsequent cycles of a repetitive loading program.
4. Different behavior in tension and compression.
5. Stiffness degradation.

None of these phenomena can be satisfactorily interpreted within the context of the classical theory of plasticity which was initially intended for ductile materials. Hence the need arises for a theory which can interpret these phenomena.

In the past two decades, the **damage mechanics** approach has emerged as viable framework for the description of distributed material damage including material stiffness gradation, microcrack initiation, damage-induced anisotropy. Damage mechanics has also been introduced to describe the inelastic behavior of brittle materials such as concrete and rock.

Keeping in mind all the above mentioned factors, a three-dimensional FEM coding is developed in which a continuum damage mechanics (CDM) model based on bounding surface concept is incorporated.

1.2 SCOPE AND OBJECTIVES

The scope of this thesis is to incorporate a continuum damage model which can predict the behavior and capture as many features as possible of brittle materials. The main objectives of this work are :

1. Develop a generalized three-dimensional finite element program for the analysis of any structure (including curved boundaries), made of brittle materials and subjected to generalized loading.

2. Use the CDM model for brittle materials as proposed by Wimal Suaris(1990) which is able to predict successfully the essential characteristics of brittle materials such as nonlinearity, stiffness degradation, shear compaction dilatancy, different behavior in tension and compression and the strain softening behavior.
3. Verify the model by running it for three different tests, namely, the Brazilian test, compression test of plain concrete cylinder, and plain concrete prism under strip loading, and comparing its predictions with results reported by Resende (1987), Suaris et al. (1990) and Gonzalez et al.(1991) for the same tests respectively.
4. Assessment of Suaris damage model based on comparisons of its predictions with those based on plasticity models.

1.3 LITERATURE REVIEW

Review of the literature indicates a limited or no work in the field of three dimensional finite element analysis of brittle materials incorporating CDM model.

Krajcinovic and Fonseka (1981) proposed an analytical model governing the mechanical response of a perfectly brittle solid under isothermal conditions. This theory is rather similar to the plasticity theory. This model restricts damage to a multitude of flat, plane penny-shaped microdefects, and is also incapable of predicting fine details of propagation of particular crack and the stress field around its tip.

23-7

Siriwardne and Desai (1983) proposed computational procedures for implementing some constitutive models and introduced them in three-, and two- dimensional finite element procedures. Variable moduli, Drucker-Prager, critical state and cap models are considered. The three-dimensional finite element analysis involved 8- to 20-noded isoparametric elements where as two-dimensional finite element involves 4- to 8-noded isoparametric elements. The above mentioned work considers only advanced plasticity models with no considerations to CDM models.

Resende and Martin (1984) introduced a constitutive model for the mechanical behavior of materials such as rock and concrete. The proposed model is based on the progressive fracturing theory for the shear behavior whereas the volumetric behavior is formulated using hydrostatic compression cap yield surfaces of plasticity fitted into a broadened progressive frame work. General constitutive equations for three-dimensional problems are presented to be implemented in finite element stress analysis. This model considers only compression behavior with no statement about tensile conditions. The unloading behavior in shear produces no permanent strains; in fact there should be some kind of coupling between elastic and inelastic deformations.

Resende (1987) proposed a rate-independent constitutive theory for the behavior of concrete in the inelastic range. The inelasticity is provided by two basic damage mechanisms, namely, shear damage and hydrostatic tension damage. The proposed model was also implemented in

two-dimensional finite element codes to solve a number of boundary value problems. This model require a number of material parameters to be defined and then need to be calibrated accordingly.

De Wolf and Kou (1987) used three- dimensional finite element analysis to study the post cracking behavior of concrete treating it as isotropic, homogeneous, linear elastic material. The discrete cracking model was introduced since the directions and approximate locations of the cracks were closely followed in the tests. The discrete cracking model is good only if experimental cracking patterns are available which in fact is a handicap. This work did not involve CDM modelling of concrete none whatsoever.

Chow and Wang (1988) presented a finite element formulation of an isotropic theory of continuum mechanics for ductile fracture. The proposed finite element analysis is only for ductile materials.

Khan and Yuan(1988) modelled the behavior of bimodular materials (materials having different moduli in tension and compression) by using three-dimensional finite element method. Iteration schemes for proportionate and non-proportionate loading are proposed, and a computer program performing elastic analysis and predicting brittle failure loads with four different failure criteria is developed. In this work only the elastic bimodular behavior is considered along with the classical failure criterion (Coulomb, Drucker-Prager) to predict the failure of brittle materials,which are inadequate for predicting failure of such materials

under non-proportionate loading. The above work did not consider CDM modelling of concrete.

Mazars and Cabot (1989) reviewed different models for concrete based on continuum damage theory. Models reviewed are unilateral damage model, scalar damage model, damage model with permanent strains and induced anisotropy, damage model for high compressive loadings. Each model has its own limitations,but can be implemented in finite element codes.

Chou, Lee and Erdman (1990) formulated a finite element model based on Lee's theory which decomposes the deformation gradient into a product of elastic and plastic parts instead of assuming that the strain rate is the combination of the elastic and plastic strain rates. This work neither considers concrete nor CDM modelling.

Gonzalez, Kotsovos and Pavlovic (1990) presented a three-dimensional FE model for structural concrete which fully allows for tri-axial effects. The model consists of generalized stress-strain relations for concrete which is uncracked at the macroscopic level, and this is valid upto a specified failure envelope; beyond this envelope instant strain-softening is assumed both in tension and compression. Smeared modelling of cracking is used. Again no CDM modelling is involved in this work. The results obtained from this work are not in correlation with the experimental results.

Gonzalez, Kotsovos and Pavlovic (1991) proposed a three-dimensional model, brittle in nature, permitting the validation of certain general concepts regarding the failure of concrete in a structure. 20-noded serendipity and 27-noded Lagrangian elements are used for concrete modelling with smeared modelling of cracking. This model assumes perfect bond with a view that aggregate interlock plays a negligible role in the load-carrying capacity of a member. The above work did not consider CDM modelling of concrete.

Seraj, Kotsovos and Pavlovic (1992) proposed a three-dimensional finite element model for structural concrete, based on the brittle constitutive relationships and applied it to the analysis of reinforced concrete members. This work is an extension of {18} to high-strength concrete mixes with special reference to T-beams.

Considering the limitations regarding the past work of researchers, a generalized three-dimensional finite element code using CDM approach is developed to study the non-linear behavior of concrete.The model selected herein is as proposed by Wimal Suaris(1990), which is simple, general and captures several features of brittle materials such as stiffness degradation ,different behavior in tension and compression etc.

1.4 ORGANIZATION OF THESIS

This thesis consists of six Chapters in which Chapter Two contains the behavior of concrete and a review of some of the existing CDM constitutive models for multiaxial behavior of concrete.

In Chapter Three, the finite element model is described. Standard formulations for 20-noded serendipity element are given.

In Chapter Four finite element program DAMAG3D for non-linear analysis of brittle materials is described. A detailed discussion of important subroutines is presented.

Chapter Five consists of the verification and comparison of results obtained by applying the model for Brazilian test, compression test of plain concrete cylinder and plain concrete prism under strip loading.

Chapter Six presents conclusions, suggestions and future scope of the work.

Chapter II
MATERIAL MODELLING

2.1 INTRODUCTION

With the advancement of finite element technique and availability of high speed computers , there has been a demand for refined and sophisticated models in order to trace the response of concrete especially in the non-linear post-cracking range. Although the use of finite element method is highly promising , yet the task of modelling the material behavior remains a great challenge. Ever since this method was applied to concrete structures , material modelling has become a very active area of research. Research has been conducted to develop a versatile , simple , and realistic model able to capture as many features as possible. With the introduction of continuum damage mechanics it is becoming possible capture several features of concrete if not all.

2.2 CONTINUUM DAMAGE MECHANICS

In the past two decades,the damage mechanics approach has emerged as a viable framework for the description of distributed material damage including material stiffness degradation, microcrack initiation, growth and coalescence of cracks as well as damage-induced anisotropy. Damage mechanics has been applied to model creep damage (Hult ,1974

;Kachanov 1958, 1984, 1987; Krajcinovic , 1983; Leckie and Hayhurst , 1974; Lemaitre , 1984; Murakami , 1985) , creep-fatigue (Lemaitre , 1979, 1984; Lemaitre and Chaboche , 1974; Lemaitre and Plumtree , 1979) , elasticity coupled with damage (Cordebois and Sidorof , 1982; Ju et al., 1989; Kachanov , 1980 , 1987; Krajcinovic and Fonseka , 1981; Ortiz , 1985; Wu ,1985) and ductile plastic damage (Cordebois and Sidorof , 1982; Dragon , 1985a; Dragon and Chihab , 1985b; Lemaitre and Dufailly , 1977; Lemaitre ,1984, 1985, 1986; Simo and Ju ,1986 , 1987a ,1987b). In addition damage mechanics has been introduced to describe the inelastic behavior of brittle materials such as concrete and rock (Francois , 1984; Kachanov , 1972, 1982; Krajcinovic and Selvaraj , 1983; Mazars, 1982, 1984, 1986; Mazars and Lemaitre, 1984; Mazars and Legendre, 1984; Mazars and Pijaudier-Cabot, 1986; Mazars and Borderie, 1987; Resende and Martin, 1984; Resende, 1987; Simo and Ju, 1987a,b;Taher,S.E.-D.F., Baluch,M.H.,AL-Gadhib,A.H., 1994)

Continuum damage mechanics is based on the thermodynamics of irreversible processes, the internal state variable theory and relevant physical considerations (e.g.,micromechanical damage variable theory,kinetic law of damage growth,nonlocal damage characterization and plasticity-damage coupling mechanism, etc.). A scalar damage variable is suitable for characterization of isotopic damage processes. Nevertheless, a tensor-valued damage variable (fourth order) is necessary in order to account for anisotropic damage effects.

It is important to clarify the term "damage" employed in the literature. The existence of microcracks and their propagation which causes stiffness degradation, dilatancy and other non-linear characteristics leading ultimately to failure is termed as "DAMAGE". There are at least three different levels of scale of "damage" in the material mechanical responses:

1. micro-scale level
2. meso-scale level
3. macro-scale level

Consider a volume element at macroscale level as shown in Figure 1 ,in which,

1. S = overall section area of volume element defined by the unit normal vector $\hat{n}$
2. S_D = total area of microcracks and cavities
3. $\overline{S}$ = effective resisting area of microcracks and cavities.

The effective resisting area takes into account S_D, microstress concentrations in the vicinity of discontinuities and interactions between closed defects, and therefore

$$\overline{S} \leq S - S_D \qquad (2.1)$$

Physically, damage variable D_n (associated with normal $\hat{n}$) can be defined as

$$D_n = \frac{S - \overline{S}}{S}, \quad or \qquad (2.2)$$

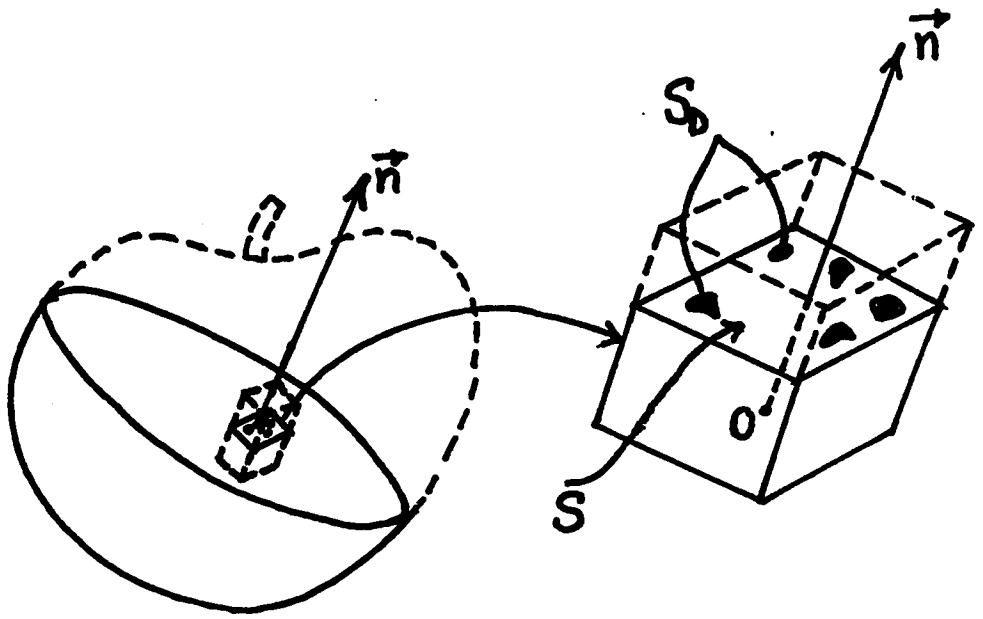

Figure 1: Volume Element from a Damaged Body

$$\overline{S} = S(1-D_n) \qquad (2.3)$$

where,

1. D_n = corrected area of cracks and cavities per unit surface cut by a plane perpendicular to $\hat{n}$
2. $D_n = 0$, corresponds to undamaged state.
3. $D_n = 1$, corresponds to rupture of material element into two parts.
4. $0 < D_n < 1$, corresponds to damaged state.

2.2.1 Isotropic Damage

In general, cracks and voids are oriented and thus D_n is a function of $\hat{n}$. This leads to an intrinsic variable of damage which can be a second order or a fourth order tensor depending upon the hypothesis mode.In isotropic damage(Lemaitre,1985), cracks and voids are equally distributed in all directions.Thus D_n does not depend upon $\hat{n}$ and intrinsic damage variable is scalar D.

The strain behavior of a damaged material is represented by constitutive equations of the virgin material (without any damage) in the potential of which the stress is simply replaced by the effective stress, $\overline{\sigma}$, where,

$$\overline{\sigma} = \frac{\sigma}{(1-D)} \qquad (2.4)$$

Therefore, for uniaxial loading $\sigma = \sigma_x$, strains may be written as:

$$\varepsilon_x = \frac{\sigma_x}{(1-D)E_o}$$

$$\varepsilon_y = \frac{-\nu\sigma_x}{(1-D)E_o} \qquad (2.5)$$

$$\varepsilon_z = \frac{-\nu\sigma_x}{(1-D)E_o}$$

2.2.2 Orthotropic Damage

For orthotropic materials, stresses in terms of strains without damage are expressed as follows:

$$\varepsilon_x = \frac{\sigma_x}{E_x} - \nu_{yx}\frac{\sigma_y}{E_y} - \nu_{zx}\frac{\sigma_z}{E_z}$$

$$\varepsilon_y = -\nu_{xy}\frac{\sigma_x}{E_x} + \frac{\sigma_y}{E_y} - \nu_{zy}\frac{\sigma_z}{E_z} \qquad (2.6)$$

$$\varepsilon_z = -\nu_{xz}\frac{\sigma_x}{E_x} - \nu_{yz}\frac{\sigma_y}{E_y} + \frac{\sigma_z}{E_z}$$

The quantities $E_x, E_y, E_z, \nu_{xy}, \nu_{xz}, \nu_{yz}$ need to be degraded as damage progresses.

In orthotropic damage, cracks and voids are distributed in all directions. Thus D_n depend upon $\hat{n}$ and intrinsic damage variable is not a

scalar D, but a vector $\hat{\omega}$ with the components $\omega_1, \omega_2, \omega_3$ acting along the principal directions of damage.

Figure 2 shows the cracks or defects in a body oriented in three principal directions. ω_i, $(i=1,2,3)$, is the area density of cracks in any plane perpendicular to axis X_i.

If the body is subjected to uniaxial tension, the cracks in the plane perpendicular to the loading will open up while those in the other directions will close. Based on this assumption, if there are three principal tensile stress directions at a point in an initially isotropic body characterized by a single modulus E_o, the modulus will be degraded only by the damage component ω_i, in the plane perpendicular to the principal stress direction i.e.,

$$
\begin{aligned}
E_1 &= E_o(1-\alpha\omega_1) \\
E_2 &= E_o(1-\alpha\omega_2) \qquad (2.7) \\
E_3 &= E_o(1-\alpha\omega_3)
\end{aligned}
$$

where, α is a constant parameter. Since, there are no cross-effects ν will not be degraded. Note that the degraded moduli as given by equation (2.7) reflect damage induced anisotropy in an initially isotropic material.

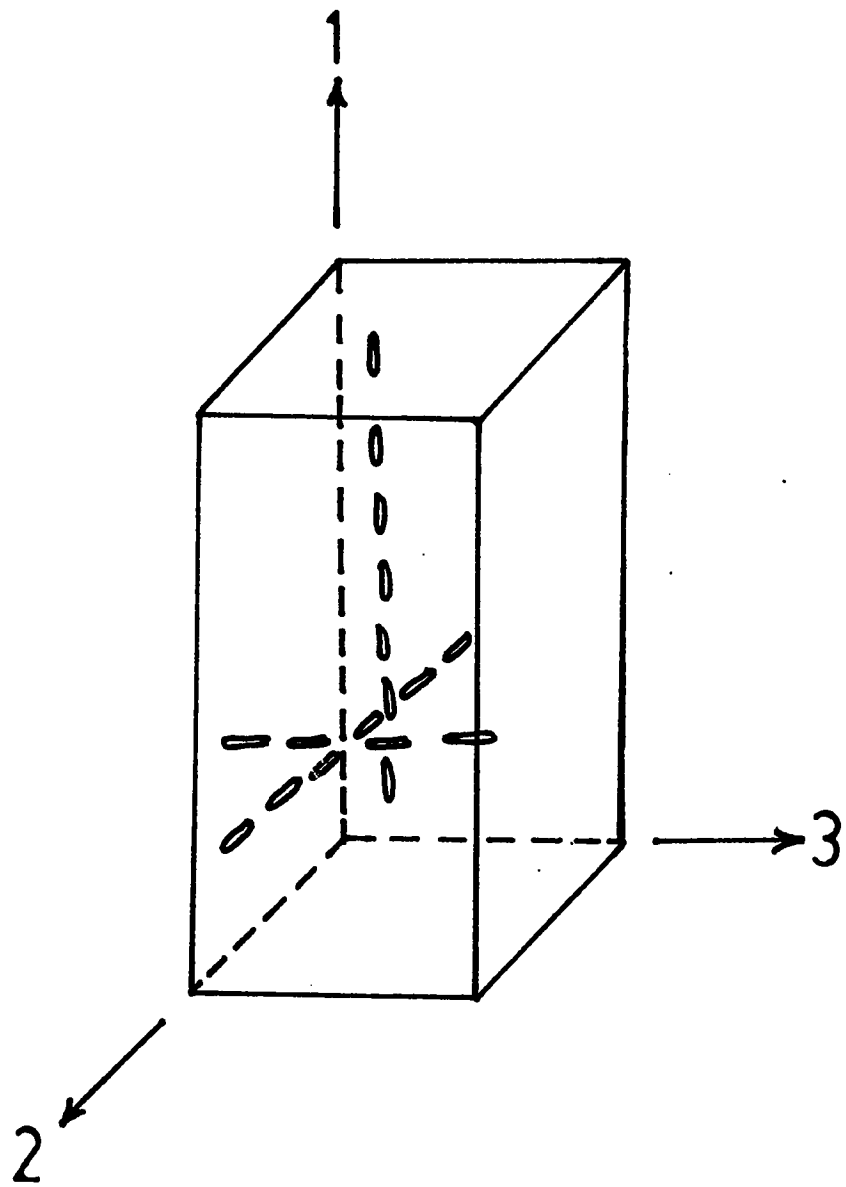

Figure 2: Distribution of Cracks in Three Principal Directions.

If the body is subjected to uniaxial compression, the cracks in the plane perpendicular to the loading will close, while in the other directions they will open up. Therefore, for the case of three principal compressive stress directions E_o will be degraded by the damage in the planes not perpendicular to the loading, i.e.,

$$
\begin{aligned}
E_1 &= E_o(1-\beta\omega_2)(1-\beta\omega_3) \\
E_2 &= E_o(1-\beta\omega_1)(1-\beta\omega_3) \\
E_3 &= E_o(1-\beta\omega_1)(1-\beta\omega_2)
\end{aligned}
\qquad (2.8)
$$

where, β is a constant parameter. Due to the cross-effects and tortuous nature of cracks ν is also degraded, i.e.,

$$
\begin{aligned}
\nu_{12} &= \frac{\nu}{(1-\omega_1)(1-\omega_2)} \\
\nu_{13} &= \frac{\nu}{(1-\omega_1)(1-\omega_3)} \\
\nu_{23} &= \frac{\nu}{(1-\omega_2)(1-\omega_3)}
\end{aligned}
\qquad (2.9)
$$

Note that degraded Poisson's ratio implies an increase in the Poisson's ratio, reflecting an effective increase in the flexibility.

2.3 BEHAVIOR OF CONCRETE

Concrete consists of cementitious matrix and aggregate particles.Wittmann (1983) outlined a classification scheme for structural levels by which the processes in the concrete can be observed : 1. micro-level ; 2. meso-level ; 3. macro-level. Most of the properties of concrete have to be measured in the second level using the concept of unit cell but the phenomenological aspects are observed in the macro-level. The most prominent modes of the irreversible changes of the micro-structure are :

1. slip on the preferred crystallographic planes
2. nucleation and growth of microcracks and microvoids

Slip is promoted by shear stresses available for moving and stacking dislocations (line defects) into preferential configuration. For material slips through the crystalline lattice , the number of bonds between particles remains practically unchanged (Krajcinovic, 1984). The plastic deformation is a phenomenological result of the slips on all active slip systems in the solid.Concrete lacks the crystalline lattice necessary for the sustained slip deformation. This phenomena are studied within the context of the theory of plasticity. Response dominated by slip in shear planes will be perceived as ductile for concrete if partially or totally confined.

Ortiz (1984) pointed out that it is important to note , however, that both the cracking and plastic flow of concrete exhibit a variety of

23-7

typical features that are not contained within the classical theories of fracture mechanics and plasticity. It is well known that when concrete is subjected to uniaxial compression it develop cracks that are parallel to the axis of loading. In some cases, these cracks become so large to be the direct cause of failure of the specimen.

Whereas plastic strain does not significantly reduce the elastic moduli, micro-cracking causes both inelastic strain and a reduction of the elastic moduli (Bazant and Shieh,1980). Micro-cracking in the cleavage mode occurs in planes perpendicular to the direction in which the direct tensile strain exceeds some threshold value reflecting the cohesive and/or adhesive strength of the solid locally.Since the microcracking involves progressive loss of bonds between adjacent particles (grains) the elastic properties of the solid are affected as well.Microcracks are actually not randomly oriented but exhibit a prevalent orientation, thus giving rise to stress- induced anisotropy of incremental elastic moduli (Bazant and Shieh, 1980).Response characterized by micro-cracking in cleavage mode is typically classified as brittle as for a concrete specimen in unconfined uniaxial compression.

The extension of microcracks, for instance, is not only known to play a decisive role in the inelasticity of concrete (Ortiz, 1984), as it results in the degradation of the elastic compliances (Hsu et al., 1963; Gardener, 1969; Karsan and Jirsa, 1969; Mills and Zimmerman, 1970,1971; Linse, 1973; Palaniswamy and Shah, 1974; Wastiels, 1979)

but also interacts with the plasticity of the material (Hueckel, 1975;1976.1977; Dafalias, 1977a,b,1978). Such an effect is known as elastoplastic coupling.

The cracking of materials results from creation, propagation and coalescence of micro-cracks.For materials characterized by ductile behavior, Chaboche(1987) considered four different levels of cracking:

1. crack nucleation;
2. micro-crack initiation;
3. macro-crack initiation;
4. breaking up.

On the other hand , one must distinguish two other types of structural materials (Bazant et al., 1991)

1. those failing at the initiation of the macroscopic crack growth (i.e., the structure just before failure contains only macroscopic cracks or other flaws, as in typical types of many ceramics and fatigue-embrittled metal structures); and
2. those failing only after large stable microscopic crack growth (which is the case of reinforced concrete structures).

These considerations give rise to the brittle damage. Damage is generally termed brittle when it occurs by decohesion without any sensible plastic strain at the mesoscale.

For concrete, the heterogeneity of its microstructure associated with great porosity of the binding material and with the presence of granulates , is an essential factor of the phenomenological aspect of the behavior. From experimental observations and from micromechanical models which were proposed by several authors the following can be described for concrete :

1. a state of initial degradation (defects of compactness , microcracks in the paste created by dilatation and shrinkage);
2. a propagation of the microcracks around the biggest grains under load ;
3. a dependence of the microporous structure of the cement paste on the hydrostatic pressure.

A salient aspect of the material behavior of concrete that can be deduced is the process of damage undergone by its elastic properties as a consequence of microcrack growth. It has been shown through crack surveys that crack textures quickly become highly anisotropic. This endows the elasticity of concrete with a strong induced anisotropy (Ortiz, 1984).

2.4 REVIEW OF SOME EXISTING DAMAGE MODELS OF CONCRETE

In this section before reviewing some of the existing models a brief description of theoretical preliminaries is discussed.

2.4.1 Theoretical Preliminaries

At constant temperature, concrete may be described by the elastic strain tensor ε^e ,the damage variable D, and the scalar effective plastic strain $\bar{\varepsilon}^p$. which may be defined as

$$\bar{\varepsilon}^p = \int_0^t \frac{1}{2} |\dot{\varepsilon}^p : \dot{\varepsilon}^p| dt \qquad (2.10)$$

in which $\dot{\varepsilon}^p$ is the rate of plastic strain tensor obtained through the partitioning of total strain rate $\dot{\varepsilon}$ into elastic and plastic strains , such that, $\dot{\varepsilon} = \dot{\varepsilon}^e + \dot{\varepsilon}^p$. The symbol : indicates the tensorial product contracted on two indices.

The mathematical definition of damage does not need to be precised at this point. Each equilibrium state is distinguished by the value of a scalar thermodynamic potential, strain energy function $W = \rho\psi$, in which ψ, is the strain energy per unit mass,and ρ is the mass density of the material.The quantity $\rho\psi$ is a function of ε^e , D , $\bar{\varepsilon}^p$. A common choice for ψ that satisfies the first principle of thermodynamics is the specific energy of a quadratic form as proposed by Lemaitre and Chaboche (1978). Following Kachanov and Lemaitre's interpretation it is

assumed that only the elastic properties of the material are affected by damage. Therefore , $\rho\psi$ can be expressed as

$$\rho\psi(\varepsilon^e, D, \bar{\varepsilon}^p) = \rho\psi^e(\varepsilon^e, D) + \rho\psi^p(\bar{\varepsilon}^p) \qquad (2.11)$$

in which ψ^e is a function of damage and elastic strains , and ψ^p is a function of the effective plastic strain. The stress tensor σ, the effective stress, $\bar{\sigma}$ and the damage energy release rate Y are defined from the specific energy as follows :

$$\sigma = \frac{\partial\rho\psi^e}{\partial\varepsilon^e};$$

$$\bar{\sigma} = -\frac{\partial\rho\psi^p}{\partial\bar{\varepsilon}^p}; \qquad (2.12)$$

$$Y = -\frac{\partial\rho\psi^e}{\partial D}.$$

The permanent strains and damage are irreversible processes leading to the conversion of mechanical energy into heat and surface creation. According to the Clausius Duhem inequality, the rate of energy dissipated $\dot{\varphi}$ must remain positive :

$$\dot{\varphi} = \sigma:\dot{\varepsilon} - \rho\dot{\psi}^e - \rho\dot{\psi}^p \geq 0 \qquad (2.13)$$

In this expression the rate of energy dissipated due to damage $\dot{\varphi}_d$ can be distinguished from that due to plasticity $\dot{\varphi}_p$:

$$\dot{\varphi}_d = \sigma:\dot{\varepsilon}^e - \rho\dot{\psi}^e; \qquad \dot{\varphi}_p = \sigma:\dot{\varepsilon}^e - \rho\dot{\psi}^p; \qquad (2.14)$$

A sufficient condition to satisfy the Clausius Duhem inequality can be $\dot{\varphi}_d \geq 0$, and $\dot{\varphi}_p \geq 0$. Since the introduction of plasticity in the models is very similar to classical developments (Ladeveze 1983) the attention is focused on the introduction of damage into the elastic constitutive laws. The potential $\rho\psi^e$ is adopted for the elastic energy :

where $\rho\psi^e = \frac{1}{2}\Lambda(D):\varepsilon^e:\varepsilon^e$

(2.15)

$\Lambda(D)$ is a fourth-order symmetric tensor, function of damage D, interpreted as the secant stiffness matrix. Taking the incremental form of Eq.(2.15) and substituting into Eqs.(2.12) and (2.14) gives

$$\sigma = \Lambda(D):\varepsilon^e; \qquad Y = -\frac{1}{2}\frac{\partial\Lambda(D)}{\partial D}:\varepsilon^e:\varepsilon^e \qquad (2.16)$$

$$\dot{\varphi}_d = -\left(\frac{1}{2}\frac{\partial\Lambda(D)}{\partial D}:\varepsilon^e:\varepsilon^e\right)\dot{D} \geq 0 \qquad (2.17)$$

The damage energy release rate Y is a quadratic form positive definite since $\frac{\partial\Lambda}{\partial D} < 0$ i.e. the stiffness decreases with increasing damage. The sufficient condition to satisfy the Clausius Duhem inequality is $\dot{D} \geq 0$ The damage growth satisfying the above condition will be governed by a loading surface of equation $f(\varepsilon, \Lambda, K_o) = 0$, in which K_o is the initial threshold of damage. Uniqueness of this function with regard to the stress-state is insured by choosing f as a function of strains, not

stresses (two strain tensors may be associated with the same stress tensor).To respect the loading condition, damage evolution equation is defined as

$$\dot{D} = 0 \text{ if } f < 0 \ \ or \ \ f = 0 \text{ and } \dot{f} = 0 \qquad (2.18)$$

$$\dot{D} = F(\varepsilon) \text{ if } f = 0 \text{ and } \dot{f} \geq 0 \qquad (2.19)$$

$F(\varepsilon)$ is a positive function of strains which is experimentally determined.

In the following sections some of the existing models are now reviewed.

2.4.2 Scalar Damage Model (Mazars)

In Mazars' scalar damage model (1984), the material is supposed to behave elastically and to remain isotropic. Based on Eq.(2.15) elastic energy may be expressed as follows:

$$\rho\psi^e = \frac{1}{2}\Lambda_o(1-D):\varepsilon^e:\varepsilon^e$$

in which, Λ_o is the initial stiffness matrix of the material and D is the damage. (2.20)

The stress σ and the damage energy release rate Y are then directly calculated from Eqs. (2.12) and (2.17) in the following form :

$$\sigma = \Lambda_o(1-D):\varepsilon^e; \qquad (2.21)$$

$$Y = \frac{1}{2}\Lambda_o:\varepsilon^e:\varepsilon^e; \qquad (2.22)$$

The dissipation rate is obtained from Eq. (2.14):

$$\dot{\phi} = YD \qquad (2.23)$$

The damage scalar theoretically ranges from 0 for the virgin material to 1 which represents the failure (zero stress) under homogeneous strain condition. The loading surface used is inspired from the St. Venant criterion of maximum principal strain, and may be expressed as

$$f(\varepsilon, \Lambda, K_o) = \tilde{\varepsilon} - K(D) \qquad (2.24)$$

where $\tilde{\varepsilon}$ is the equivalent strain, defined as :

$$\tilde{\varepsilon} = \sqrt{\sum_{1}^{3} (<\varepsilon_i>_+^2}; \qquad (2.25)$$

$$\left(<x>_+ = \frac{|x| + x}{2}, \quad \varepsilon_i \textit{ are the principal strains} \right) \qquad (2.26)$$

The hardening-softening parameter K(D) takes the largest value of the equivalent strain $\tilde{\varepsilon}$ ever reached by the material at the considered point to retain the previous loading history, and is initially equal to K_o. The response in tension or compression is described by the following laws coupling two types of damage, namely, D_t and D_c which correspond to damage measured in uniaxial tension and uniaxial compression respectively. The total damage D is expressed as the weighted sum of D_t and D_c such that

$$D = \alpha_t D_t + \alpha_c D_c; \text{and} \qquad (2.27)$$

$$D_t = F_t(\tilde{\varepsilon}) \text{ and } D_c = F_c(\tilde{\varepsilon}) \qquad (2.28)$$

where, α_t and α_c are the weighted functions depending on the strain state.

The stress tensor σ is decomposed into positive and negative parts, such that σ_+ and σ_- are the tensors which contain only the positive and negative principal stress, respectively, and $\varepsilon_t, \varepsilon_c$ the strain tensors defined as :

$$\varepsilon_t = \Lambda^{-1}:\sigma_+ ; \varepsilon_c = \Lambda^{-1}:\sigma_- \qquad (2.29)$$

It can be noted that in uniaxial tension $\alpha_t = 1$, and $\alpha_c = 0$, $D \doteq D_t$ and vice versa in compression.

2.4.3 Unilateral Damage Model (Ladevezé ; Mazars)

In the unilateral model Ladeveze(1983) and Mazars(1985), instead of using average set in Eq.(2.21) which defines the kinematics of damage , proposed that, it may be useful to distinguish damage due to tension from that due to compression. Since damage cannot diminish (Clausius Duhem inequality) two independent scalars, damage D_t and D_c, are used.Depending on the sign of stress, the apparent damage will be either D_t for positive stresses or D_c for negative stresses. If the loads are complex, damage may be a combination of D_t and D_c, The stress tensor is decomposed into positive and negative parts. The material is assumed to remain elastic and consequently the complementary potential function Ω^e may be expressed as:

23-7

$$\Omega^e = \Omega^e(\sigma_+) + \Omega^e(\sigma_-)$$

$$= \frac{1}{2}\left\{ \frac{1}{E_o(1-D_t)}[(1+\nu_o)(\sigma_+ : \sigma_+) - \nu_o(tr\sigma_+)^2] \right\} +$$

$$\frac{1}{2}\left\{ \frac{1}{E_o(1-D_c)}[(1+\nu_o)(\sigma_- : \sigma_-) - \nu_o(tr\sigma_-)^2] \right\} \qquad (2.30)$$

where $tr\sigma = \sigma_{kk}$ and E_o and ν_o are the initial modulus of elasticity and Poisson's ratio respectively. Tension and compression are distinguished by the sign of stress. The corresponding constitutive laws may be obtained from $\varepsilon^e = \frac{\partial \Omega^e}{\partial \sigma}$ as follows:

$$\varepsilon^e = \frac{1}{E_o(1-D_t)}[(1+\nu_o)\sigma_+ - \nu_o < tr\sigma_+ > I] +$$

$$\frac{1}{E_o(1-D_c)}[(1+\nu_o)\sigma_- - \nu_o < tr\sigma_- > I] \qquad (2.31)$$

where I is the identity tensor. In the Clausius Duhem inequality two damage energy release rates related to each damage scalar appear:

$$\dot{\varphi}_d = Y_t D_t + Y_c D_c; \qquad (2.32)$$

$$Y_t = -\frac{\partial \Omega^e}{\partial D_t}; \qquad Y_c = -\frac{\partial \Omega^e}{\partial D_c} \qquad (2.33)$$

A sufficient condition to satisfy Eq.(2.7) is that the two rates of damage D_t and D_c remain positive. The damage loading surface is expressed in term of the energy release rate as :

$$f_t(\varepsilon,\Lambda,K_o) = Y_t - K_t(D_t) \qquad (2.34)$$

$$f_c(\varepsilon,\Lambda,K_o) = Y_c - K_c(D_c) \qquad (2.35)$$

K_t and K_c are the hardening-softening parameters similar to K(D) in Eq.(2.18). The evolution of laws of each damage scalars are the following functions of the energy release rates, $D_t = F_t(Y_t)$ and $D_c = F_c(Y_c)$. For this model the damage produced by tension has no effect on the response in compression and vice versa. The two damage parameters grow independently, each one describing the corresponding secant stiffness of the material subjected to uniaxial loading of positive or negative sign.

2.4.4 Damage Model with Permanent Strains and Induced Anisotropy (Collumbet)

Collumbet(1985), proposed the following thermodynamic potential,from which a formulation including the effect of induced anisotropy can be derived :

$$\rho\psi = \frac{1}{2}[\Lambda_D:\varepsilon^e]:(\varepsilon^e + \varepsilon^p) \qquad (2.36)$$

Permanent strains ε^p appear in this potential and Λ_D is the stiffness matrix of an orthotropic material. Its dependence on damage is defined as $\Lambda_D^{-1}:\sigma = \Lambda_o^{-1}:[L_D:\sigma]$ in which Λ_o is the initial stiffness matrix of the material, the damage variable called L_D Is a fourth-order symmetric

tensor. Since the material is orthotropic, there are in general nine damage variables. Collumbet restricted the identification to the axisymmetric case where four variables are needed Eq.(2.37). The damage loading surface is identical to the one used previously in the one scalar damage model Eq.(2.24)

$$L^D:\sigma = \begin{bmatrix} l_1 & l_{12} & l_{23} \\ l_{12} & l_1 & l_{23} \\ l_{23} & l_{23} & l_3 \end{bmatrix} \begin{bmatrix} \sigma_1 \\ \sigma_2 \\ \sigma_3 \end{bmatrix} \qquad (2.37)$$

The constitutive laws are derived from the potential Eq.(2.36) :

$$\varepsilon = \Lambda_D^{-1}:\sigma + \varepsilon^p \qquad (2.38)$$

This model may not be applied to stress states where the hydrostatic pressure is high.

2.4.5 Constitutive Model for Concrete in Cyclic Compression (Chen)

In this work by Chen (1984), an overall assessment of the damage is based on the evaluation of the plastic volumetric strain ε_v^p and the plastic octahedral shear strain γ_o^p The coupling of these two effects is achieved through a shear compaction-dilatancy factor. The damage accumulation is proposed to be evaluated by the use of a damage parameter,K, which is related to γ_o^p The realistic modelling of damage accumulation under complex stress paths is achieved by defining K in an incremental form as

$$dK = \frac{d\gamma_o^p}{F_1(I_1, 0)} \qquad (2.39)$$

$$\text{and } K = \int_{loading\ history} dK \qquad (2.40)$$

The failure criterion used in this model is represented by a failure surface defined in stress space. This failure surface, called a bounding surface, as shown in Figure 3 , encloses all possible stress points and shrinks in size as damage accumulates.The bounding surface is a function of stress invariants and damage parameter.In this model the bounding surface,F, is proposed to be a function of σ_{ij} (or stress invariants) and K_{max} = the maximum value of K ever experienced by the material :

$$F(\sigma_{ij}, K_{max}) = 0 \qquad (2.41)$$

$$F(\sigma_{ij}, K_{max}) = \frac{1.85(\sqrt{J_2} + 0.378 J_2)(12 + 11\cos 3\theta)^{1/6}}{I_1 + 0.3} - \frac{40}{K_{max}^2 + 39} = 0 \qquad (2.42)$$

where,

I_1 = the first stress invariant ,

J_2 = second deviatoric stress invariant.

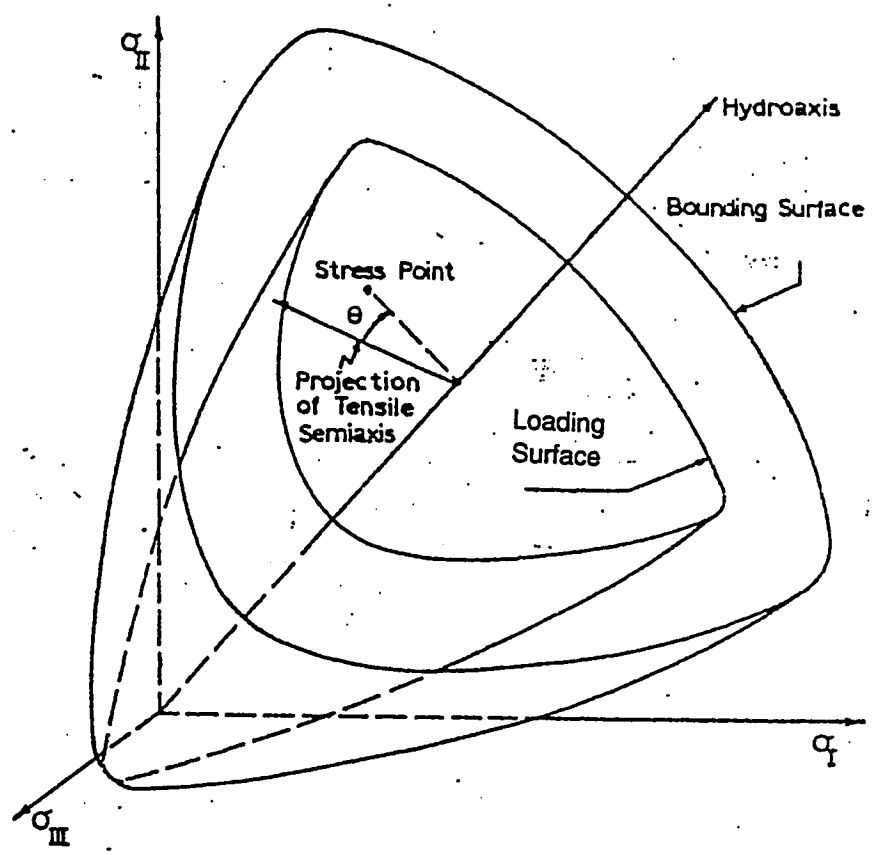

Figure 3: Bounding Surface in Principal Stress Space

θ = angle between projection of the position vector of principal stress and that of any semiaxis on deviatoric plane (angle of similarity).

The present formulation adopts that the distance between the stress point and the bounding surface is measured along the S_{ij} direction. By this definition, the octahedral stress-strain behavior can be characterized. Since the bounding surface on the deviatoric plane is I_1 dependent , a normalized measure D is introduced for this purpose:

$$D = \frac{r}{R} \qquad (2.43)$$

in which r is the distance from the projection of current stress point on the deviatoric plane to the hydrostatic axis; and R is the distance of the bounding surface from the hydroaxis along the S_{ij} direction. Thus, when D = 1, the material is assumed to have failed.

Strain increment $d\varepsilon_{ij}$ is decomposed into its deviatoric and volumetric components :

$$d\varepsilon_{ij} = de_{ij} + \delta_{ij}\frac{d\varepsilon_{kk}}{3} \; ; (k=1,2,3) \qquad (2.44)$$

The deviatoric strain increment can be further decomposed into elastic and plastic components, de^{e}_{ij} and de^{p}_{ij}

$$de_{ij} = de^{e}_{ij} + de^{p}_{ij} \qquad (2.45)$$

23-7

The elastic deviatoric strain increment ε_{ij}^{e} can be related to the stress increment following Hooke's Law

$$de_{ij}^{e} = \frac{1}{H^{e}} dS_{ij} \qquad (2.46)$$

in which H^{e} = the generalized elastic shear modulus; and dS_{ij} = the deviatoric stress increment.The plastic strain increment de_{ij}^{p} is assumed to be independent of any volumetric change, and the projection of de_{ij}^{p} on the deviatoric plane is assumed directly along the projection of the position vector of the stress point.In other words, de_{ij}^{p} is proportional to S_{ij} ·This proportionality yields

$$\frac{de_{ij}^{p}}{S_{ij}} = \frac{d\gamma_{o}^{p}}{\tau_{o}} \qquad (2.47)$$

and assuming incremental linearity one can write

$$d\gamma_{o}^{p} = \frac{d\tau_{o}}{H^{p}} \qquad (2.48)$$

in which the generalized plastic shear modulus H^{p} , depends on the history of the stress and strain.

The portion of $d\varepsilon_{kk}$ caused by dI_1 , $d\varepsilon_{kk,0}$ is calculated as

23-7

$$d\varepsilon_{kk,0} = \frac{dI_1}{3K_t} \qquad (2.49)$$

in which tangent bulk modulus K_t is assumed to be a function of I_1 The remaining portion of $d\varepsilon_{kk}$, $d\varepsilon_{kk,d}$, is directly associated with the plastic octahedral shear strain increment, $d\gamma_o^p$, by the linear relationship

$$d\varepsilon_{kk,d} = \beta d\gamma_o^p \qquad (2.50)$$

in which shear compaction-dilatancy factor β is also a function of the stress and strain , and

$$d\varepsilon_{kk} = d\varepsilon_{kk,0} + d\varepsilon_{kk,d} \qquad (2.51)$$

Combining Eqs.(2.38-2.45) and by expressing

$$d\tau_o = \frac{\partial\tau_o}{\partial\sigma_{km}} d\sigma_{km} = S_{km}\frac{d\sigma_{km}}{3\tau_o}, (k,m=1,2,3) \qquad (2.52)$$

the following relationship between $d\varepsilon_{ij}$ and $d\sigma_{ij}$ is obtained:

$$d\varepsilon_{ij} = \frac{d\sigma_{ij}}{H^e} + \frac{1}{3H^p\tau_o}\left[\frac{S_{ij}}{\tau_o} + \delta_{ij}\frac{\beta}{3}\right]S_{km}d\sigma_{km} +$$

$$\delta_{ij}\left(\frac{1}{9K_t} - \frac{1}{3H^e}\right)d\sigma_{kk};\ (k,m=1,2,3) \qquad (2.53)$$

2.4.6 Damage Model for Cyclic Loading of Concrete (Suaris)

Suaris (1990), in his model, derived the damage growth, using a concept formally similar to the bounding surface hypothesis used in plasticity. In this method, a limit fracture surface (which defines the onset of damage), a loading surface and a bounding surface are defined. Damage growth would occur only when the loading surface is outside of the limit fracture surface. The bounding surface is obtained by applying a mapping rule to the loading surface. The damage growth rate is defined as a function of the distance between a point on the loading surface and the corresponding image point on the bounding surface.

The elastic complementary free-energy function (Λ) is a function of the stress tensor σ_{ij}, temperature t, and current damage state. If the damage can be represented by three components , ω_i, along the principal tensile stress directions, then the function, Λ , can be expressed as

$$\Lambda = \Lambda(\sigma_{ij}, t, \omega_i) \qquad (2.54)$$

The constitutive relations and the generalized thermodynamic force conjugates (R_j) of the damage components, derived subject to thermodynamic restrictions, are given by

$$\varepsilon_{ij} = \rho \frac{\partial \Lambda}{\partial \sigma_{ij}}(\sigma_{ij}, t, \omega_i) \qquad (2.55)$$

$$R_j = \rho \frac{\partial \Lambda}{\partial \omega_i} \qquad (2.56)$$

23-7

The entropy production rate (the Clausius Duhem inequality) can be written as

$$\rho\dot{\eta} = -\varepsilon_{ij}\dot{\sigma}_{ij} + \rho\Lambda > 0 \qquad (2.57)$$

Expanding and substituting $\varepsilon_{ij} = \rho\frac{\partial\Lambda}{\partial\sigma_{ij}}$ and assuming that the process is isothermal, Eq.(2.57) can be reduced to the form

$$\rho\dot{\eta} = R_j\dot{\omega}_j > 0 \qquad (2.58)$$

The loading function (f) is defined in terms of the thermodynamic-force conjugate as

$$f = (R_iR_i)^{\frac{1}{2}} - \frac{R_c}{b} = 0 \qquad (2.59)$$

where R_c is a constant with a value of 0.63 and b is the mapping parameter , which varies from infinity to 1 with the growth of the loading function,

A bounding surface F is defined as

$$F = (\overline{R}_i\overline{R}_i)^{\frac{1}{2}} - R_c = 0 \qquad (2.60)$$

where $\overline{R}_i$ = an image point on $F = 0$ associated with a given point R_i on $f = 0$, defined through a noninvertible continuous mapping rule as

$$\overline{R}_i = bR_i \qquad (2.61)$$

Bounding, loading and limit fracture surfaces are shown in Figure 4

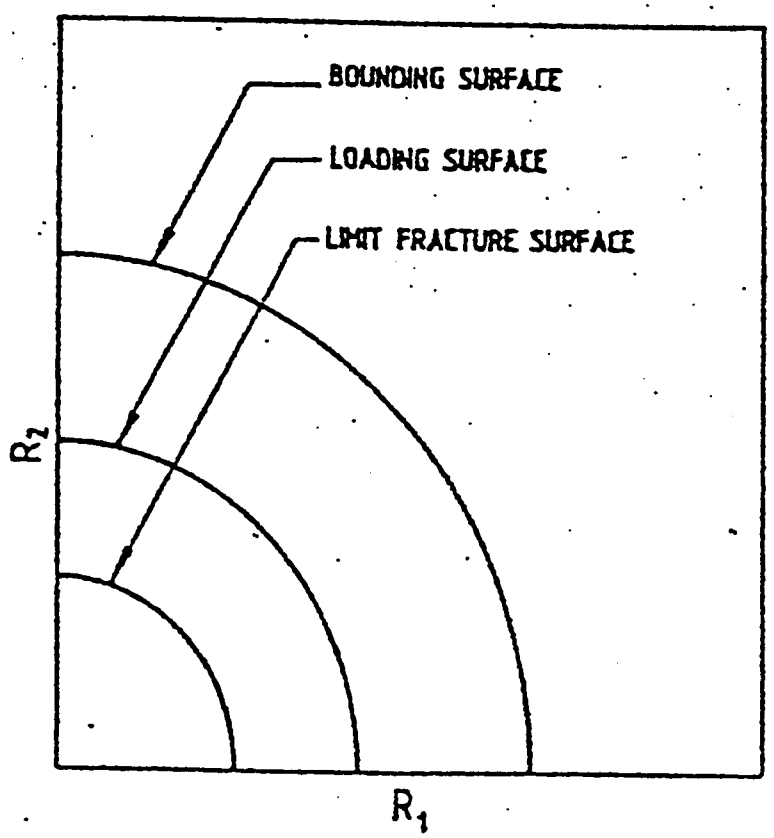

Figure 4: Illustration of Bounding, Loading and Limit Fracture Surfaces

The damage-growth rate is determined from the loading function by using an associated flow rule as

$$\dot{\omega}_i = L\left[\frac{\partial f}{\partial R_i}\right] \qquad (2.62)$$

where L = a loading index selected so that Eq.(2.58) is satisfied.The loading index L is defined by

$$L = \frac{c}{H}\left[\frac{\partial f}{\partial R_j}R_j\right] \qquad (2.63)$$

where

$$c = 1 \quad \text{if } f = 0 \text{ and } \left[\frac{\partial f}{\partial R_j}\right]R_j > 0$$

$$c = 0 \quad \textit{otherwise} \qquad (2.64)$$

The damage modulus H is expressed as a function of the distance between the loading and the bounding surface, given by

$$H = \frac{D\delta}{<\delta_{in} - \delta>} \qquad (2.65)$$

where $D = 2.65$ is a constant; and < > are Macaulay brackets that set the quantity within to zero if the value is negative.

The normalized distance δ between the loading and bounding surfaces is given by

23-7

$$\delta = \frac{(\bar{R}_i\bar{R}_i)^{\frac{1}{2}} - (R_iR_i)^{\frac{1}{2}}}{(\bar{R}_i\bar{R}_i)^{\frac{1}{2}}} = 1 - \frac{1}{b} \qquad (2.66)$$

and is shown in Figure 5.

The stress tensor is decomposed into its positive and negative eigenvalues given by

$$\sigma = [\sigma]^{+} + [\sigma]^{-} \qquad (2.67)$$

The complementary free-energy function is then introduced in terms of the positive and negative eigenvalues as

$$\rho\Lambda = \frac{1}{2}(\sigma^{+}C_{I}\sigma^{+} + \sigma^{-}C_{II}\sigma^{-}) \qquad (2.68)$$

where C_I and C_{II} are the compliance matrices for tensile and compressive stresses.

The decomposition of the elastic potential into tensile and compressive portions enables the modelling of the different crack mechanisms in tension and compression.The compliance matrices for tension and compression are derived using the concept of orthotropic damage as discussed in sec.2.2.2.The compliance matrix for tensile stresses C_I is defined as

$$C_I = \frac{1}{E_o}\begin{bmatrix} \frac{1}{(1-\alpha\omega_1)} & \frac{-\nu}{1} & \frac{-\nu}{-\nu} \\ \frac{-\nu}{-\nu} & \frac{1}{(1-\alpha\omega_2)} & \frac{1}{(1-\alpha\omega_3)} \end{bmatrix} \qquad (2.69)$$

23-7

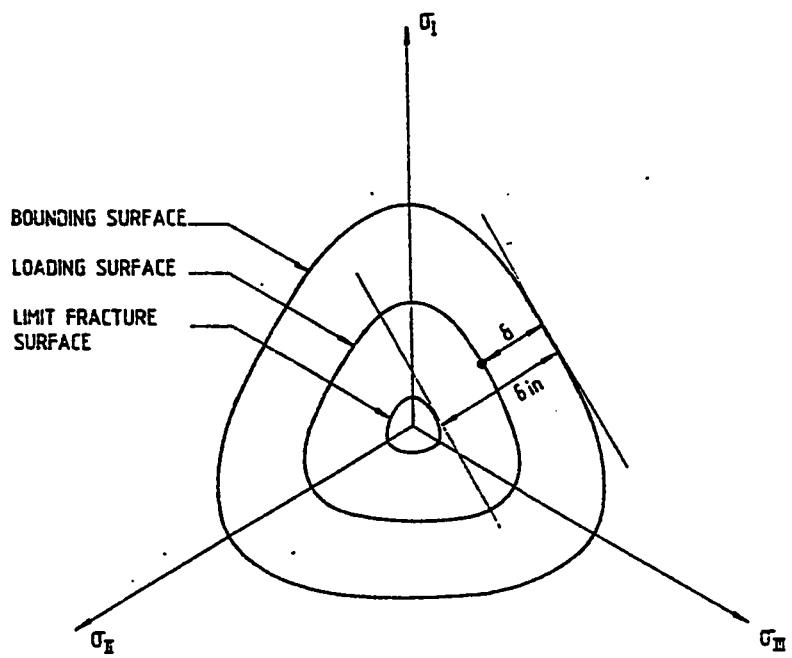

Figure 5: **Definition of Normalized Distance in Deviatoric Plane**

where E_o = the modulus of elasticity; and ν = the Poisson's ratio of the uncracked concrete, and $\omega_1, \omega_2, \omega_3$ = the components of damage in the three principal tensile stress directions respectively.

The compliance matrix C_{II} for compression is defined as

$$C_{II} = \frac{1}{E_o}\begin{bmatrix} \frac{1}{(1-\beta\omega_2)(1-\beta\omega_3)} & -\frac{\nu}{(1-\omega_1)(1-\omega_2)} & -\frac{\nu}{(1-\omega_1)(1-\omega_3)} \\ -\frac{\nu}{(1-\omega_1)(1-\omega_2)} & \frac{1}{(1-\beta\omega_1)(1-\beta\omega_3)} & -\frac{\nu}{(1-\omega_2)(1-\omega_3)} \\ -\frac{\nu}{(1-\omega_1)(1-\omega_3)} & -\frac{\nu}{(1-\omega_2)(1-\omega_3)} & \frac{1}{(1-\beta\omega_1)(1-\beta\omega_2)} \end{bmatrix} \tag{2.70}$$

where $\omega_i (i=1,2,3)$ are the accumulated damage values in planes perpendicular to axes $x_i (i=1,2,3)$ respectively. α and β are the constant parameters of the model, which are selected by calibrating the model to results obtained by for uniaxial tensile and compressive tests.

This model can be viewed as a generalization of the effective stress concept previously used for concrete. The proposed compliance relations are however valid only when the axes of principal stress and strain coincide and do not rotate.A larger 6 x 6 compliance matrix (with all nonzero elements) should be introduced to relate six independent components of stress to the six oriented strain components, if the model is to exhibit these features i.e., the axes of principal stress and strain do not coincide and do rotate.

2.4.6.1 Physical interpretation of Rc

The damage process gives rise to initiation of a macrocrack for a critical value of $(R_i R_i)^{\frac{1}{2}}$, which is a characteristic for each material.

This characteristic value , $(R_i R_i)^{\frac{1}{2}} = R_c$, corresponds to a critical value of damage variable $D = D_{cr}$, which can be determined experimentally from uniaxial tension case for rupture conditions.

Lemaitre {46},has expressed R_c in terms of rupture stress, σ_R, and critical damage variable, D_{cr}, for the isotropic damage as follows:

$$R_c = \frac{\sigma_R^{\ 2}}{2E(1-D_{cr})^2} \qquad (2.71)$$

Similar expression for R_c can de derived from the Suaris damage model for uniaxial tension case, which is as follows:

The thermodynamic force conjugates R_k may be obtained by expressing Eq.(2.56) as follows:

$$R_k = \frac{1}{2}\left(\sigma_i^+ \frac{\partial C_{ij}^{I}}{\partial \omega_k}\sigma_j^+ + \sigma_i^- \frac{\partial C_{ij}^{II}}{\partial \omega_k}\sigma_j^-\right) \qquad (2.72)$$

For uniaxial tension case, there will be only one component of R_k i.e.,

R_1. At failure, $R_1 = R_c$ and $\sigma_+ = f_t'$. Substituting in Eq.(2.72) yields the following expression :

$$R_c = \frac{f_t'^2 \alpha}{2E_o(1-\alpha\omega)^2} \qquad (2.73)$$

Expressing f_t' in terms of uniaxial compressive strength, f_c, yields the following relationship

$$R_c = \frac{(0.1 f_c')^2 \alpha}{2E_o(1-\alpha\omega)^2} \qquad (2.74)$$

The above expression shows that, there exists a relationship between R_c and uniaxial compressive strength, f_c', which should be determined experimentally for different strengths of concrete. The relationship $R_c = R_c(f_c')$ should be in the form of an expression that can be used to determine the critical strain energy release rate for different strengths of concrete.

2.4.7 Damage Model for Concrete using Bounding Surface Concept (Voyiadjis and Taher)

Voyiadjis and Taher (1993) in their model, also use the concept of bounding surface as the failure criterion. The damage bounding surface ,F, which is the innermost locus of stress points, is proposed to be a function of the states σ_{ij} (or stress invariants) and the damage parame-

ter , $\overline{D}$:

$$F(\sigma_{ij},\overline{D}) = 0 \qquad (2.75)$$

The mathematical function chosen for the damage bounding surface is as follows:

$$F(\sigma_{ij},\overline{D}) = aJ_2+\lambda\sqrt{J_2}+bI_1-g(\overline{D}) = 0 \qquad (2.76)$$

where a b, and λ are constants as given by Ottosen (1977) in his work on elasto-plastic constitutive modelling of concrete.It may be noted that form of F does not explicitly involve strain energy release rates R_i as in the Suaris model {69}. $g(\overline{D})$ = a function of damage accumulation. According to the nonuniform hardening rule (Han and Chen 1985) each loading surface can be characterized by a shape factor , K , and expressed in the form:

$$f(\sigma_{ij},\overline{D}) = aJ_2+\lambda K\sqrt{J_2}+K^2bI_1-K^2g(\overline{D}) = 0 \qquad (2.77)$$

where the damage parameter, D , takes the values $0 \le D \le 0.7$. The initial fracture surface is expressed in the form :

$$f_o(\sigma_{ij},\overline{D}_o) = aJ_2+\lambda K\sqrt{J_2}+K^2bI_1-K^2\frac{50+\overline{D}_o}{50.05} = 0 \qquad (2.78)$$

where $\overline{D}_o$ = the accumulated damage $(\overline{D})$ at the beginning of any cycle.

Instead of averaging D_t and D_c as proposed by Mazars(1986), a different loading surface is defined for each variable. A damage due to tension D_t will grow independently from the compression damage D_c. From the loading surface in (2.77) ,the compressive and tensile loading damage surfaces may be expressed as:

$$f_t = aJ_{2_t} + \lambda_t K\sqrt{J_{2_t}} + K^2 bI_{1_t} - K^2 g_t(\overline{D}) = 0 \qquad (2.79)$$

$$f_c = aJ_{2_c} + \lambda_c K\sqrt{J_{2_c}} + K^2 bI_{1_c} - K^2 g_c(\overline{D}) = 0 \qquad (2.80)$$

where D_t and D_c = the damage due to tension and compression respectively. (D_{1t}, D_{2t}, D_{3t}) and (D_{1c}, D_{2c}, D_{3c}) = principal values of damage tensor in tension and compression, respectively. The stress tensor is decomposed into positive(tension) σ^+ and negative(compression) σ^- parts , such that:

$$\sigma = \sigma^+ + \sigma^- \text{ and } tr\sigma = tr\sigma^+ + tr\sigma^- \qquad (2.81)$$

where σ_+ and σ^- are built with the positive and negative eigenvalues which appear only in the positive and negative principal stresses respectively.

The damage growth rate may be expressed as

$$(\dot{D}_{ij})_l = \frac{1}{h}\frac{\partial f_l}{\partial \sigma_{ij}}\frac{\partial f_l}{\partial \sigma_{mn}}\dot{\sigma}_{mn};\ l = t, c \qquad (2.82)$$

Differentiating (2.70 and 2.71) with respect to σ_{ij},

$$\frac{\partial f_l}{\partial \sigma_{ij}} = A_l S_{ij} + B_l \delta_{ij} \qquad (2.83)$$

where

$$A_l = a + \lambda_l K \frac{1}{2\sqrt{J_2}} \qquad (2.84)$$

$$B_l = 2\bar{a}\lambda_l[1 + I_{1_l}]\sqrt{J_{2_l}} + 4\bar{a}bK[1 + I_{1_l}]I_{1_l} - 4\bar{a}K[1 + I_{1_l}]g(\bar{D}) + bK^2$$

$$(2.85)$$

Substituting equations (2.83) to (2.85) into (2.81), the damage growth rate can be written as :

$$\dot{D}_{ij_l} = \frac{1}{h_l}[A_l^2 S_{ij} S_{mn} \dot{\sigma}_{mn} + B_l^2 \delta_{ij} \dot{\sigma}_{mn} + A_l B_l (\delta_{ij} S_{mn} \dot{\sigma}_{mn} + S_{ij} \dot{\sigma}_{mn})]$$

$$(2.86)$$

where S_{ij} = the deviatoric stress and δ_{ij} = the Kronecker delta. The damage modulus h is derived using the concept of the bounding surface, in which it may be given as :

$$h = \hat{h}(\delta, \bar{D}) \qquad (2.87)$$

where δ = the distance between the stress point on the loading surface and the corresponding point on the bounding surface measured along the deviatoric stress direction.

The constitutive relationships are the same as that given by Suaris (1990).

In the models reviewed herein, only two models i.e.,(Suaris (1990) and Voyiadjis and Taher (1993)),consider the three dimensionality.It is interesting to note that, almost all models claim that they can be incorporated in the finite element method, but the models are presented in a stress controlled form i.e., the constitutive relationships are given for strains in terms of stresses,which is not conducive for application in a stiffness based finite element method, since, in this approach strains are used to calculate stresses. Therefore, in order to use any of these models, the constitutive relationships need to be first inverted and expressed explicitly for implementation in finite element codes.

2.5 WHY SUARIS DAMAGE MODEL

Of the existing models, the model proposed by Wimal Suaris (1990) is selected to be incorporated in a finite element code for following reasons :

1. Generality of the model, as it takes into account three dimensions.
2. Simplicity
3. Fewer parameters to calibrate the model
4. It captures certain essential features of brittle materials including stiffness degradation and stress induced anisotropy.

23-7

2.5.1 Inversion of Constitutive Relations

Inversion of constitutive relationships involves the inversion of C matrices which leads to lengthy expressions for D matrices. The task becomes even more complicated when constitutive relationships are expressed in incremental form.

Strain tensor is decomposed into its positive and negative eigenvalues as :

$$\varepsilon = [\varepsilon]^{+} + [\varepsilon]^{-} \qquad (2.88)$$

The strain-energy function is introduced in terms of positive and negative eigenvalues as

$$\rho\Psi = \frac{1}{2}(\varepsilon^{+} D_{I} \varepsilon^{+} + \varepsilon^{-} D_{II} \varepsilon^{-}) \qquad (2.89)$$

The $[D]$ for tensile and compressive strains are determined as $[C_I]^{-1}$ and $[C_{II}]^{-1}$ respectively. Detailed expressions for D matrices can be seen in Appendix C.

Constitutive relationship is expressed as

$$\sigma_{ij} = \rho \frac{\partial \Psi}{\partial \varepsilon_{ij}}(\varepsilon_{ij}, t, \omega_i) \qquad (2.90)$$

Expanding (2.90), σ may be expressed as:

$$\sigma_{ij} = (D^{I}_{ij} \varepsilon^{+}_{ij} + D^{II}_{ij} \varepsilon^{-}_{ij}) \qquad (2.91)$$

Incremental form of σ can be written as

$$d\sigma_{ij} = (D^{I}_{ij} d\varepsilon^{+}_{ij} + D^{II}_{ij} d\varepsilon^{-}_{ij}) + (dD^{I}_{ij} \varepsilon^{+}_{ij} + dD^{II}_{ij} \varepsilon^{-}_{ij}) \qquad (2.92)$$

2.5.2 Equations for the Evolution of Damage

The equations used in the model cannot be implemented readily in the finite element code, therefore, they need to be expressed explicitly. In incremental form R_k may be expressed as

$$dR_k = \frac{1}{2}\Big(\sigma^{+}_{i} \frac{\partial C^{I}_{ij}}{\partial \omega_k} d\sigma^{+}_{j} + d\sigma^{+}_{i} \frac{\partial C^{I}_{ij}}{\partial \omega_k} \sigma^{+}_{j} + \sigma^{-}_{i} \frac{\partial C^{II}_{ij}}{\partial \omega_k} d\sigma^{-}_{j} +$$

$$d\sigma^{-}_{i} \frac{\partial C^{II}_{ij}}{\partial \omega_k} \sigma^{-}_{j} + \sigma^{+}_{i} \frac{\partial}{\partial \omega_l}\left[\frac{\partial C^{I}_{ij}}{\partial \omega_k}\right] d\omega_l \sigma^{+}_{j} +$$

$$\sigma^{-}_{i} \frac{\partial}{\partial \omega_l}\left[\frac{\partial C^{II}_{ij}}{\partial \omega_k}\right] d\omega_l \sigma^{-}_{j}\Big) \qquad (2.94)$$

The damage growth rate is determined from the loading function as

$$\dot{\omega} = L\left[\frac{\partial f}{\partial R_i}\right] \qquad (2.95)$$

In Eq.(2.95), $\left[\frac{\partial f}{\partial R_i}\right]$ may be expressed as,

$$\left[\frac{\partial f}{\partial R_i}\right] = \frac{1}{2}(R_j R_j)^{-\frac{1}{2}}\left[\frac{\partial R_j}{\partial R_i} R_j\right] \qquad (2.96)$$

and the loading index, L , is expressed as,

$$L = \frac{1}{H(R_i R_i)^{\frac{1}{2}}}(R_1 dR_1 + R_2 dR_2 + R_3 dR_3) \qquad (2.97)$$

The limit fracture surface which defines the initiation of damage is defined as

$$f_o = 0.08 + 0.0015\overline{\omega}$$

where,

$$\overline{\omega} = (\omega_{io} : \omega_{io}) \qquad (2.98)$$

and, ω_{io} = the component of accumulated damage (ω_i) at the beginning of any cycle.

Chapter III
FINITE ELEMENT MODEL

3.1 INTRODUCTION

A computer code 'DAMAG3D' has been developed for three dimensional structures made up of brittle materials using the twenty noded isoparametric hexahedral element.Three degrees of freedom are specified at each nodal point, corresponding to three displacements at that node.Stresses, strains and change in the characteristics of material are monitored at Gauss integration points in each element. Any Gauss point may remain elastic or undergoes damage or fail. Normal integration scheme is employed using normal 3 x 3 x 3 integration rule.

In this chapter the governing equilibrium equations are derived by using minimization of the total potential energy, and the finite element discretization is presented for 20- noded isoparametric hexahedral element.

3.2 FINITE ELEMENT FORMULATION

The governing equilibrium equations are derived by minimizing the total potential energy of the system.

23-7

3.2.1 Total Potential Energy of the System

If the structural system is subjected to a set of body forces $\{\tilde{b}\}$ and boundary tractions $\{\tilde{t}\}$ over the volume and surface of the domain Ω and Γ , respectively, then the total potential energy can be written as :

$$\pi = \frac{1}{2}\int_{\Omega}\{\tilde{\varepsilon}\}^{T}\{\tilde{\sigma}\}d\Omega - \int_{\Omega}\{\tilde{u}\}^{T}\{\tilde{b}\}d\Omega - \int_{\Gamma}\{\tilde{u}\}^{T}\{\tilde{t}\}d\Gamma \qquad (3.1)$$

where $\{\tilde{u}\}$ is the global displacement vector.

The displacement function $\{\tilde{u}\}$ and the strain field $\{\tilde{\varepsilon}\}$ may be expressed in terms of the interpolation function N and its derivative B such that :

$$\{\tilde{u}\} = [N]\,\{\tilde{d}\} \qquad (3.2)$$

$$\{\tilde{\varepsilon}\} = [B]\,\{\tilde{d}\} \qquad (3.3)$$

where $[N]$ and $[B]$ are row vectors, and

$$\{\tilde{d}\}$$

is the global displacement vector.

Equation 3.1 can now be expressed as

$$\pi = \frac{1}{2}\int\{\tilde{d}\}^{T}[B]^{T}\{\tilde{\sigma}\}d\Omega - \int\{\tilde{d}\}^{T}[N]^{T}[\tilde{b}]d\Omega - \int\{\tilde{d}\}^{T}[N]^{T}\{\tilde{t}\}d\Gamma \qquad (3.4)$$

Further, upon using

$$\{\sigma\} = [D]\,\{\varepsilon\} \qquad (3.5)$$

23-7

($[D]$ being elastic or damaged) into (3.4) and minimizing total potential energy with respect to nodal displacements,

$$\frac{d\pi}{d\{d\}} = 0 \qquad (3.6)$$

one obtains

$$\int [B]^T [D][B]\{\tilde{d}\} d\Omega - \int [N]^T \{b\} d\Omega - \int [N]^T \{\tilde{t}\} d\Gamma = 0 \qquad (3.7)$$

Equation 3.7 can now be recast into the following form

$$[K]\{\tilde{d}\} = \{\tilde{f}\} \qquad (3.8)$$

where :

$$[K] = \int [B]^T [D] [B] \, d\Omega \qquad (3.9)$$

is the global stiffness matrix $\{\tilde{d}\}$ is the global displacement vector and

$$\{\tilde{f}\} = \int [N]^T \{b\} \, d\Omega + \int [N]^T \{\tilde{t}\} \, d\Gamma \qquad (3.10)$$

is the global load vector

3.2.2 Element Stiffness Matrix

In order to determine the global stiffness matrix and the global load vector of the system , the contribution from each element needs to be determined. Expression 3.4 for the total potential energy can be written as the sum of the contributions from each element π^e such that

$$\pi = \sum_{e=1}^{n} \pi^e \qquad (3.11)$$

Minimization of the total potential energy with respect to global displacements implies minimization of potential energy of every element with respect to its own displacement vector $\{\tilde{d}^e\}$ therefore equation (3.6) can be written for individual elements as:

$$\frac{d\pi^e}{d\{d^e\}} = 0 \qquad (3.12)$$

and consequently the element stiffness matrix may be written as:

$$[K^e] = \int [B^e]^T [D^e] [B^e] \, d\Omega^e \qquad (3.13)$$

with element load vector

$$\{f^e\} = \int [N^e]^T \{b^e\} \, d\Omega^e + \int [N^e]^T \{\tilde{t}\} \, d\Gamma^e \qquad (3.14)$$

where $[N^e]$ and $[B^e]$ are the element shape function matrix and element strain matrix respectively, described in the next section of this chapter.The $[D^e]$ is the element constitutive matrix.

It remains here to say that both $[K^e]$ and $\{f^e\}$ should be expressed with respect to the global frame and consequently all the matrices and vectors used in evaluation of $[K^e]$ and $\{f^e\}$ need also to be with respect to the global frame. If one, however, decides to use different system then the appropriate transformation is necessary. For example, it is more convenient to use natural coordinate system to perform the integration and therefore one need to apply proper transformation from one system to another as will be described in the next sections.

3.2.3 Finite Element Discretization

3.2.3.1 Element Geometry

In the isoparametric formulation the coordinates of a point within the element (x, y, z) are obtained by applying the element shape functions to the nodal coordinates. For defining the element geometry a natural coordinate system (ξ, η, ζ) is used, as shown in Figure 6.

Thus at any point (ξ, η, ζ) within an element the x, y and z coordinates may be obtained from the expressions

$$x(\xi,\eta,\zeta) = \sum_{i=1}^{n} N_i^e(\xi,\eta,\zeta) x_i^e,$$

$$y(\xi,\eta,\zeta) = \sum_{i=1}^{n} N_i^e(\xi,\eta,\zeta) y_i^e, \qquad (3.15)$$

$$z(\xi,\eta,\zeta) = \sum_{i=1}^{n} N_i^e(\xi,\eta,\zeta) z_i^e.$$

The shape functions must satisfy the conditions

$$\sum N_i^e(\xi,\eta,\zeta) = 1 \qquad (3.16)$$

and

$$N_i^e(\xi,\eta,\zeta) = \begin{cases} 1 \text{ if } i=j \\ 0 \text{ if } i \neq j \end{cases} \qquad (3.17)$$

where (i,j = 1,.....20)

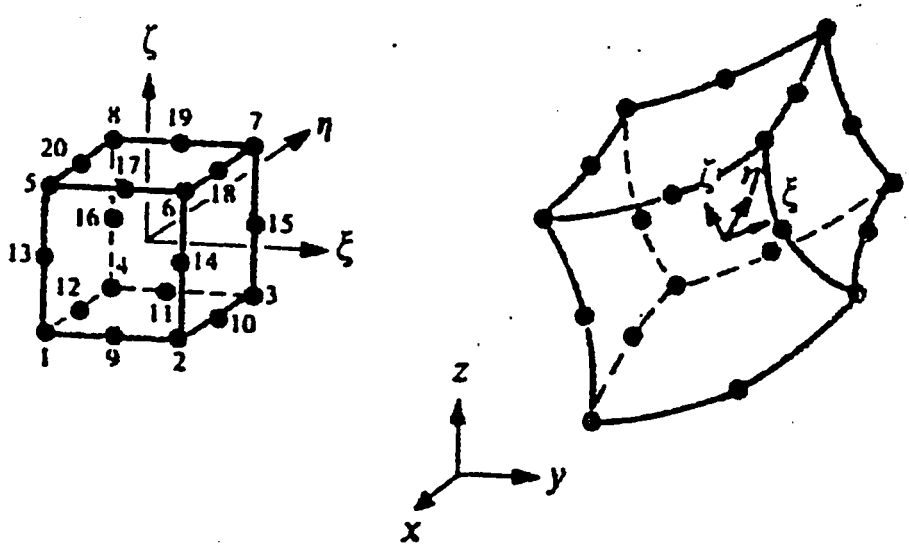

Figure 6: 20- Noded Isoparametric Element

3.2.3.2 Displacement Field

The displacement field $\{u\} = [u, v, w]$ at any point in the structure in direction x, y and z respectively, is defined by the three degrees of freedom at each nodal point corresponding to its three displacements at the node.

$$\begin{bmatrix} u \\ v \\ w \end{bmatrix} = \sum_{k=1}^{n} N_k \begin{bmatrix} u_k \\ v_k \\ w_k \end{bmatrix} \qquad (3.18)$$

The contribution to the global displacements from a given node k is

$$\begin{bmatrix} u \\ v \\ w \end{bmatrix} = \begin{bmatrix} N_k & 0 & 0 \\ 0 & N_k & 0 \\ 0 & 0 & N_k \end{bmatrix} \begin{bmatrix} u_k \\ v_k \\ w_k \end{bmatrix} \qquad (3.19)$$

or

$$\underline{u}_k = \underline{N}_k \, \underline{\delta}_k \qquad (3.20)$$

For the complete element , the displacement field is

$$\underline{u}^e = \sum_{k=1}^{n} \underline{N}_k(\xi, \eta, \zeta) \underline{\delta}_k \qquad (3.21)$$

where n is the number of nodes in the element.

3.2.4 20- Node Hexahedral Element

The shape functions for the 20-node rectangular hexahedral shown in Figure 7 , are given by Hinton and Owen {19} as follows:

for corner nodes

$$N_i^e(\xi,\eta,\zeta) = \frac{1}{8}(1+\xi_i\xi)(1+\eta_i\eta)(1+\zeta_i\zeta)(\xi_i\xi+\eta_i\eta)(\zeta_i\zeta-2),\ i=1,2,3,4,5,6,7,8$$

at mid side nodes

$$N_i^e(\xi,\eta,\zeta) = \frac{1}{4}(1-\xi^2)(1+\eta_i\eta)(1+\zeta_i\zeta),\ i=9,11,17,19$$

$$N_i^e(\xi,\eta,\zeta) = \frac{1}{4}(1-\eta^2)(1+\xi_i\xi)(1+\zeta_i\zeta),\ i=10,12,18,20 \qquad (3.22)$$

$$N_i^e(\xi,\eta,\zeta) = \frac{1}{4}(1-\zeta^2)(1+\xi_i\xi)(1+\eta_i\eta),\ i=13,14,15,16$$

it should be noted that :

1. The shape functions contain a complete polynomial of order two plus the terms $\xi^2\eta, \xi^2\zeta, \eta^2\xi, \eta^2\zeta, \zeta^2\xi, \zeta^2\eta, \xi\eta\zeta, \xi^2\eta\zeta, \eta^2\xi\zeta, \zeta^2\xi\eta$.
2. The shape functions satisfy the conditions listed above.
3. The element is C(0) continuous.

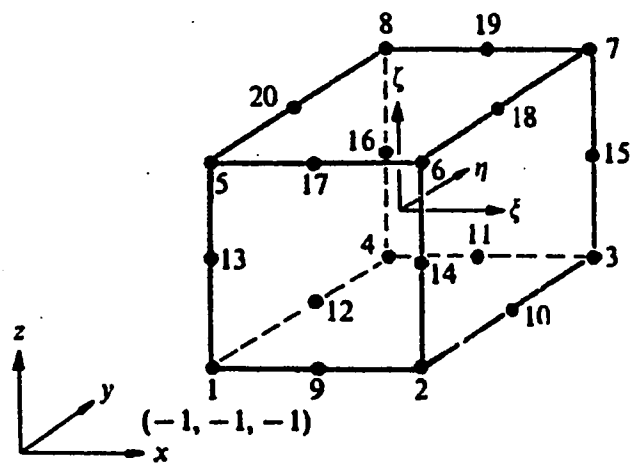

Figure 7: Arrangement of Nodes in 20-Noded Hexahedral

3.2.4.1 Strain Displacement Relationship

Using small deformation theory , the six strains are expressed as:

$$\{\varepsilon\} = \begin{bmatrix} \varepsilon_x \\ \varepsilon_y \\ \varepsilon_z \\ \gamma_{xy} \\ \gamma_{xz} \\ \gamma_{yz} \end{bmatrix} = \begin{bmatrix} \dfrac{\partial u}{\partial x} \\ \dfrac{\partial v}{\partial y} \\ \dfrac{\partial w}{\partial z} \\ \dfrac{\partial u}{\partial y} + \dfrac{\partial v}{\partial x} \\ \dfrac{\partial u}{\partial z} + \dfrac{\partial w}{\partial x} \\ \dfrac{\partial v}{\partial z} + \dfrac{\partial w}{\partial y} \end{bmatrix} \qquad (3.23)$$

Substituting equation (3.18) in equation (3.23) gives the strain-displacement relationship for an element e as follows:

$$\{\varepsilon\} = \begin{bmatrix} \varepsilon_x \\ \varepsilon_y \\ \varepsilon_z \\ \gamma_{xy} \\ \gamma_{xz} \\ \gamma_{yz} \end{bmatrix} = \begin{bmatrix} \sum_{k=1}^{n} \frac{\partial N_k}{\partial x} & 0 & 0 \\ 0 & \sum_{k=1}^{n} \frac{\partial N_k}{\partial y} & 0 \\ 0 & 0 & \sum_{k=1}^{n} \frac{\partial N_k}{\partial z} \\ \sum_{k=1}^{n} \frac{\partial N_k}{\partial y} & \sum_{k=1}^{n} \frac{\partial N_k}{\partial x} & 0 \\ \sum_{k=1}^{n} \frac{\partial N_k}{\partial z} & 0 & \sum_{k=1}^{n} \frac{\partial N_k}{\partial x} \\ 0 & \sum_{k=1}^{n} \frac{\partial N_k}{\partial z} & \sum_{k=1}^{n} \frac{\partial N_k}{\partial y} \end{bmatrix} \begin{bmatrix} u_k \\ v_k \\ w_k \end{bmatrix} \qquad (3.24)$$

Contribution from a node to the element strain matrix $|B|^r$ is

$$[B_i]^e = \begin{bmatrix} \frac{\partial N_i}{\partial x} & 0 & 0 \\ 0 & \frac{\partial N_i}{\partial y} & 0 \\ 0 & 0 & \frac{\partial N_i}{\partial z} \\ \frac{\partial N_i}{\partial y} & \frac{\partial N_i}{\partial x} & 0 \\ \frac{\partial N_i}{\partial z} & 0 & \frac{\partial N_i}{\partial x} \\ 0 & \frac{\partial N_i}{\partial z} & \frac{\partial N_i}{\partial y} \end{bmatrix} \qquad (3.25)$$

The Cartesian shape function derivatives $\frac{\partial N_i^e}{\partial \xi}$, $\frac{\partial N_i^e}{\partial \eta}$ and $\frac{\partial N_i^e}{\partial \zeta}$, in the strain matrix may be obtained by using the chain rule of partial differentiation :

$$\frac{\partial N_i^e}{\partial \xi} = \frac{\partial N_i^e}{\partial x}\frac{\partial x}{\partial \xi} + \frac{\partial N_i^e}{\partial y}\frac{\partial y}{\partial \xi} + \frac{\partial N_i^e}{\partial z}\frac{\partial z}{\partial \xi}$$

$$\frac{\partial N_i^e}{\partial \eta} = \frac{\partial N_i^e}{\partial x}\frac{\partial x}{\partial \eta} + \frac{\partial N_i^e}{\partial y}\frac{\partial y}{\partial \eta} + \frac{\partial N_i^e}{\partial z}\frac{\partial z}{\partial \eta} \qquad (3.26)$$

$$\frac{\partial N_i^e}{\partial \zeta} = \frac{\partial N_i^e}{\partial x}\frac{\partial x}{\partial \zeta} + \frac{\partial N_i^e}{\partial y}\frac{\partial y}{\partial \zeta} + \frac{\partial N_i^e}{\partial z}\frac{\partial z}{\partial \zeta}$$

In matrix form:

$$\begin{bmatrix} \dfrac{\partial N_i^e}{\partial \xi} \\ \dfrac{\partial N_i^e}{\partial \eta} \\ \dfrac{\partial N_i^e}{\partial \zeta} \end{bmatrix} = \begin{bmatrix} \dfrac{\partial x}{\partial \xi} & \dfrac{\partial y}{\partial \xi} & \dfrac{\partial z}{\partial \xi} \\ \dfrac{\partial x}{\partial \eta} & \dfrac{\partial y}{\partial \eta} & \dfrac{\partial z}{\partial \eta} \\ \dfrac{\partial x}{\partial \zeta} & \dfrac{\partial y}{\partial \zeta} & \dfrac{\partial z}{\partial \zeta} \end{bmatrix} \begin{bmatrix} \dfrac{\partial N_i^e}{\partial x} \\ \dfrac{\partial N_i^e}{\partial y} \\ \dfrac{\partial N_i^e}{\partial z} \end{bmatrix} \qquad (3.27)$$

$$\begin{bmatrix} \dfrac{\partial N_i^e}{\partial \xi} \\ \dfrac{\partial N_i^e}{\partial \eta} \\ \dfrac{\partial N_i^e}{\partial \zeta} \end{bmatrix} = [J_i^e] \begin{bmatrix} \dfrac{\partial N_i^e}{\partial x} \\ \dfrac{\partial N_i^e}{\partial y} \\ \dfrac{\partial N_i^e}{\partial z} \end{bmatrix} . \qquad (3.28)$$

where $[J^e]$ is the Jacobian matrix given by

$$[J^e] = \begin{bmatrix} \dfrac{\partial x}{\partial \xi} & \dfrac{\partial y}{\partial \xi} & \dfrac{\partial z}{\partial \xi} \\ \dfrac{\partial x}{\partial \eta} & \dfrac{\partial y}{\partial \eta} & \dfrac{\partial z}{\partial \eta} \\ \dfrac{\partial x}{\partial \zeta} & \dfrac{\partial y}{\partial \zeta} & \dfrac{\partial z}{\partial \zeta} \end{bmatrix} \qquad (3.29)$$

The cartesian derivatives $\frac{\partial N_i^e}{\partial x}$, $\frac{\partial N_i^e}{\partial y}$ and $\frac{\partial N_i^e}{\partial z}$, are now calculated as:

$$\begin{bmatrix} \frac{\partial N_i^e}{\partial x} \\ \frac{\partial N_i^e}{\partial y} \\ \frac{\partial N_i^e}{\partial z} \end{bmatrix} = [J_i^e]^{-1} \begin{bmatrix} \frac{\partial N_i^e}{\partial \xi} \\ \frac{\partial N_i^e}{\partial \eta} \\ \frac{\partial N_i^e}{\partial \zeta} \end{bmatrix} \qquad (3.30)$$

The discretized elemental volume is given in the isoparametric formulation as

$$dV = dx.dy.dz = \det J \, d\xi d\eta d\zeta \qquad (3.31)$$

A typical submatrix of $[K^e]$ linking nodes i and j may be expressed as :

$$[K^e_{ij}] = \int [B^e_i]^T [D^e] \int B^e_j] \, d\Omega^e = \iiint [B^e_i]^T [D^e] \, [B^e_j] \det J d\xi d\eta d\zeta \qquad (3.32)$$

or,

$$[K^e_{ij}] = \sum_{i=1}^{n} \sum_{j=1}^{n} \sum_{k=1}^{n} [B^e_i]^T [D^e] \, [B^e_j] \, W_i W_j W_k \det J \qquad (3.33)$$

3.2.5 CONSISTENT NODAL FORCES DUE TO DISTRIBUTED SURFACE LOADING

Consistent nodal forces due to distributed surface loading are calculated following Brebbia and Connors {3}. Consider the $\zeta = +1$ face shown in Figure 8.

The consistent nodal forces over the face are defined in terms of two-dimensional interpolation functions,

$$N_i^*(\xi,\eta) = N_i(\xi,\eta,+1), \qquad (3.34)$$

as well as the pressure intensities acting over the face.

Let t^*, be a vector, containing the pressure intensities for the $\zeta = +1$ face.

$$N_i^* = N_i^*(\xi,\eta) \qquad (3.35)$$

$$\tilde{t} = \varphi(x,y)t^* \qquad (3.36)$$

where, $\varphi(x,y)$ is the variation of loading over the surface.

The consistent nodal force matrix can now be expressed as

$$f^* = [\int_\eta\int_\xi (N_i^*)^T \varphi(x,y)dS]t^* \qquad (3.37)$$

The differential surface area dS can be expressed in terms of $d\xi$ and $d\eta$. By definition,

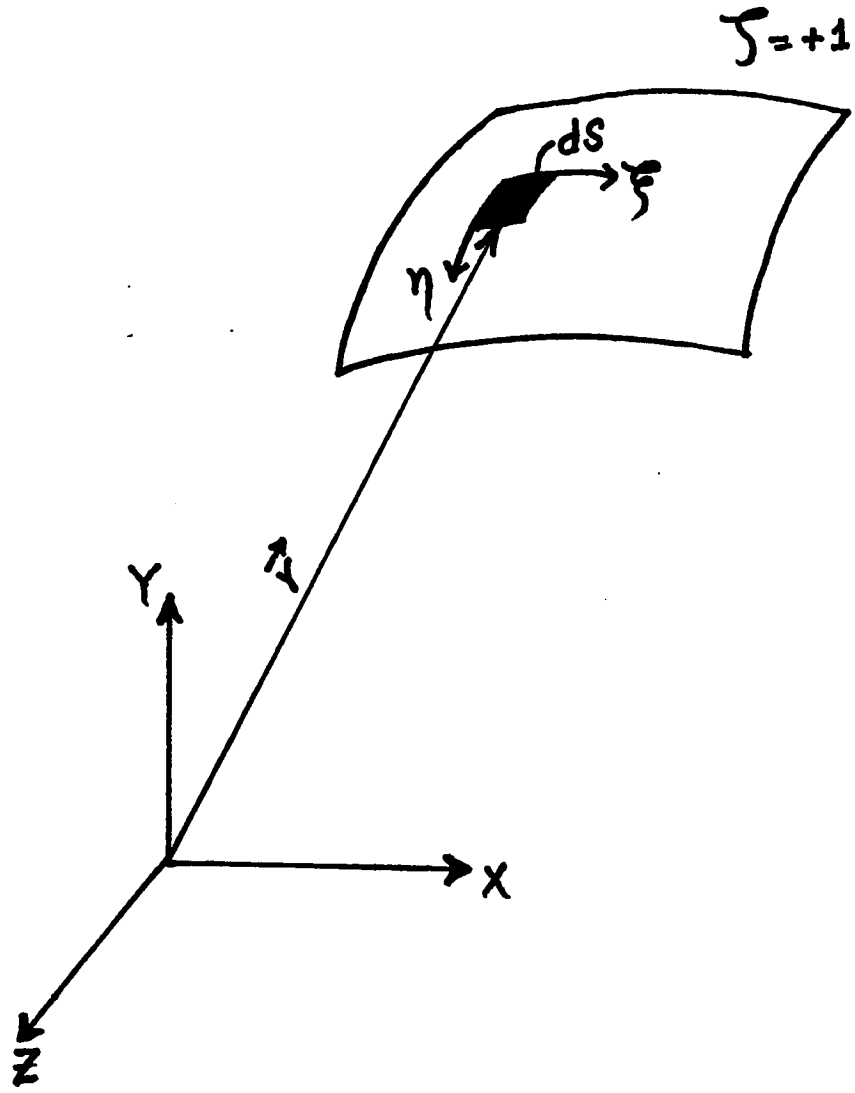

Figure 8: Surface Loaded with Distributed Loading

$$dS = d\xi d\eta \left| \frac{\partial \vec{r}}{\partial \xi} X \frac{\partial \vec{r}}{\partial \eta} \right|_{\zeta = +1} = G d\xi d\eta \qquad (3.38)$$

Expanding the vector cross product in eq.(3.38) leads to

$$G = (g_1^2 + g_2^2 + g_3^2)^{\frac{1}{2}} \qquad (3.39)$$

where,

$$g_1 = \left(\frac{\partial y}{\partial \xi}\frac{\partial z}{\partial \eta} - \frac{\partial y}{\partial \eta}\frac{\partial z}{\partial \xi}\right)_{\zeta = +1}$$

$$g_2 = \left(\frac{\partial x}{\partial \xi}\frac{\partial z}{\partial \eta} - \frac{\partial x}{\partial \eta}\frac{\partial z}{\partial \xi}\right)_{\zeta = +1} \qquad (3.40)$$

$$g_3 = \left(\frac{\partial x}{\partial \xi}\frac{\partial y}{\partial \eta} - \frac{\partial x}{\partial \eta}\frac{\partial y}{\partial \xi}\right)_{\zeta = +1} \qquad (3.41)$$

All these terms are the part of the Jacobian.

Substituting eq.(3.38) in eq.(3.37), the consistent nodal force vector can be expressed as

$$f^* = \int_\eta \int_\xi (N_i^*)^T \varphi[x(\xi,\eta,\zeta), y(\xi,\eta,\zeta)]_{\zeta = +1} G t^* d\xi d\eta \qquad (3.42)$$

Chapter IV
FINITE ELEMENT IMPLEMENTATION

4.1 INTRODUCTION

This chapter presents a detailed discussion regarding the implementation of the material model and the finite element model discussed in Chapters 2 and 3 respectively. Program 'DAMAG3D' is written in FORTRAN code in a modular form consisting of various subroutines called from the master and from within themselves. This program is written along the same format as outlined by Prof. Owen and Hinton at the University College of Swansea in their books on finite element modelling {19,20}. In the following sections , the description of the functions of the various subroutines are presented.

4.2 PROGRAM DAMAG3D PARAMETERS

(a) Type of element

- 20-node isoparametric parallelopoid

(b) Solution Algorithm

- Initial stiffness method
- Tangential stiffness calculation at each iteration
- Tangential stiffness calculation at first iteration of first increment
- Tangential stiffness calculation at second iteration

of each increment

(c) Integration scheme

- Normal integration

(d) Load cases

- Gravity Loading (Body Forces)
- Concentrated Loading
- Uniformly Distributed Loading

(e)Output of Converged / Unconverged results at different interval of increments

- Displacements Only
- Displacements and reactions
- Displacements ,reactions, stresses , strains and damage

(f) Boundary conditions can be precisely defined using three degrees of freedom per node

(g) Convergence criteria

- Residual force norm

(h) Maximum number of iterations and tolerance for convergence

(i) Material model

- Continuum damage model as proposed by Suaris (1990)

4.3 FLOW OF OPERATIONS

Figure 9 illustrates the flow of operations for the nonlinear incremental-iterative procedure schematically.

4.4 METHODOLOGY

The main features of the nonlinear incremental-iterative solution are presented as follows :

Before entering the increment loop all the arrays of stresses, strains, displacements, reactions, damage, are initialized to zero in subroutine INITAL.

At the beginning of the rth load increment , the displacements $\{d\}^{r-1}$ and the stresses $\{\sigma\}^{r-1}$ are known, as well as the unbalanced nodal forces $\{\psi\}^{r-1}$ resulting from the previous load increment. At the beginning of the next increment, the incremental nodal forces are equal to the unbalanced nodal forces and may be written as

$$\{\psi\}^{r} = \{\psi\}^{r-1} + \{df\}^{r} \qquad (4.1)$$

where $\{df\}^{r}$ is the rth load increment.

The iterative process is performed with the following steps for a generic iteration, i:

1. The stiffness matrix $[K]$ is updated or unchanged depending on the solution algorithm adopted. This algorithm is directed from the subroutine NONAL.

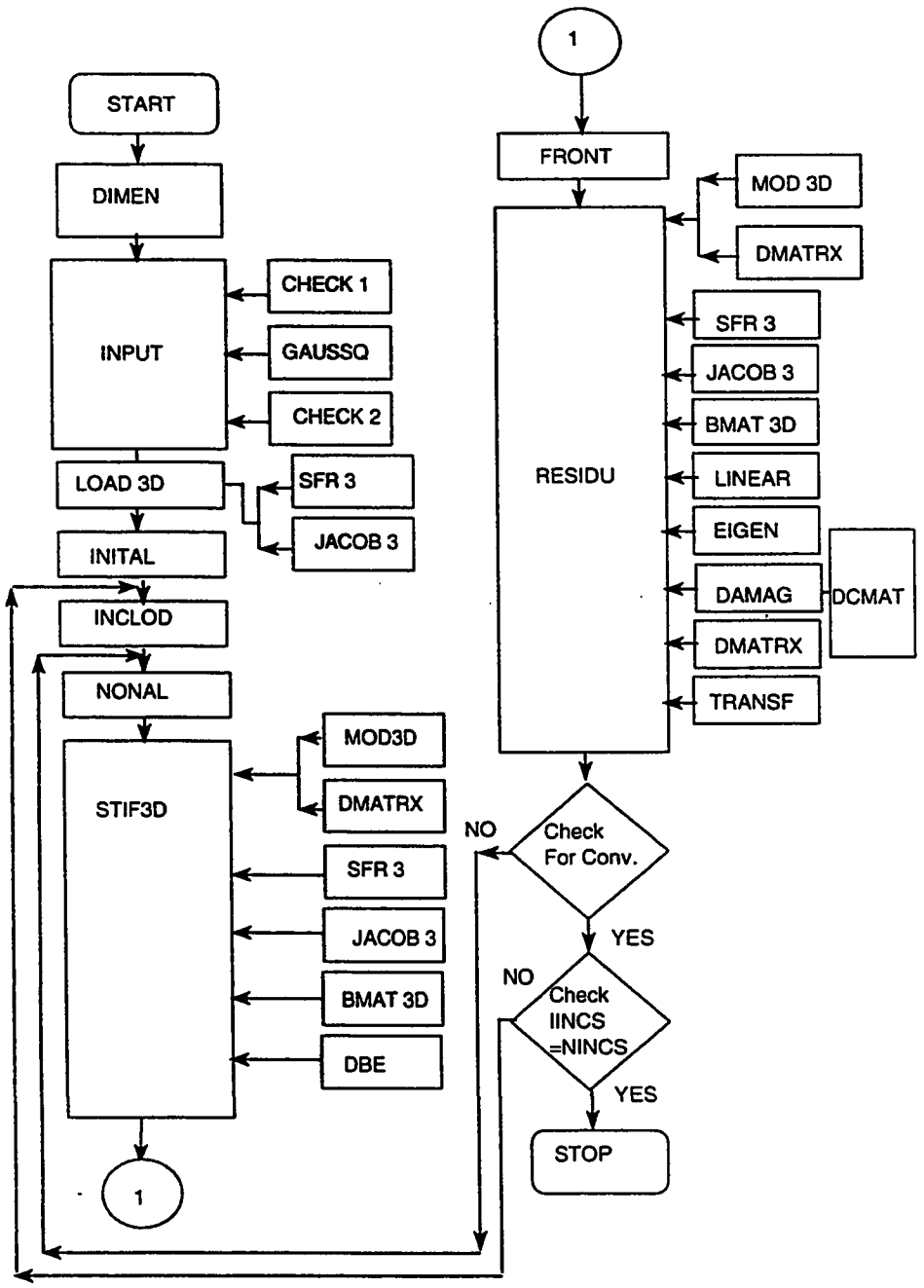

Figure 9: Flow of Operations

2. The incremental displacements $\{\Delta d\}^i$ are evaluated using the equilibrium equations

$$\{\Delta d\}^i = -[K]^{-1}\{\psi\}^{r-1} \qquad (4.2)$$

where $\{\psi\}^{r-1}$ are the nodal forces resulting from the previous iteration. The total displacement vector $\{d\}^i$ is then updated,

$$\{d\}^i = \{d\}^{i-1} + \{\Delta d\}^i \qquad (4.3)$$

3. The incremental strains $\{d\varepsilon\}^i$ and the total strains $\{\varepsilon\}^i$ are evaluated

$$\{d\varepsilon\}^i = [B]\,\{\Delta d\}^i \qquad (4.4)$$

$$\{\varepsilon\}^i = [B]\,\{d\}^i \qquad (4.5)$$

where $[B]$ is the strain matrix at a Gauss point

4. The incremental stress $\{d\sigma\}^i$ and the total stress $\{\sigma\}^i$ are calculated ,

$$\{d\sigma\}^i = [D]\,\{d\varepsilon\}^i \qquad (4.6)$$

$$\{\sigma\}^i = \{\sigma\}^{i-1} + \{d\sigma\}^i \qquad (4.7)$$

where $[D]$ is the updated constitutive matrix at each iteration.

5. The stresses are corrected according to the material constitutive equations.

4.5 DESCRIPTION OF SUBROUTINES

A detailed discussion now follows of the function of major subroutines contained in computer program DAMAG3D.

4.5.1 Dynamic Dimensioning

For any given problem the maximum dimensions are first calculated by program DIMEN and required storage is specified in the top of the program.The maximum dimensions are passed to all subroutines as arguments. This approach has the advantage that the maximum dimensions can be updated in a very simple and straightforward manner. This helps in saving a considerable amount of core space and results in the optimum use of core storage with minimal chance of errors related to dimensions.

4.5.2 Input and Output Module

The subroutine DATA first reads the various parameters defining various options, element connectivity, nodal coordinates, boundary conditions, material properties and applied loading conditions. It also reads Gauss point locations and their weights through subroutine GAUSSQ. After reading all the data it calls two diagnostic subroutines CHECK1 and CHECK2 for verification of the data already read for any possible errors before going for expensive runs.If the error is diagnosed then the rest of the data is echoed by subroutine ECHO and the program terminates.

23-7

Subroutine LOAD3D reads first the control parameters to identify the types of loading applied. Then it calculates the consistent nodal forces due to each type of the given loading.

Subroutine OUTPUT displays the output selectively depending upon the options given as control parameters in subroutine INCLOD. In INCLOD ,the load factors, values of tolerance for convergence and maximum number of iterations required for convergence for each increment are provided.

4.5.3 Stiffness and Solution Module

In subroutine STIF3D ,the $|D|$ matrix is calculated for each Gauss point depending upon the state of material as elastic or damaged, using subroutines MOD3D and DMATRX respectively.Shape functions and their derivatives are calculated using subroutine SFR3.These are used in calculating the Jacobian matrix and the Cartesian derivatives of the shape functions in subroutine JACOB3. In subroutine BMAT3D, $|B|$ is calculated. Using $|B|$ and $|D|$ matrices the element stiffness matrix $|K^e|$ is evaluated by performing numerical integration .

In FRONT , equations of equilibrium are then assembled and variables are eliminated at the same time using the frontal technique introduced by Irons{26}.In this technique, as soon as the coefficients of an equation are completely assembled from the contributions of all relevant elements ,the corresponding variable can be eliminated. A detailed description of this technique is outlined in {20}.

4.6 SUBROUTINE RESIDU

This subroutine is the most important component of the nonlinear iterative-incremental computational algorithm. During the application of an increment of load to the structure, a particular Gauss point of an element may undergo damage whilst others may remain elastic.At the end of every iteration ,stresses, strains and damage at each Gauss point are stored in different arrays. At the subsequent iteration ,all the previous information is passed to the subroutine STIF3D to update the stiffness matrix as the material degrades. Eventually in this subroutine equivalent nodal forces are evaluated corresponding to the corrected stress field. The difference of applied nodal loads and these equivalent nodal loads gives the residual forces which are reduced in successive iterations to a tolerable value to meet the desired degree of convergence which is achieved in subroutine CONVER. The corrected stress field is calculated by using the updated $|D|$ for that particular Gauss point. Since at the start of every increment the values of previous damage components are known, another iteration loop is used within the initial iteration loop to get the correct stresses according to the present damage values as illustrated in Figure 10.

23-7

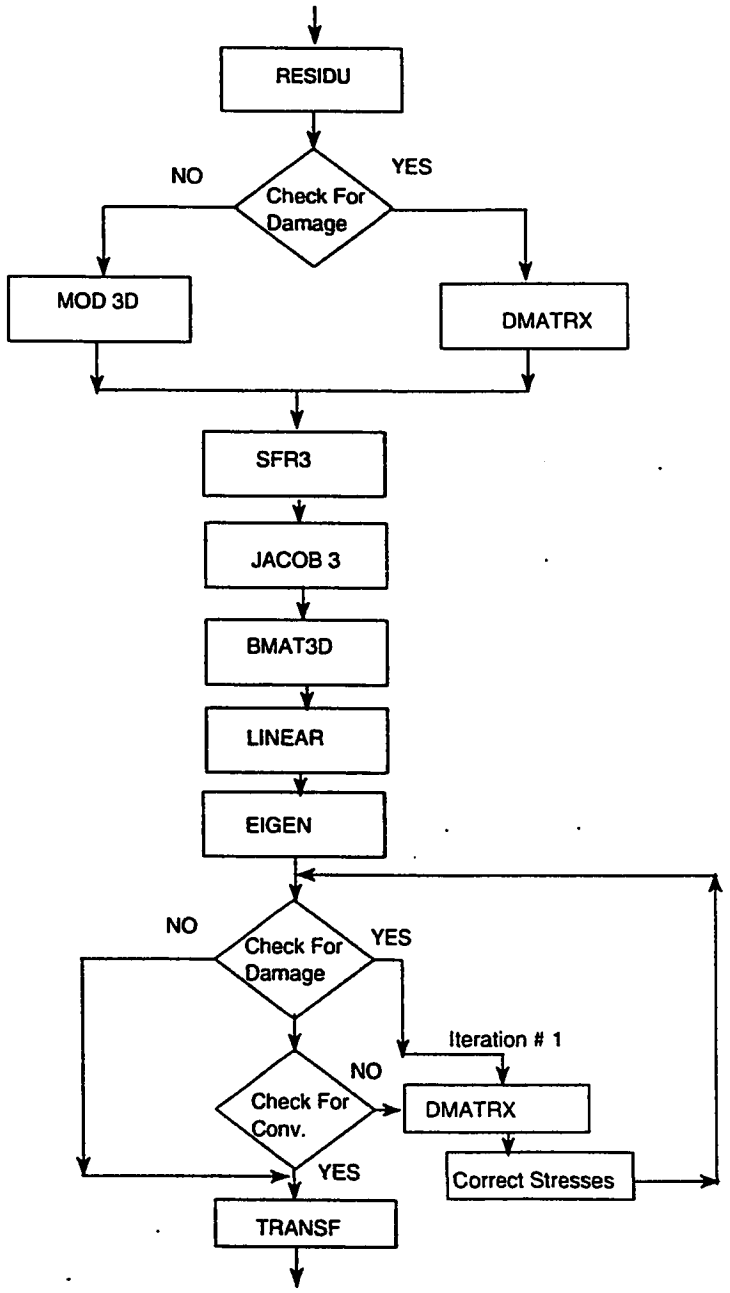

Figure 10: **Flow Chart for Iteration within each Iteration**

Chapter V
RESULTS

In order to verify the finite element model incorporating continuum damage mechanics model for prediction of response of brittle materials , results in terms of ultimate load and stress-strain curves are compared with the data as reported in the literature. Three test examples were chosen i.e. uniaxial compression test of plain concrete cylinder, plain concrete prism under strip loading and the Brazilian test. Load deflection curves and contours of damage are also plotted. Also numerical study of model parameters α and β is conducted in order to calibrate the model.

5.1 PARAMETRIC STUDY

In the continuum damage mechanics model as proposed by Suaris {69}, the two parameters α and β are chosen so as to calibrate the model, using results of the uniaxial tensile and compressive tests respectively. Suaris {69} has suggested the use of $\alpha = 4$ and $\beta = 0.1$. In the numerical parametric study following effects were considered :

1. Effect of β on uniaxial tensile test results.
2. Effect of α on uniaxial compressive test results.

23-7

5.1.1 Effect of Beta on Uniaxial Tensile Test Results

It was found by using different values of β that it has no effect on the ultimate load as predicted in the simulated uniaxial tensile test as can be seen in Figure 11. The value of α was taken as 4.

5.1.2 Effect of Alpha on Uniaxial Compressive Test Results

It was found by varying the values of α that it has nominal effect on the ultimate load as predicted in the simulated uniaxial compression test. The value of β was taken as 0.1. Effect of α on uniaxial compressive test results is shown in Figure 12.

The study of variation of these factors reveals that the use of $\alpha = 4$ and $\beta = 0.08$ will yield the same results as Suaris is reporting. Therefore, it is recommended that following values should be used, i.e.,

$\alpha = 4$ and

$\beta = 0.08$

23-7

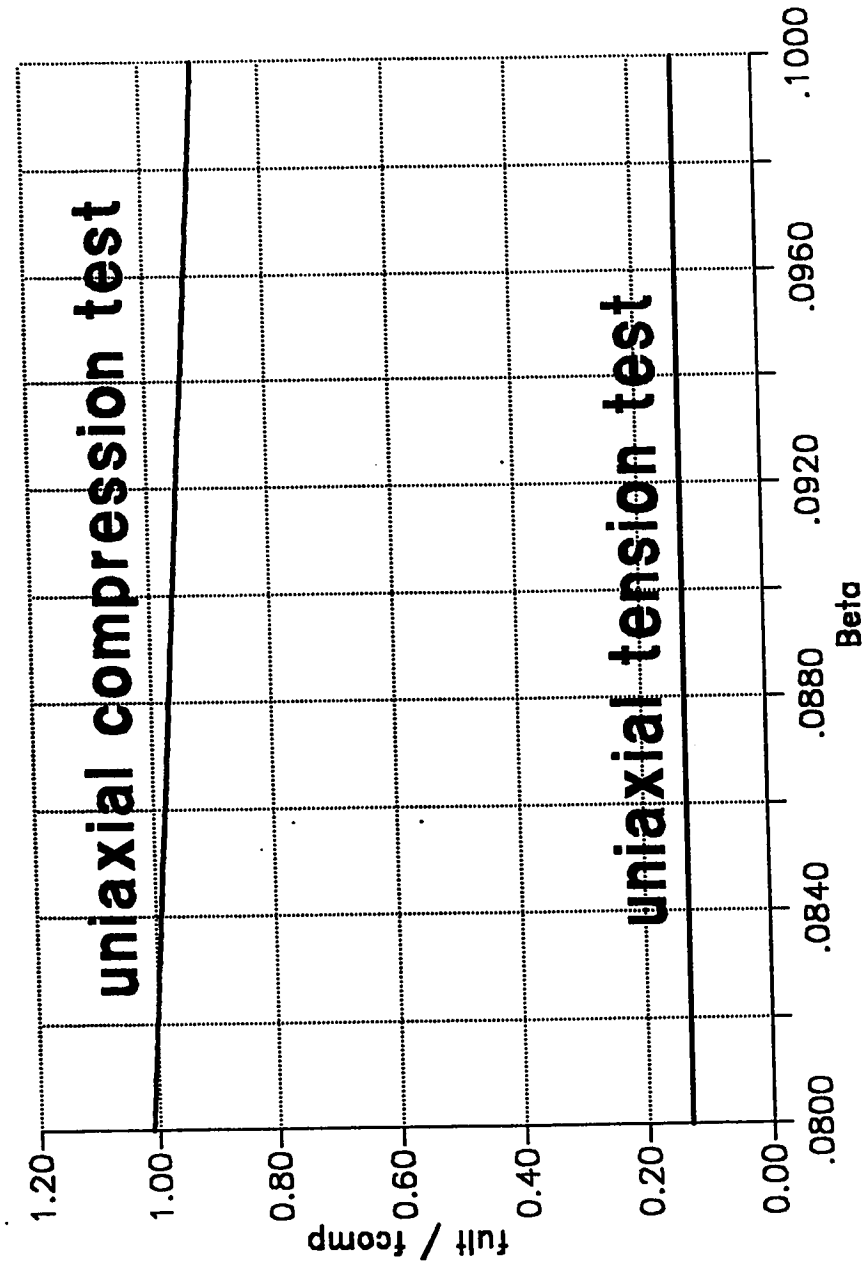

Figure 11: Effect of Beta on Uniaxial Tensile Test Results

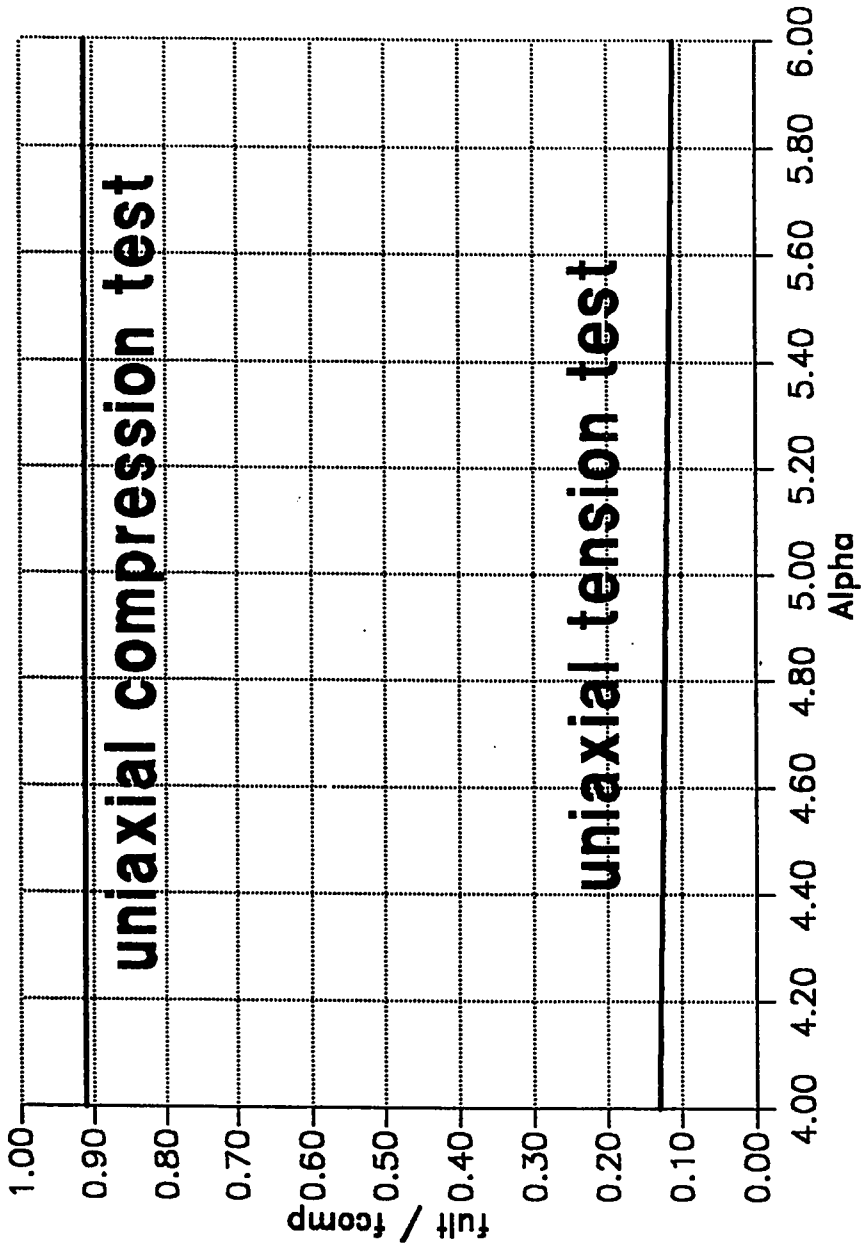

Figure 12: Effect of Alpha on Uniaxial Compressive Test Results

5.2 GEOMETRY AND MATERIAL PROPERTIES

5.2.1 Uniaxial Compression Test

For uniaxial compression test the standard cylinder is used i.e. 3 in. dia. x 6 in. height (75 mm x 150 mm). The geometry and finite element discretization of the cylinder is shown in Figure 13 .Using the triaxial symmetry, one-eighth of the cylinder discretized into eight elements,is used for analysis.

5.2.2 Plane Concrete Prism Under Strip Loading

For plain concrete prism under strip loading the prism tested by Nayogi {58} is chosen. The dimensions of the prism were 8 in. x 8 in. x 16 in.(200 mm x 200 mm x 400 mm). The geometry and finite element discretization of the prism is shown in Figure 14 .Using the triaxial symmetry,one-eighth of the prism discretized into four elements,is used for analysis.

5.2.3 Brazilian Test

For Brazilian test, cylinder with 6 in. dia. x 12 in. height (150 mm x 300 mm) is used. The geometry and finite element discretization of the cylinder is shown in Figure 15 .Using the triaxial symmetry,one-eighth of the cylinder discretized into nine elements,is used for analysis.Applied load is distributed uniformly over the width of the element. Material properties used in the numerical analysis are shown in Table 1.

23-7

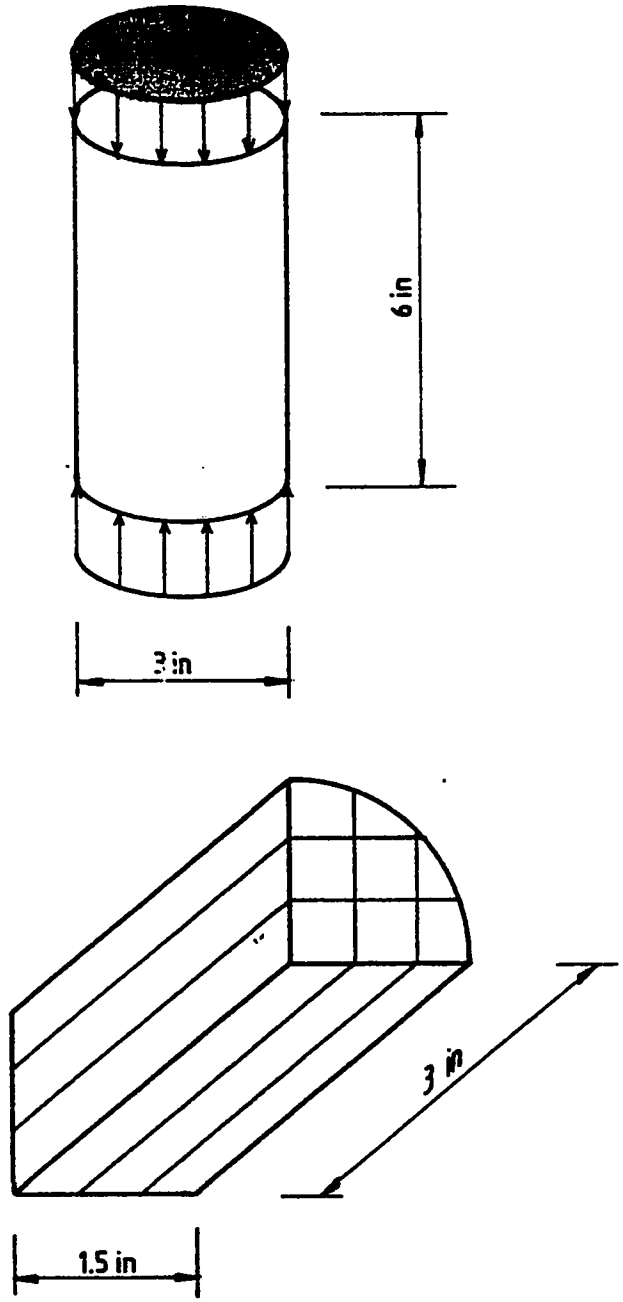

Figure 13: Finite Element Mesh of Cylinder for Uniaxial Compression Test

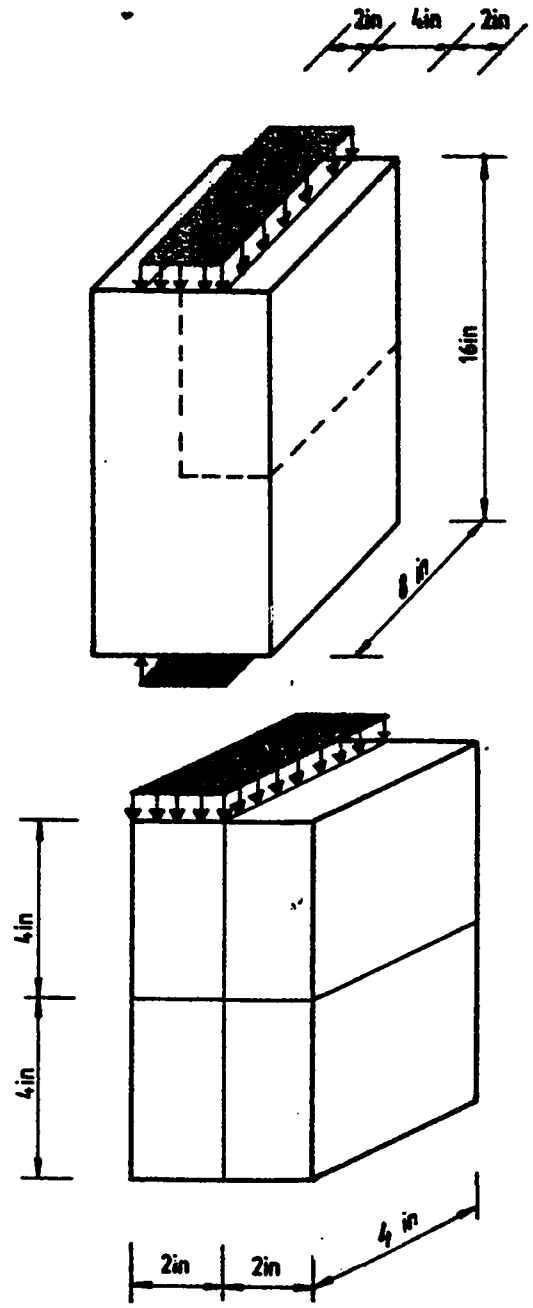

Figure 14: Finite Element Mesh of Plain Concrete Prism

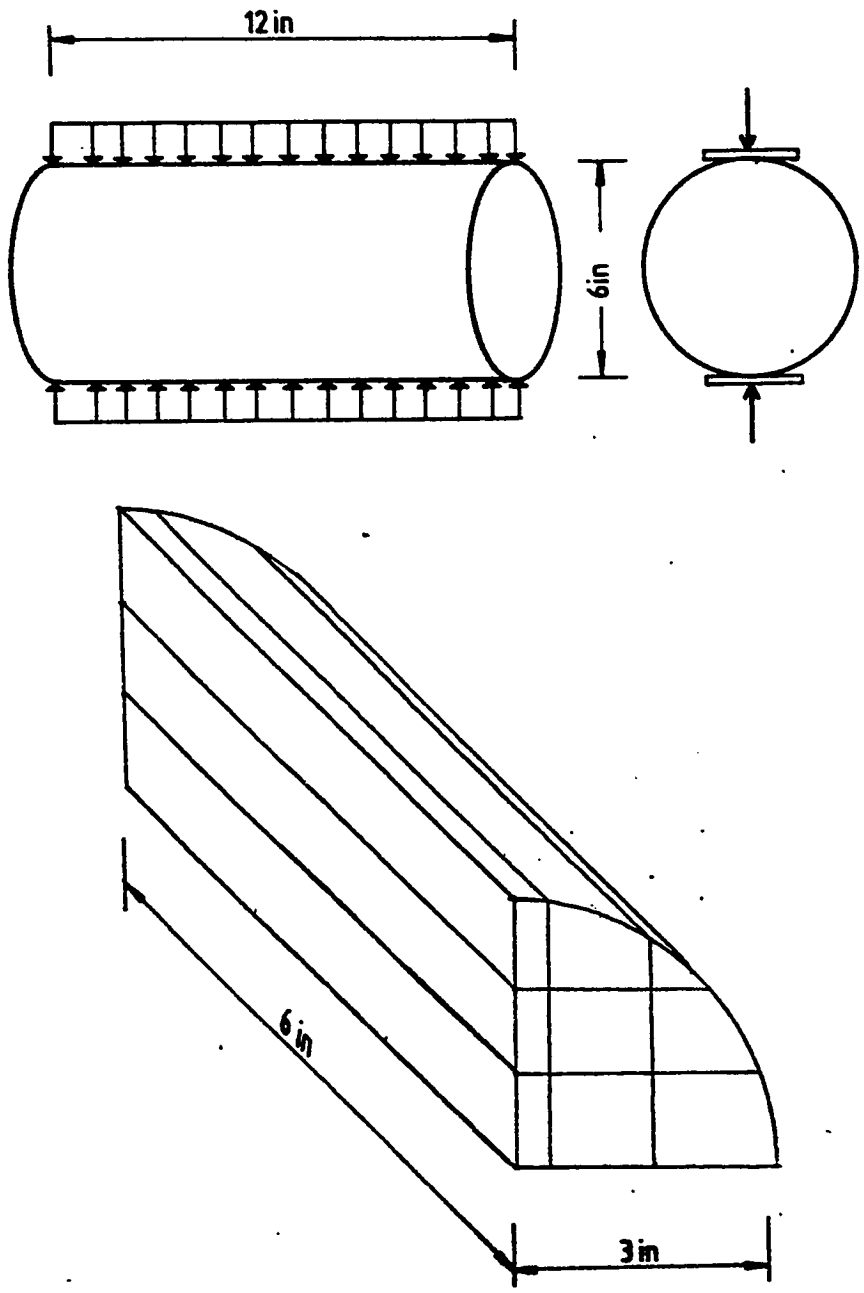

Figure 15: Finite Element Mesh of Cylinder for Brazilian Test

Table 1: Specimen Geometry and Material Properties

Specimen	Size in. (mm)	Material Properties	
		Uniaxial Comp. Strength (psi) (Mpa)	Young's Modulus (psi) (Mpa)
Cylinder	3 x 6 (75 x 150)	5,600(38.61)	4.7*1E6(32,406)
Prism1	8 x 8 x 16 (200x200x400)	3,900(26.89)	3.56*1E6(24,546)
Cylinder	6 x 12 (150 x 300)	4,650(32.06)	4.7*1E6(32,406)
Prism2	8 x 8 x 16 (200x200x400)	5,600(38.61)	4.7*1E6(32,406)

Initial stiffness matrix was used.Maximum number of iterations allowed for convergence was 20 with a convergence tolerance of one percent force residual norm.

5.3 RESULTS

The predicted results and the results available in the literature are compared in Table 2. and shown in Figs. 16 to 26. Results shows that uniaxial compression test is one dimensional problem since the major component of stress is the stress which is in the direction of the loading.In Brazilian Test,the stress component in the direction of the length is not zero and it varies with the depth.At the points near the centre it is negligible, but directly under the load it is almost twenty five percent of the vertical stress and there is no significant change

over the length. Therefore,it is not a simple two dimensional problem and a triaxial state of stress exists directly under the load.Similarly, the case of PC prism under strip loading reflects the three dimensionality of the problem.

5.3.1 Failure Loads

Table 2 shows that in most of the cases there is reasonably good agreement between the predicted failure loads and those available in the literature for the various cases considered. For the case of prism1 under strip loading the result is away from the available result. This difference is due to the limitations of the model used herein. In the equation of the bounding surface the critical strain energy release rate, R_c, fixed as 0.63 is good only for concretes which have strengths equal or close to the strength Suaris has used. This is verified by running the case of PC prism under strip loading with $f_c' =$ 5600 psi.The predicted failure load compares well with the experiment.

23-7

Table 2: Comparison of Failure Loads

Specimen	Failure Loads (lbs / KN)		
	Experiment	Alternative model	FEM(damage)
Cylinder	39,584(176) (Suaris)	39,584(176) (Suaris)	37,605(167)
Prism1 (Strip loading)	80,754(359) (Niyogi)	88,150(392) (Gonzalez)	124,800(555)
Cylinder	-	40,800(181) (Resende)	53,010(235)
Prism2 (Fully loaded)	358,400(1594)	-	369,184(1610)
Prism2 (Strip loading)	115,954(516) (Niyogi)	126,574(563) (Gonzalez)	125,440(557)

5.3.2 Stress-Strain Curves

Stress-strain curves were available for uniaxial compression test{69}. Stress-strain curves are presented in Figs. 16 to 19. The predicted stress-strain curves shows no strain softening part while the available curve do show the strain softening part, this may be due to the fact that the present analysis had been carried out by simulating stress controlled conditions.

Since,the damage model by Suaris does not takes into account the plastic strains,in order to include the effect of plastic strains,it has been suggested by him to modify the strains due to damage by a factor γ, whose value ranges from 1.0 to 1.5,i.e., $\varepsilon^p = \gamma\varepsilon^d$. Using his sug-

gestions,modified stress-strain curve is plotted for uniaxial compression test as shown in Fig. 17. In Fig. 17 the modified stress-strain curve for the uniaxial compression test is compared with the available experimental stress-strain curve in Fig. 17.

123-7

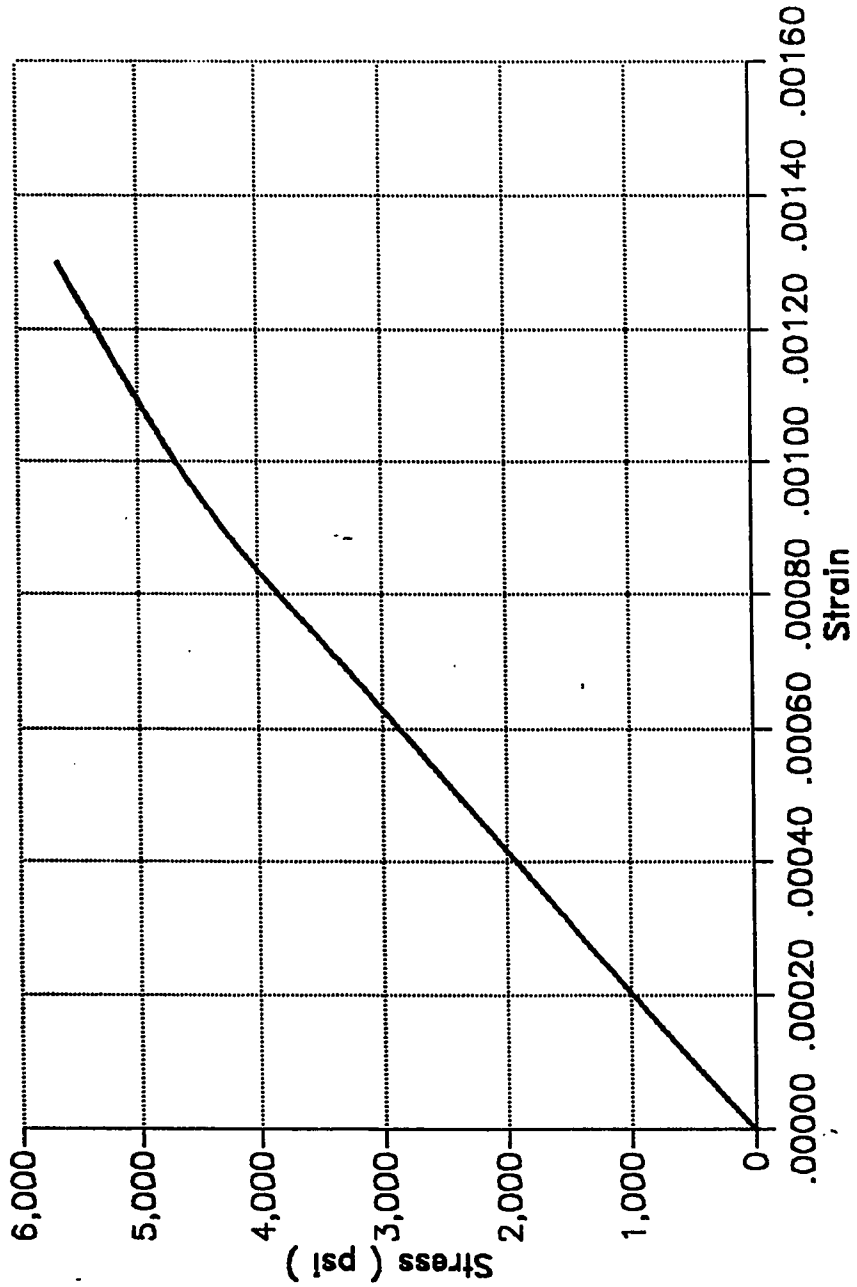

Figure 16: Stress-Strain Curve for Uniaxial Compression Test.

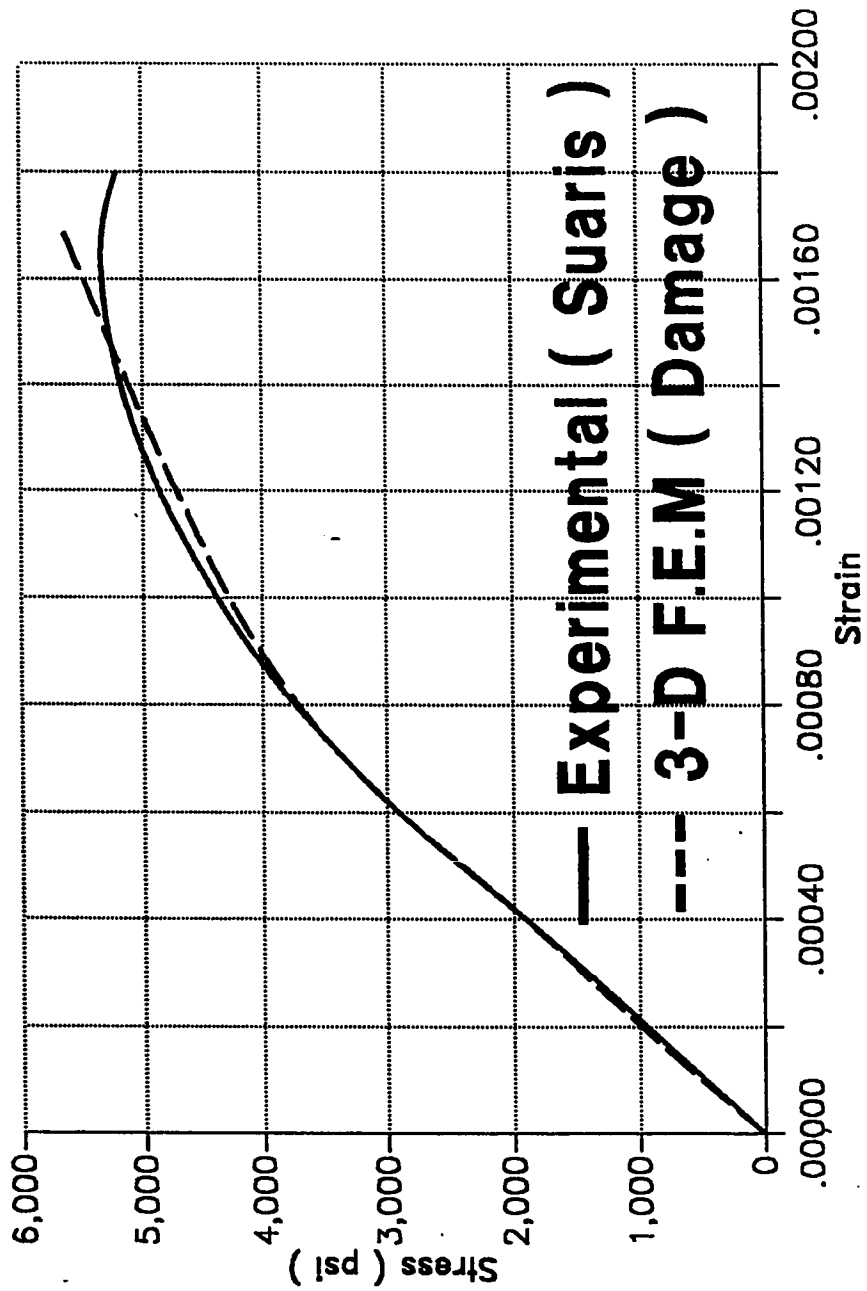

Figure 17: Modified Stress-Strain Curve for Uniaxial Compression Test.

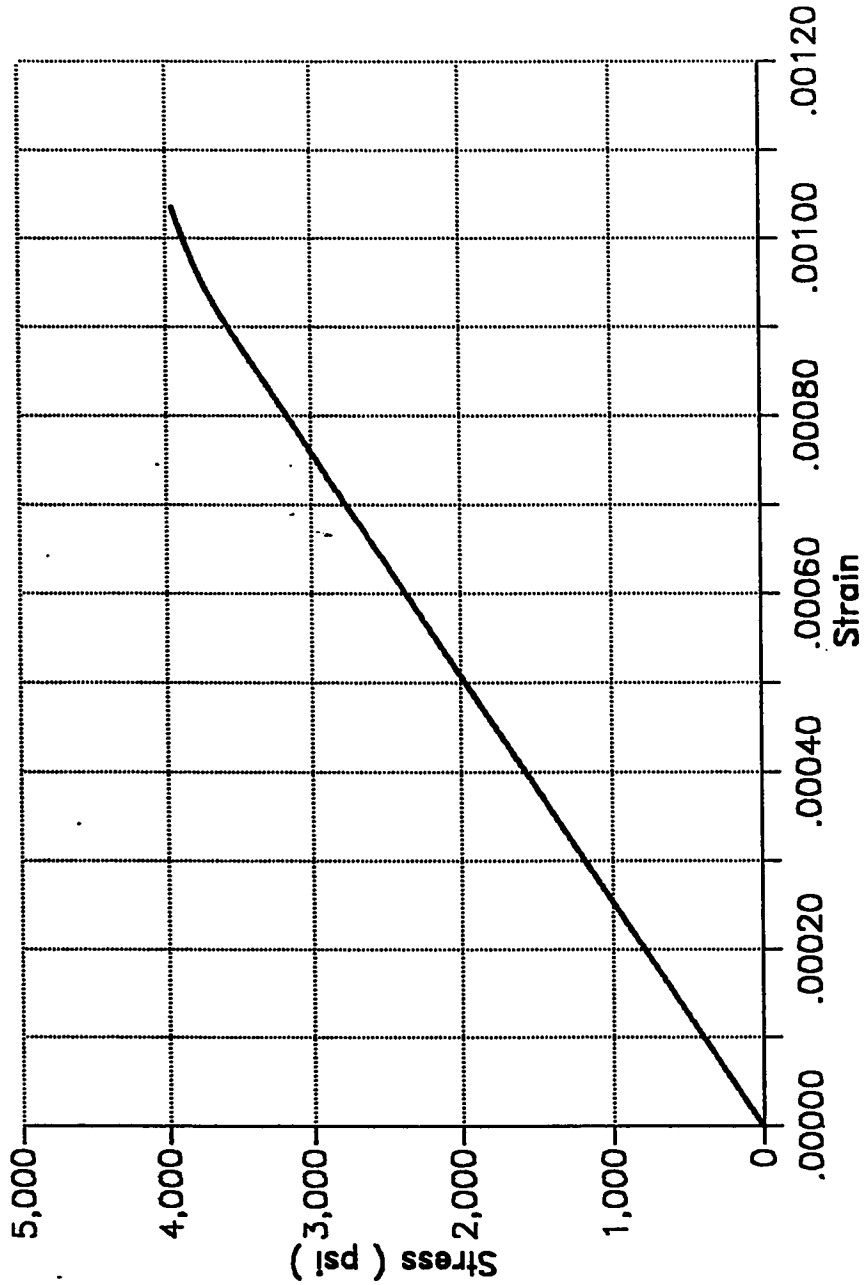

Figure 18: Stress-Strain Curve for PC Prism under Strip Loading.

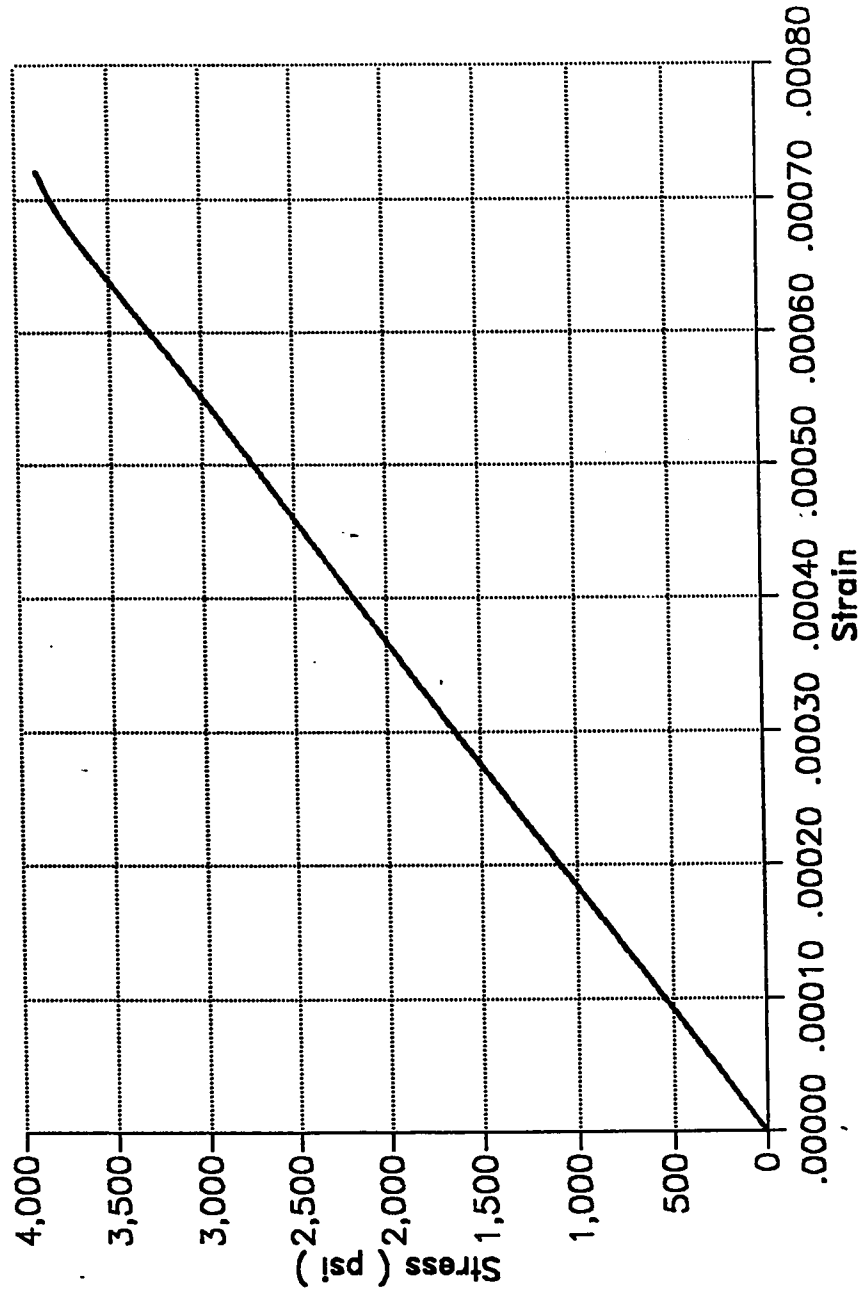

Figure 19: Stress-Strain Curve for Brazilian Test.

5.3.3 Contours of Damage Distribution

Contours of damage distribution over the faces were plotted for PC prism under strip loading ,Brazilian test and PC prism under patch load as shown in Figs. 20 to 26. For uniaxial compression test they are uniform over the cross-section and throughout the depth,therefore instead of plotting them,the percentage of maximum damage at different load levels is plotted in Fig. 20 and presented in Table 3.

Table 3: % of Maximum Damage at Different Stages

% of Applied Load	% of Maximum Uniform Damage
20	0.0
40	0.0
60	5.0
80	28.0
100	94.0

For PC prism these contours are plotted at the failure loads for two different cases i.e., prism under strip loading and prism under patch loading. Distribution of damage varies as the loading varies. For prism under strip loading, it is maximum at the centre of the loaded strip and decreases as it reaches the end of the loaded strip.For prism under patch loading, it is maximum at the centre and decreases as it reaches the end of the load.

For the Brazilian test, Resende(1987) has drawn such contours.When compared with those contours,it was found that the effected zone by

damage is the same,but the maximum damage for his case is not directly under the load,whereas,it is under the applied load for our case.The distribution of damage is found to be uniform throughout the length except at the edges,where it is extended a bit more.

In Fig.25 damage surface for Brazilian test is presented which represents the percentage of damage over the cross-section.It is clear from the figure that the maximum damage is directly under the load and it decreases as we go down.Fig.26 represents the damage surface for the same test over the length i.e., in the third direction.The damage is again maximum under the load and at the edges,elsewhere it is almost uniform througout the length and decreases with the depth.

23-7

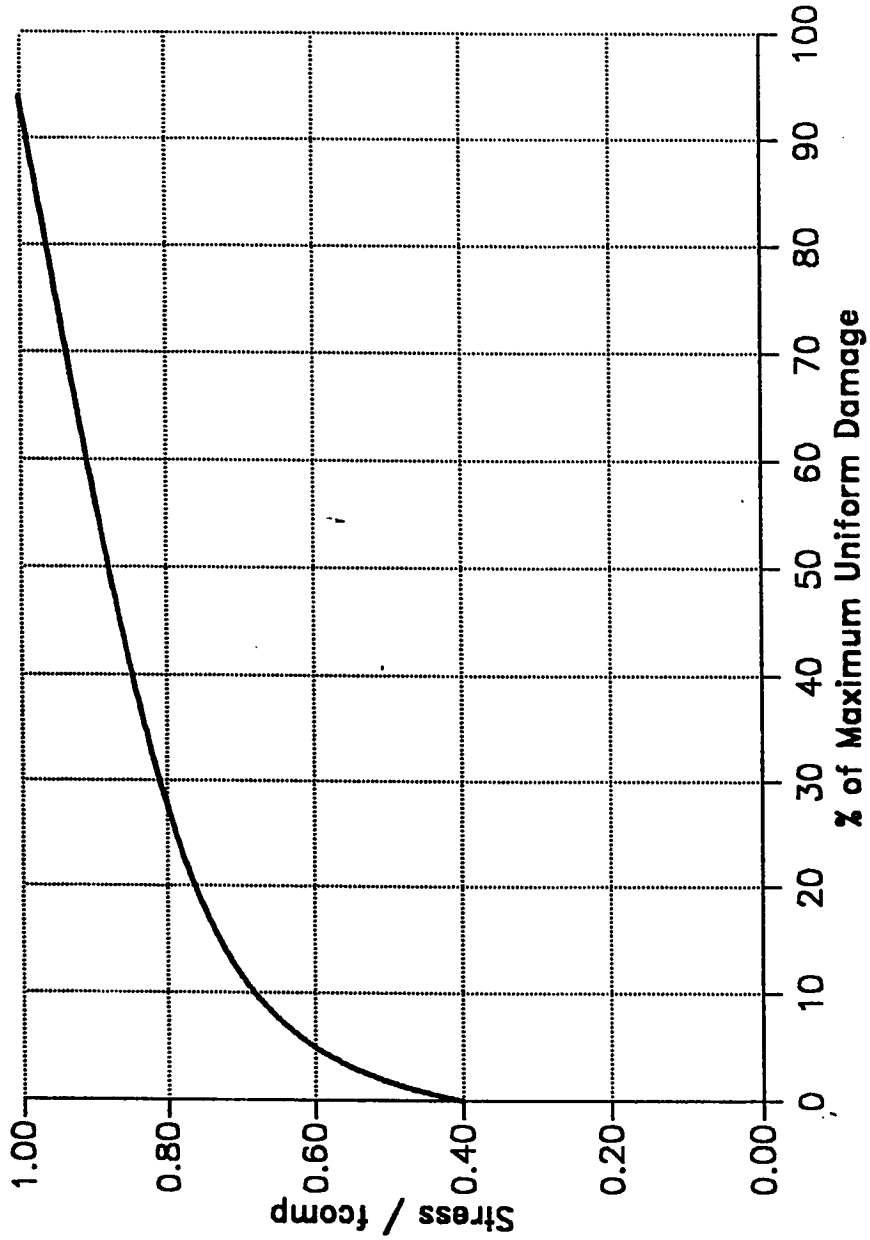

Figure 20: % of Maximum Damage at Different Load Levels.

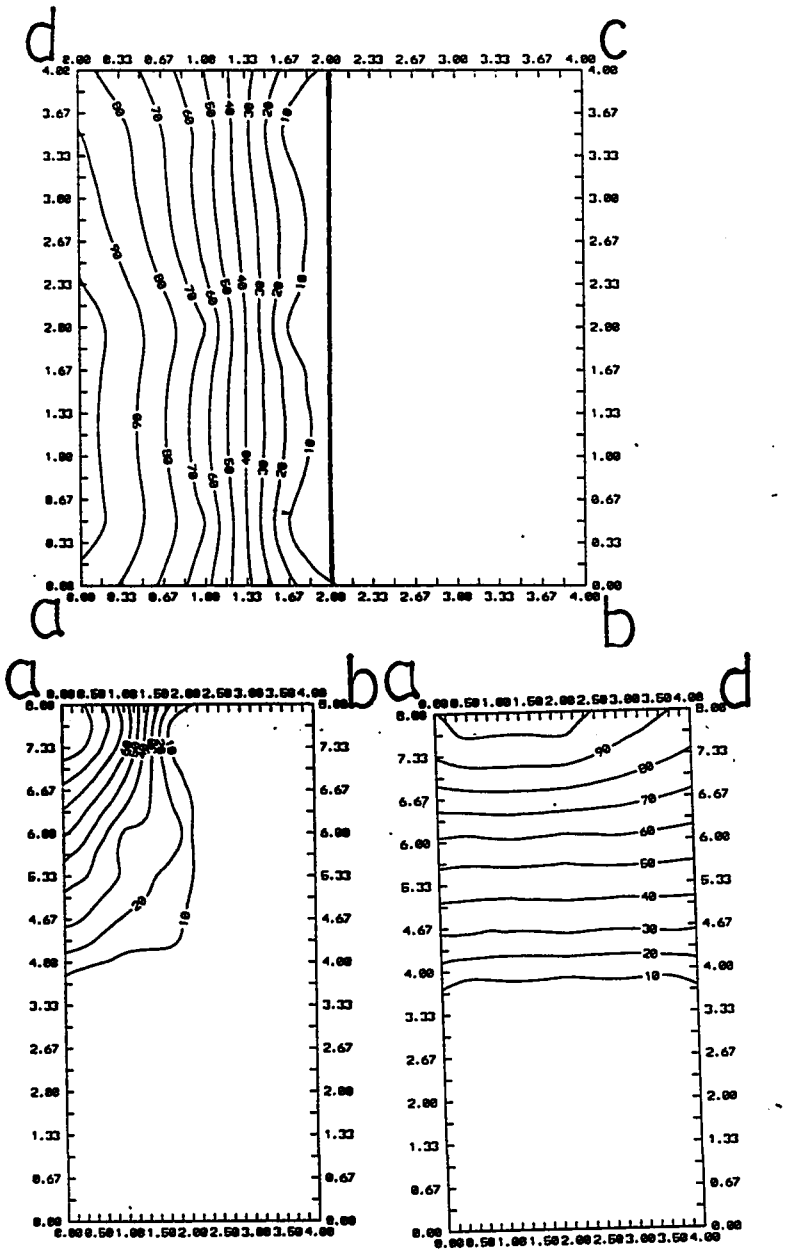

Figure 21: Distribution of Damage for PC Prism under Strip Loading.

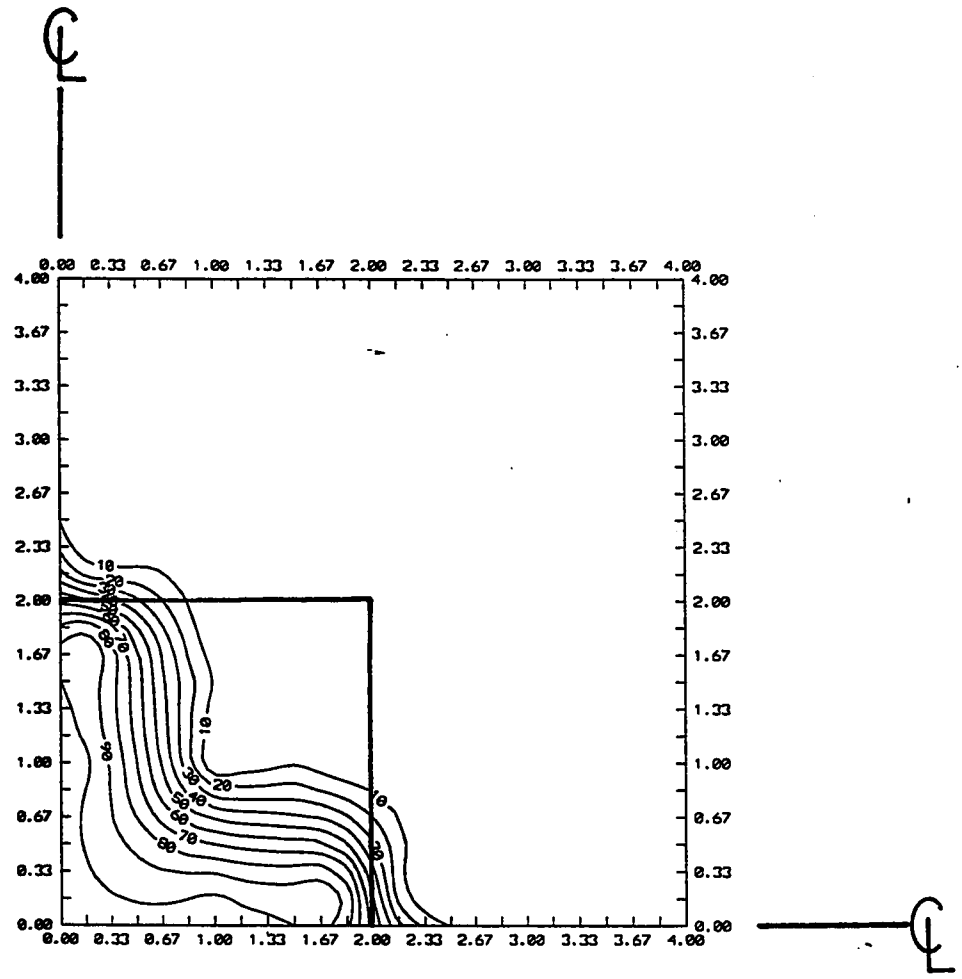

Figure 22: Distribution of Damage for PC Prism under Patch Load.

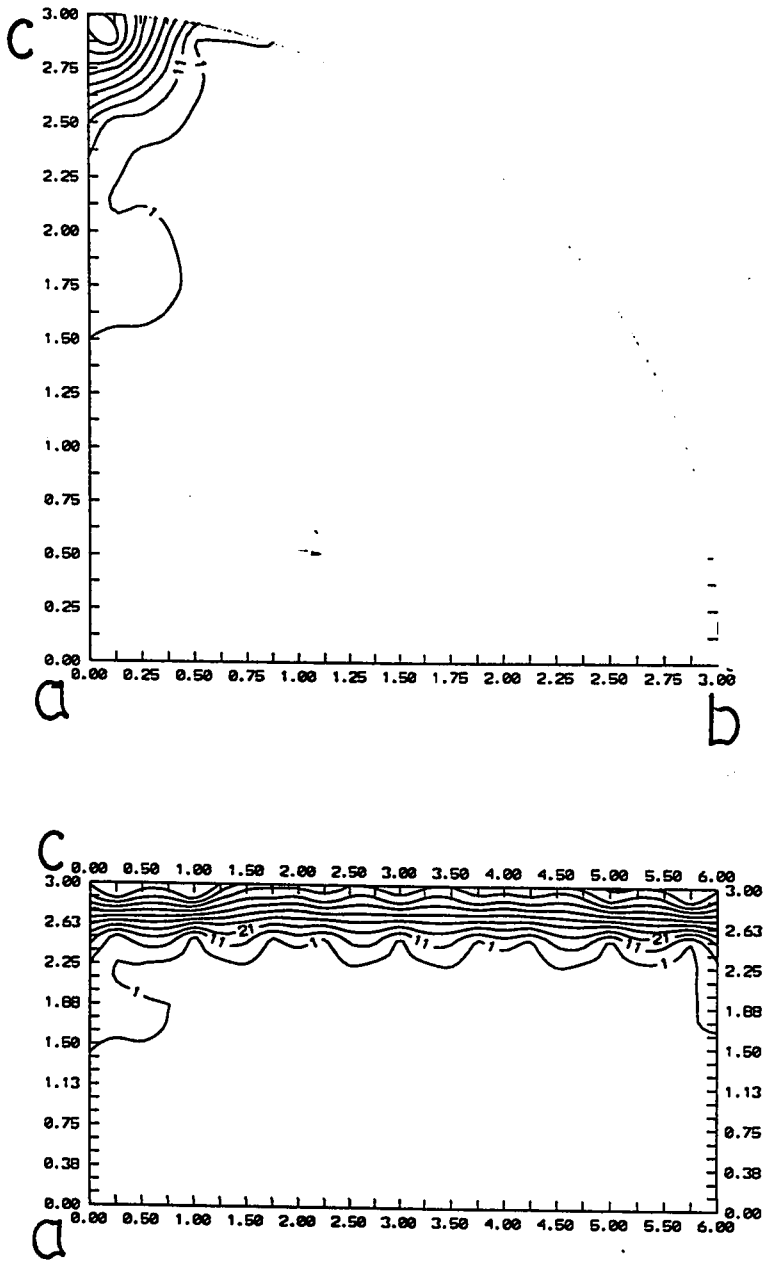

Figure 23: Damage Distribution for Brazilian Test.

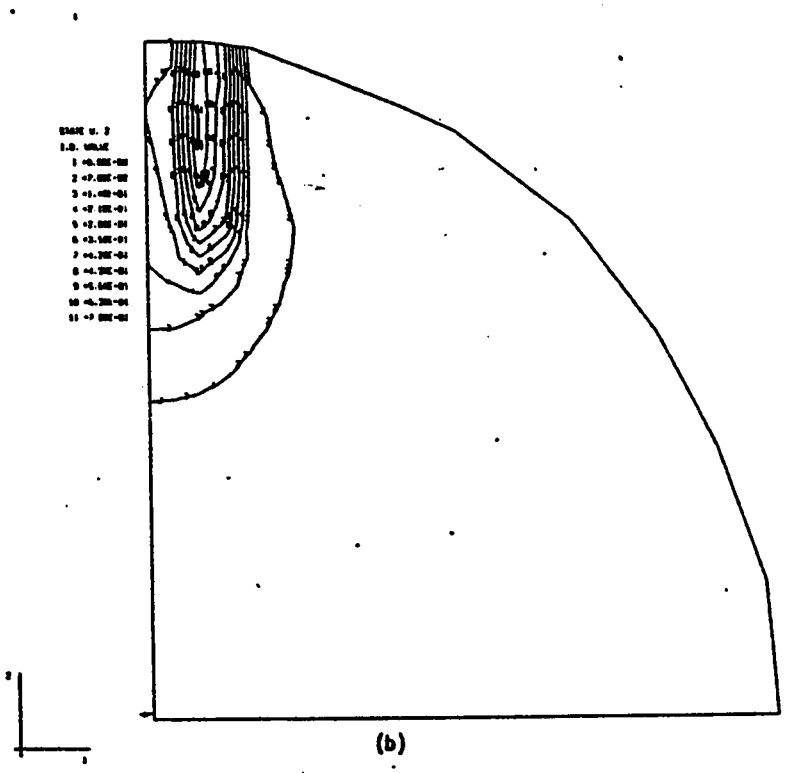

Figure 24: Damage Distribution for Brazilian Test (Resende)

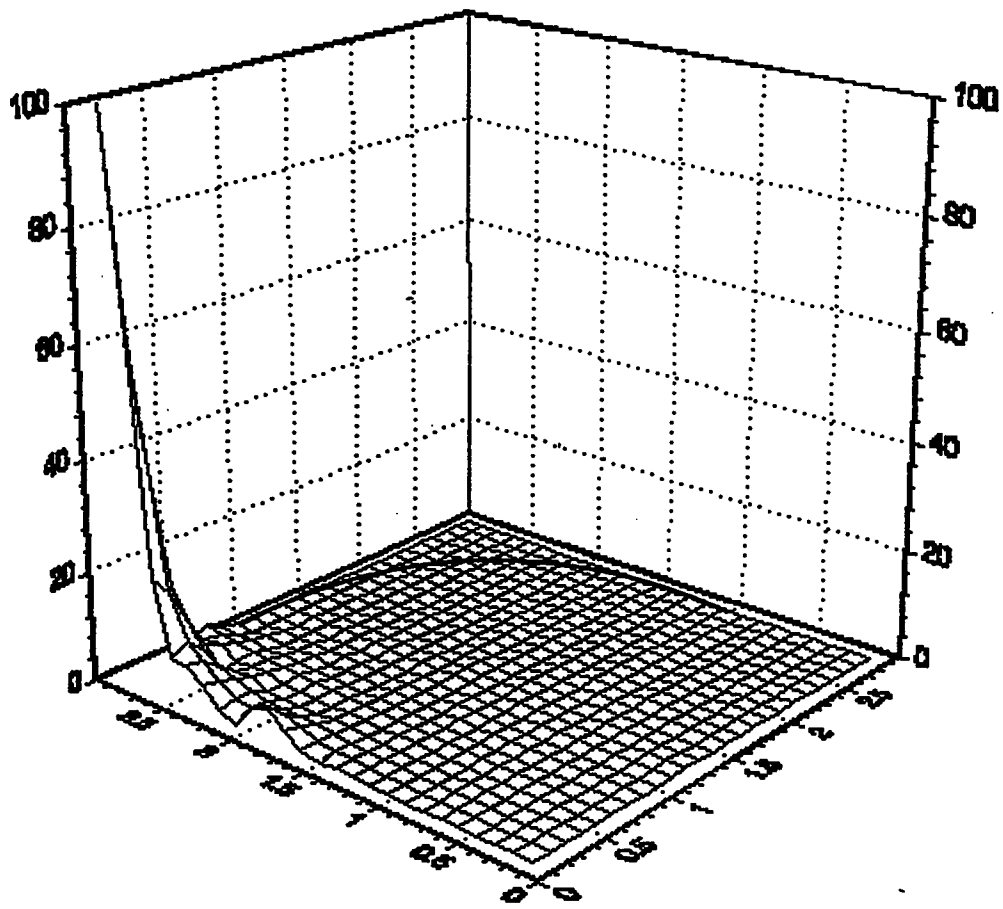

Figure 25: Damage Surface for Brazilian Test

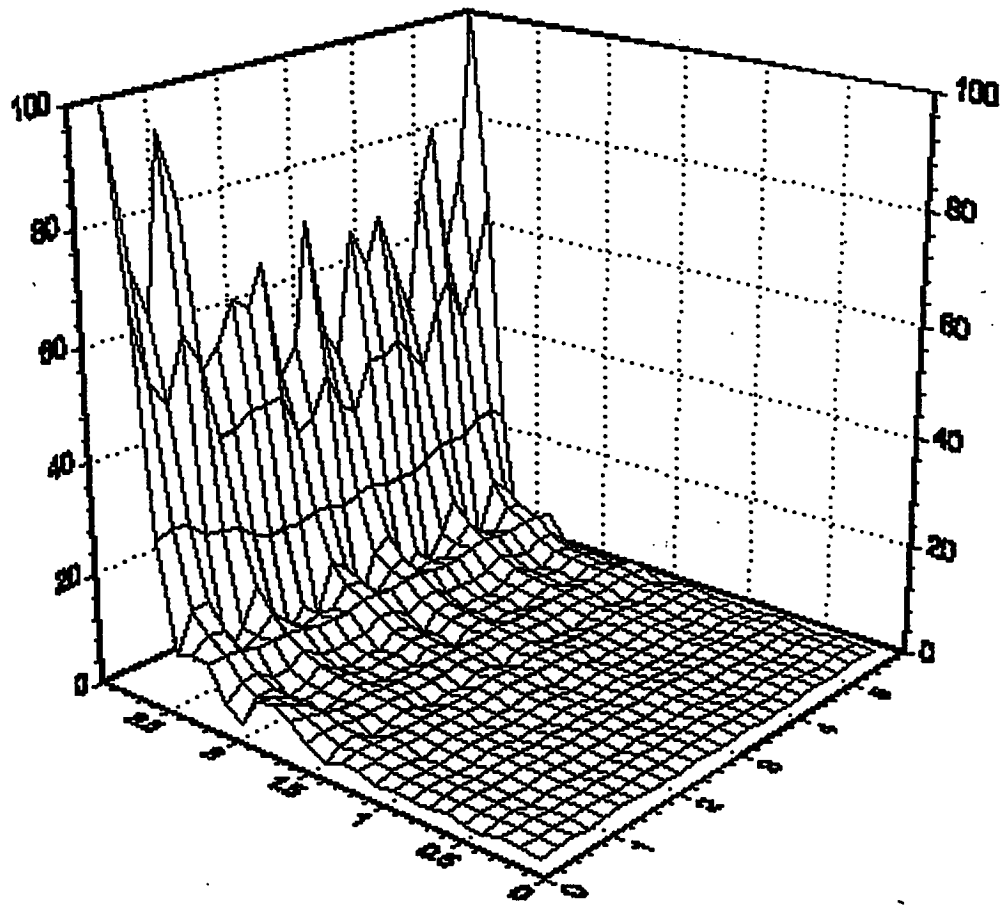

Figure 26: Damage Surface for Brazilian Test over the Length.

Chapter VI
CONCLUSIONS

6.1 CONCLUSIONS

The main conclusions drawn from the following work are as follows:

1. Within the framework of continuum damage mechanics theory, several features of brittle materials can be captured effectively, which cannot be captured within the framework of plasticity or fracture mechanics.

2. Continuum damage mechanics model incorporated in three dimensional finite element code simulates the response of uniaxially loaded brittle materials reasonably accurately, since the model has been calibrated using uniaxial tension and compression tests.Therefore, to be used effectively in three dimensional analysis it should be calibrated accordingly.

3. R_c, critical strain energy release rate and D, are two material parameters which depends on the uniaxial compressive strength of the material. An explicit relationship between these parameters and uniaxial compressive strength needs to be determined experimentally.

4. The model,when incorporated in three dimensional finite element code fails to capture the strain softening part.This may be due

23-7

to the fact that in the present study stress controlled conditions were simulated.

5. Three dimensional analysis reflects the true response of the material, and with the availability of high speed digital computers, efficient solution algorithms and sophisticated models it should be used instead of idealizing the situations.

6.2 RECOMMENDATIONS

The present work can be further extended/modified to address the following problems of practical significance:

1. Incorporation of more refined and sophisticated continuum damage model/models.
2. Modification of the code to handle ductile materials such as reinforcement in RC-members so that it can be used to analyse reinforced concrete members.
3. Modification of the code to handle cyclic loading, which will help in predicting the fatigue failure of the structures.
4. Study of the size effect.
5. Study of the relationship between R_c and D with the uniaxial compressive strength.

Appendix A
INSTRUCTIONS FOR PREPARING DATA FOR PROGRAM DAMAG3D

CARD SET 1 - Title card - one card

Title of the problem CARD SET 2 - Control Data Card - two cards

First Card - Title Card

Second card

NPOIN -Total number of nodal points

NELEM -Total number of elements

NVFIX -Total number of points where one or more degrees of freedom are prescribed

NNODE -Number of nodes per element

NMATS -Total number of different materials

NGAUS -Number of Gauss points

NSTRE -Number of stresses

NALGO -Nonlinear solution algorithm to be used

= 1 - Initial stiffness method

= 2 - Tangential stiffness method

= 3 - Stiffness matrix is recalculated in the first iteration of each increment

= 4 - Stiffness matrix is recalculated in the second

iteration of each increment

NINCS -Total number of load increments

CARD SET 3 - Element Cards-two title cards and one card for each element

NUMEL -ELement number

MATNO(NUMEL) -Material number of each element

LNODS(NUMEL) -Node numbers of each element (1 - 20)

CARD SET 4 - Nodal coordinates card - one title card - one card for each node whose coordinates must be input

IPOIN -Node number

COORD(IPOIN,1) - X- coordinate

COORD(IPOIN,2) - Y- coordinate

COORD(IPOIN,3) - Z- coordinate

CARD SET 5 - Restrained node Cards - two title cards - one card for each restrained node

NOFIX(IVFIX) -Restrained node number

IFPRE -Condition of the degree of freedom :

0 - Free

1 - Restrained

u - displacement (x-dir)

v - displacement (y-dir)

w - displacement (z-dir)

CARD SET 6 - Material Cards - two title cards - one card for each material

NUMAT -Material identification number

PROPS(NUMAT,1) Young's Modulus

PROPS(NUMAT,2) Poisson's ratio

PROPS(NUMAT,3) Ultimate compressive strength

PROPS(NUMAT,4) ALpha (factor controlling tensile strength)

PROPS(NUMAT,5) Beta (factor controlling compressive strength)

PROPS(NUMAT,6) G (shear modulus)

CARD SET 7 - Applied Loading Cards - two title cards -

one card for identification of loading condition

one card for number of loaded nodes or surfaces

one card for each loaded node or surface and the applied node or surface

CARD SET 8 - Load increment control cards - NINCS cards

FACTO -Applied load factor for the current increment

TOLER -Convergence tolerance factor

MITER -Maximum number of iterations allowed

NOUTP(1) -Controls output parameter of the unconverged results after the first iteration

= 1 for displacements only

= 2 for displacements and reactions

= 3 for displacements, reactions, stresses, strains and damage

NOUTP(2) -Controls output parameter of the converged results after the first iteration

= 1 for displacements only

= 2 for displacements and reactions

= 3 for displacements, reactions, stresses, strains and damage

123-7

Appendix B

SAMPLE INPUT DATA AND OUPUT FILES FOR PROGRAM DAMAG3D

DATA FILE

```
PC PRISM UNDER STRIP LOADING
NPOIN NELEM NVFIX NNODE NMATS NGAUS NSTRE NALGO NINCS
 51     4    35    20     1     3     6     1     1
ELEMENT CONNECTIVITY DATA
ELEMENT MAT          NODE NUMBERS
1         1  1 9 39 31 3 11 41 33 6 25 36 22 2 10 40 32 7 26 37 23
2         1  3 11 41 33 5 13 43 35 7 26 37 23 4 12 42 34 8 27 38 24
3         1  9 17 47 39 11 19 49 41 14 28 44 25 10 18 48 40 15 29 45 26
4         1  11 19 49 41 13 21 51 43 15 29 45 26 12 20 50 42 16 30 46 27
NODAL COORDINATES
NODE   X       Y       Z
1    0.0     0.0     0.0
2    0.0     0.0     2.0
3    0.0     0.0     4.0
4    0.0     0.0     6.0
5    0.0     0.0     8.0
6    1.0     0.0     0.0
7    1.0     0.0     4.0
8    1.0     0.0     8.0
9    2.0     0.0     0.0
10   2.0     0.0     2.0
11   2.0     0.0     4.0
12   2.0     0.0     6.0
13   2.0     0.0     8.0
14   3.0     0.0     0.0
15   3.0     0.0     4.0
16   3.0     0.0     8.0
17   4.0     0.0     0.0
18   4.0     0.0     2.0
19   4.0     0.0     4.0
20   4.0     0.0     6.0
21   4.0     0.0     8.0
22   0.0     2.0     0.0
23   0.0     2.0     4.0
24   0.0     2.0     8.0
25   2.0     2.0     0.0
26   2.0     2.0     4.0
27   2.0     2.0     8.0
28   4.0     2.0     0.0
29   4.0     2.0     4.0
30   4.0     2.0     8.0
31   0.0     4.0     0.0
32   0.0     4.0     2.0
33   0.0     4.0     4.0
34   0.0     4.0     6.0
35   0.0     4.0     8.0
36   1.0     4.0     0.0
37   1.0     4.0     4.0
38   1.0     4.0     8.0
39   2.0     4.0     0.0
40   2.0     4.0     2.0
41   2.0     4.0     4.0
42   2.0     4.0     6.0
43   2.0     4.0     8.0
44   3.0     4.0     0.0
```

```
45   3.0    4.0    4.0
46   3.0    4.0    8.0
47   4.0    4.0    0.0
48   4.0    4.0    2.0
49   4.0    4.0    4.0
50   4.0    4.0    6.0
51   4.0    4.0    8.0
PRESCRIBED BOUNDARIES
NODE    CODE    VALUES
1       111     0.0 0.0 0.0
2       110     0.0 0.0 0.0
3       110     0.0 0.0 0.0
4       110     0.0 0.0 0.0
5       110     0.0 0.0 0.0
6       011     0.0 0.0 0.0
7       010     0.0 0.0 0.0
8       010     0.0 0.0 0.0
9       011     0.0 0.0 0.0
10      010     0.0 0.0 0.0
11      010     0.0 0.0 0.0
12      010     0.0 0.0 0.0
13      010     0.0 0.0 0.0
14      011     0.0 0.0 0.0
15      010     0.0 0.0 0.0
16      010     0.0 0.0 0.0
17      011     0.0 0.0 0.0
18      010     0.0 0.0 0.0
19      010     0.0 0.0 0.0
20      010     0.0 0.0 0.0
21      010     0.0 0.0 0.0
22      101     0.0 0.0 0.0
23      100     0.0 0.0 0.0
24      100     0.0 0.0 0.0
25      001     0.0 0.0 0.0
28      001     0.0 0.0 0.0
31      101     0.0 0.0 0.0
32      100     0.0 0.0 0.0
33      100     0.0 0.0 0.0
34      100     0.0 0.0 0.0
35      100     0.0 0.0 0.0
36      001     0.0 0.0 0.0
39      001     0.0 0.0 0.0
44      001     0.0 0.0 0.0
47      001     0.0 0.0 0.0
MATERIAL PROPERTIES
NUMAT YOUNG    POISSON  FCOMP  ALPHA BETA   G
1     3.56E06  0.17     3900   4     0.08   0
APPLIED PRESSURE
IPLOD IGRAV ISURF
 0     0     1
1
 2 5 8 13 27 43 38 35 24
3900 0 0 3900 0 0 3900 0 0 3900 0 0 3900 0 0 3900 0 0 3900 0 0 3900 0 0
 0.4 1.0 20 0 3
```

OUTPUT FILES

PC PRISM UNDER STRIP LOADING

NPOIN =	51	NELEM =	4	NVFIX =	35	NNODE =	20
NMATS =	1	NGAUS =	3	NEVAB =	60	NSTRE =	6
NALGO =	1	NINCS =	1	NSVAB =	153		

ELEMENT	PROPERTY	NODE NUMBERS															
1	1	1	9	39	31	3	11	41	33	6	25	36	22	2	10	40	32
2	1	3	11	41	33	5	13	43	35	7	26	37	23	4	12	42	34
3	1	9	17	47	39	11	19	49	41	14	28	44	25	10	18	48	40
4	1	11	19	49	41	13	21	51	43	15	29	45	26	12	20	50	42

NODE	X	Y	Z
1	0.000	0.000	0.000
2	0.000	0.000	2.000
3	0.000	0.000	4.000
4	0.000	0.000	6.000
5	0.000	0.000	8.000
6	1.000	0.000	0.000
7	1.000	0.000	4.000
8	1.000	0.000	8.000
9	2.000	0.000	0.000
10	2.000	0.000	2.000
11	2.000	0.000	4.000
12	2.000	0.000	6.000
13	2.000	0.000	8.000
14	3.000	0.000	0.000
15	3.000	0.000	4.000
16	3.000	0.000	8.000
17	4.000	0.000	0.000
18	4.000	0.000	2.000
19	4.000	0.000	4.000
20	4.000	0.000	6.000
21	4.000	0.000	8.000
22	0.000	2.000	0.000
23	0.000	2.000	4.000
24	0.000	2.000	8.000
25	2.000	2.000	0.000
26	2.000	2.000	4.000
27	2.000	2.000	8.000
28	4.000	2.000	0.000
29	4.000	2.000	4.000
30	4.000	2.000	8.000
31	0.000	4.000	0.000
32	0.000	4.000	2.000
33	0.000	4.000	4.000
34	0.000	4.000	6.000
35	0.000	4.000	8.000
36	1.000	4.000	0.000
37	1.000	4.000	4.000

38	1.000	4.000	8.000
39	2.000	4.000	0.000
40	2.000	4.000	2.000
41	2.000	4.000	4.000
42	2.000	4.000	6.000
43	2.000	4.000	8.000
44	3.000	4.000	0.000
45	3.000	4.000	4.000
46	3.000	4.000	8.000
47	4.000	4.000	0.000
48	4.000	4.000	2.000
49	4.000	4.000	4.000
50	4.000	4.000	6.000
51	4.000	4.000	8.000

NODE	CODE	FIXED VALUES		
1	111	0.000000	0.000000	0.000000
2	110	0.000000	0.000000	0.000000
3	110	0.000000	0.000000	0.000000
4	110	0.000000	0.000000	0.000000
5	110	0.000000	0.000000	0.000000
6	11	0.000000	0.000000	0.000000
7	10	0.000000	0.000000	0.000000
8	10	0.000000	0.000000	0.000000
9	11	0.000000	0.000000	0.000000
10	10	0.000000	0.000000	0.000000
11	10	0.000000	0.000000	0.000000
12	10	0.000000	0.000000	0.000000
13	10	0.000000	0.000000	0.000000
14	11	0.000000	0.000000	0.000000
15	10	0.000000	0.000000	0.000000
16	10	0.000000	0.000000	0.000000
17	11	0.000000	0.000000	0.000000
18	10	0.000000	0.000000	0.000000
19	10	0.000000	0.000000	0.000000
20	10	0.000000	0.000000	0.000000
21	10	0.000000	0.000000	0.000000
22	101	0.000000	0.000000	0.000000
23	100	0.000000	0.000000	0.000000
24	100	0.000000	0.000000	0.000000
25	1	0.000000	0.000000	0.000000
28	1	0.000000	0.000000	0.000000
31	101	0.000000	0.000000	0.000000
32	100	0.000000	0.000000	0.000000
33	100	0.000000	0.000000	0.000000
34	100	0.000000	0.000000	0.000000
35	100	0.000000	0.000000	0.000000
36	1	0.000000	0.000000	0.000000
39	1	0.000000	0.000000	0.000000
44	1	0.000000	0.000000	0.000000
47	1	0.000000	0.000000	0.000000

NUMBER ELEMENT PROPERTIES

23-7

```
    1      0.356000E+07  0.170000E+00  0.390000E+04  0.400000E+01
       0.800000E-01  0.000000E+00


 MAXIMUM FRONTWIDTH ENCOUNTERED =    75
0   APP  LIED   PRE  SSUR  E
    0    0    1
0     NO. OF LOADED SURFACES =     1
0     LIST OF LOADED SURFACES AND APPLIED LOADS
         2         5    8   13   27   43   38   35   24

  3900.000       0.000       0.000
  3900.000       0.000       0.000
  3900.000       0.000       0.000
  3900.000       0.000       0.000
  3900.000       0.000       0.000
  3900.000       0.000       0.000
  3900.000       0.000       0.000
  3900.000       0.000       0.000
0       TOTAL NODAL FORCES FOR EACH ELEMENT
    1        0.0000E+00  0.0000E+00  0.0000E+00
             0.0000E+00  0.0000E+00  0.0000E+00
             0.0000E+00  0.0000E+00  0.0000E+00
             0.0000E+00  0.0000E+00  0.0000E+00
             0.0000E+00  0.0000E+00  0.0000E+00
             0.0000E+00  0.0000E+00  0.0000E+00
             0.0000E+00  0.0000E+00  0.0000E+00
             0.0000E+00  0.0000E+00  0.0000E+00
             0.0000E+00  0.0000E+00  0.0000E+00
             0.0000E+00  0.0000E+00  0.0000E+00
             0.0000E+00  0.0000E+00  0.0000E+00
             0.0000E+00  0.0000E+00  0.0000E+00
             0.0000E+00  0.0000E+00  0.0000E+00
             0.0000E+00  0.0000E+00  0.0000E+00
             0.0000E+00  0.0000E+00  0.0000E+00
             0.0000E+00  0.0000E+00  0.0000E+00
             0.0000E+00  0.0000E+00  0.0000E+00
             0.0000E+00  0.0000E+00  0.0000E+00
             0.0000E+00  0.0000E+00  0.0000E+00
    2        0.0000E+00  0.0000E+00  0.0000E+00
             0.0000E+00  0.0000E+00  0.0000E+00
             0.0000E+00  0.0000E+00  0.0000E+00
             0.0000E+00  0.0000E+00  0.0000E+00
             0.9207E-02  0.4572E-02  0.2600E+04
            -0.8932E-02  0.4572E-02  0.2600E+04
            -0.8932E-02 -0.5031E-02  0.2600E+04
             0.9207E-02 -0.5031E-02  0.2600E+04
             0.0000E+00  0.0000E+00  0.0000E+00
             0.0000E+00  0.0000E+00  0.0000E+00
             0.0000E+00  0.0000E+00  0.0000E+00
             0.0000E+00  0.0000E+00  0.0000E+00
             0.0000E+00  0.0000E+00  0.0000E+00
             0.0000E+00  0.0000E+00  0.0000E+00
             0.0000E+00  0.0000E+00  0.0000E+00
```

23-7

```
          0.0000E+00  0.0000E+00  0.0000E+00
         -0.4178E-02  0.6861E-02 -0.1040E+05
         -0.1375E-01  0.6144E-03 -0.1040E+05
         -0.1332E-02 -0.5943E-02 -0.1040E+05
          0.1044E-01  0.1681E-02 -0.1040E+05
   3      0.0000E+00  0.0000E+00  0.0000E+00
          0.0000E+00  0.0000E+00  0.0000E+00
          0.0000E+00  0.0000E+00  0.0000E+00
          0.0000E+00  0.0000E+00  0.0000E+00
          0.0000E+00  0.0000E+00  0.0000E+00
          0.0000E+00  0.0000E+00  0.0000E+00
          0.0000E+00  0.0000E+00  0.0000E+00
          0.0000E+00  0.0000E+00  0.0000E+00
          0.0000E+00  0.0000E+00  0.0000E+00
          0.0000E+00  0.0000E+00  0.0000E+00
          0.0000E+00  0.0000E+00  0.0000E+00
          0.0000E+00  0.0000E+00  0.0000E+00
          0.0000E+00  0.0000E+00  0.0000E+00
          0.0000E+00  0.0000E+00  0.0000E+00
          0.0000E+00  0.0000E+00  0.0000E+00
          0.0000E+00  0.0000E+00  0.0000E+00
          0.0000E+00  0.0000E+00  0.0000E+00
          0.0000E+00  0.0000E+00  0.0000E+00
          0.0000E+00  0.0000E+00  0.0000E+00
   4      0.0000E+00  0.0000E+00  0.0000E+00
          0.0000E+00  0.0000E+00  0.0000E+00
          0.0000E+00  0.0000E+00  0.0000E+00
          0.0000E+00  0.0000E+00  0.0000E+00
          0.0000E+00  0.0000E+00  0.0000E+00
          0.0000E+00  0.0000E+00  0.0000E+00
          0.0000E+00  0.0000E+00  0.0000E+00
          0.0000E+00  0.0000E+00  0.0000E+00
          0.0000E+00  0.0000E+00  0.0000E+00
          0.0000E+00  0.0000E+00  0.0000E+00
          0.0000E+00  0.0000E+00  0.0000E+00
          0.0000E+00  0.0000E+00  0.0000E+00
          0.0000E+00  0.0000E+00  0.0000E+00
          0.0000E+00  0.0000E+00  0.0000E+00
          0.0000E+00  0.0000E+00  0.0000E+00
          0.0000E+00  0.0000E+00  0.0000E+00
          0.0000E+00  0.0000E+00  0.0000E+00
          0.0000E+00  0.0000E+00  0.0000E+00
          
```

0 LOAD FACTOR = 0.40000

0 DISPLACEMENTS

0

NODE	X-DISP.	Y-DISP.	Z-DISP.
1	0.000000E+00	0.000000E+00	0.000000E+00
2	0.000000E+00	0.000000E+00	-0.468073E-03
3	0.000000E+00	0.000000E+00	-0.100228E-02
4	0.000000E+00	0.000000E+00	-0.164336E-02
5	0.000000E+00	0.000000E+00	-0.244508E-02
6	0.494787E-04	0.000000E+00	0.000000E+00
7	0.841390E-04	0.000000E+00	-0.949048E-03
8	-0.190109E-03	0.000000E+00	-0.227785E-02
9	0.100377E-03	0.000000E+00	0.000000E+00
10	0.121215E-03	0.000000E+00	-0.439098E-03
11	0.145148E-03	0.000000E+00	-0.883479E-03
12	0.137125E-03	0.000000E+00	-0.134786E-02
13	-0.356970E-03	0.000000E+00	-0.178288E-02
14	0.140846E-03	0.000000E+00	0.000000E+00
15	0.201943E-03	0.000000E+00	-0.810423E-03
16	-0.380111E-03	0.000000E+00	-0.122897E-02
17	0.184182E-03	0.000000E+00	0.000000E+00
18	0.202645E-03	0.000000E+00	-0.420399E-03
19	0.233329E-03	0.000000E+00	-0.762748E-03
20	0.141369E-03	0.000000E+00	-0.898420E-03
21	-0.388956E-03	0.000000E+00	-0.827575E-03
22	0.000000E+00	0.701028E-04	0.000000E+00
23	0.000000E+00	0.837348E-04	-0.100443E-02
24	0.000000E+00	0.157187E-03	-0.245326E-02
25	0.104206E-03	0.691760E-04	0.000000E+00
26	0.150652E-03	0.704943E-04	-0.887914E-03
27	-0.365431E-03	0.108649E-03	-0.179173E-02
28	0.188965E-03	0.655092E-04	0.000000E+00
29	0.241866E-03	0.462189E-04	-0.775035E-03
30	-0.383234E-03	0.381888E-04	-0.835592E-03
31	0.000000E+00	0.142485E-03	0.000000E+00
32	0.000000E+00	0.143586E-03	-0.475273E-03
33	0.000000E+00	0.158748E-03	-0.102273E-02
34	0.000000E+00	0.229378E-03	-0.169389E-02
35	0.000000E+00	0.353916E-03	-0.253104E-02
36	0.528845E-04	0.140817E-03	0.000000E+00
37	0.100991E-03	0.153339E-03	-0.966792E-03
38	-0.153119E-03	0.310211E-03	-0.235225E-02
39	0.106935E-03	0.139819E-03	0.000000E+00
40	0.133979E-03	0.137285E-03	-0.441770E-03
41	0.174803E-03	0.138357E-03	-0.894950E-03
42	0.196591E-03	0.163997E-03	-0.137948E-02
43	-0.291913E-03	0.219399E-03	-0.183253E-02
44	0.147889E-03	0.138090E-03	0.000000E+00
45	0.239598E-03	0.116588E-03	-0.816237E-03
46	-0.297410E-03	0.116407E-03	-0.125418E-02
47	0.191203E-03	0.136600E-03	0.000000E+00
48	0.218103E-03	0.123811E-03	-0.423729E-03
49	0.274363E-03	0.932688E-04	-0.775104E-03
50	0.218566E-03	0.529405E-04	-0.918735E-03
51	-0.296703E-03	0.309422E-04	-0.843353E-03

0 LOAD FACTOR = 0.40000

0 REACTIONS

0

NODE	X-REAC.	Y-REAC.	Z-REAC.
1	0.156880E+03	-0.347243E+01	-0.543868E+03
2	-0.528967E+03	0.343750E+01	0.000000E+00
3	-0.449170E+02	-0.338807E+02	0.000000E+00
4	0.212627E+03	0.756021E+02	0.000000E+00
5	0.348328E+03	0.221997E+02	0.000000E+00
6	0.000000E+00	-0.266821E+01	0.213948E+04
7	0.000000E+00	0.479106E+02	0.000000E+00
8	0.000000E+00	0.203015E+03	0.000000E+00
9	0.000000E+00	-0.614966E+01	-0.104777E+04
10	0.000000E+00	0.176868E+02	0.000000E+00
11	0.000000E+00	0.250354E+01	0.000000E+00
12	0.000000E+00	-0.412878E+02	0.000000E+00
13	0.000000E+00	0.254852E+02	0.000000E+00
14	0.000000E+00	0.210923E+02	0.201819E+04
15	0.000000E+00	-0.730107E+02	0.000000E+00
16	0.000000E+00	-0.156344E+03	0.000000E+00
17	0.000000E+00	-0.148926E+00	-0.497218E+03
18	0.000000E+00	0.224663E+02	0.000000E+00
19	0.000000E+00	0.299002E+02	0.000000E+00
20	0.000000E+00	-0.149603E+03	0.000000E+00
21	0.000000E+00	-0.458109E+01	0.000000E+00
22	-0.473106E+03	0.000000E+00	0.212907E+04
23	-0.104573E+04	0.000000E+00	0.000000E+00
24	0.162496E+04	0.000000E+00	0.000000E+00
25	0.000000E+00	0.000000E+00	0.415533E+04
28	0.000000E+00	0.000000E+00	0.205306E+04
31	0.151812E+03	0.000000E+00	-0.542314E+03
32	-0.573672E+03	0.000000E+00	0.000000E+00
33	-0.933025E+02	0.000000E+00	0.000000E+00
34	-0.943921E+01	0.000000E+00	0.000000E+00
35	0.274437E+03	0.000000E+00	0.000000E+00
36	0.000000E+00	0.000000E+00	0.214505E+04
39	0.000000E+00	0.000000E+00	-0.104855E+04
44	0.000000E+00	0.000000E+00	0.201574E+04
47	0.000000E+00	0.000000E+00	-0.497715E+03

```
0       LOAD FACTOR =   0.40000
0 G.P.     STRESS1      STRESS2      STRESS3      STRAIN1      STRAIN2      STRAIN3
0      ELEMENT NO. =    1
    1    0.572871E+02 -0.105728E+00 -0.789350E+03  0.537906E-04  0.349408E-04 -0.224458E-03
    2    0.994661E+02  0.187746E+01 -0.864892E+03  0.691516E-04  0.371057E-04 -0.247786E-03
    3    0.150826E+03  0.122576E+02 -0.940626E+03  0.866994E-04  0.411606E-04 -0.272007E-03
    4    0.629833E+02  0.256349E+01 -0.787738E+03  0.551863E-04  0.353314E-04 -0.224405E-03
    5    0.104770E+03 -0.171756E+01 -0.867604E+03  0.709424E-04  0.379366E-04 -0.248629E-03
    6    0.160374E+03  0.335327E+01 -0.946562E+03  0.900900E-04  0.384835E-04 -0.273706E-03
    7    0.682697E+02  0.377644E+01 -0.794256E+03  0.569245E-04  0.357281E-04 -0.226546E-03
    8    0.118568E+03 -0.498241E+01 -0.876765E+03  0.754119E-04  0.348057E-04 -0.251706E-03
    9    0.187608E+03 -0.337140E+01 -0.957615E+03  0.985890E-04  0.358264E-04 -0.277790E-03
   10    0.540823E+02 -0.795425E+00 -0.785748E+03  0.527516E-04  0.347148E-04 -0.223260E-03
   11    0.751715E+02  0.693085E+00 -0.833398E+03  0.608799E-04  0.364020E-04 -0.237723E-03
   12    0.107024E+03  0.823120E+01 -0.883757E+03  0.718719E-04  0.394023E-04 -0.253750E-03
   13    0.588467E+02  0.158551E+01 -0.784883E+03  0.539350E-04  0.351159E-04 -0.223358E-03
   14    0.782576E+02 -0.201239E+01 -0.836994E+03  0.620477E-04  0.356674E-04 -0.238751E-03
   15    0.113317E+03  0.137720E+01 -0.890939E+03  0.743101E-04  0.375192E-04 -0.255740E-03
   16    0.638997E+02  0.312025E+01 -0.789221E+03  0.554880E-04  0.356126E-04 -0.224892E-03
   17    0.907402E+02 -0.376462E+01 -0.844323E+03  0.659878E-04  0.349281E-04 -0.241322E-03
   18    0.138492E+03 -0.262932E+01 -0.900862E+03  0.820469E-04  0.356658E-04 -0.259539E-03
   19    0.523103E+02 -0.280014E+00 -0.774862E+03  0.517093E-04  0.344242E-04 -0.220142E-03
   20    0.520497E+02 -0.158159E+01 -0.795281E+03  0.526733E-04  0.350461E-04 -0.225803E-03
   21    0.647367E+02  0.753036E+00 -0.821456E+03  0.573754E-04  0.363458E-04 -0.233873E-03
   22    0.562948E+02  0.197015E+01 -0.773939E+03  0.526772E-04  0.348219E-04 -0.220181E-03
   23    0.531445E+02 -0.323720E+01 -0.799029E+03  0.532390E-04  0.347076E-04 -0.226829E-03
   24    0.683020E+02 -0.394980E+01 -0.829396E+03  0.589806E-04  0.352337E-04 -0.236049E-03
   25    0.612891E+02  0.399762E+01 -0.775320E+03  0.540490E-04  0.352193E-04 -0.220904E-03
   26    0.646239E+02 -0.327975E+01 -0.803916E+03  0.566988E-04  0.343845E-04 -0.228748E-03
   27    0.920853E+02 -0.499168E+01 -0.837977E+03  0.661210E-04  0.342150E-04 -0.239545E-03
0      ELEMENT NO. =    2
    1    0.205093E+03  0.104351E+02 -0.105684E+04  0.107579E-03  0.436315E-04 -0.307156E-03
    2    0.159128E+02 -0.320051E+02 -0.128599E+04  0.674080E-04  0.516717E-04 -0.360464E-03
    3   -0.173000E+03 -0.736445E+03 -0.163677E+04  0.673951E-04 -0.118406E-03 -0.414775E-03
    4    0.220424E+03  0.786117E+01 -0.106059E+04  0.112470E-03  0.423841E-04 -0.308830E-03
    5    0.408333E+02 -0.907129E+01 -0.128652E+04  0.733385E-04  0.569364E-04 -0.362899E-03
    6   -0.127006E+03 -0.712754E+03 -0.163478E+04  0.791843E-04 -0.114434E-03 -0.417798E-03
    7    0.253991E+03  0.351510E+01 -0.108946E+04  0.125325E-03  0.412180E-04 -0.318388E-03
    8    0.117764E+03  0.196150E+02 -0.130445E+04  0.944347E-04  0.621756E-04 -0.372979E-03
    9   -0.643938E+02 -0.606124E+03 -0.164265E+04  0.912843E-04 -0.879896E-04 -0.428764E-03
   10    0.163563E+03 -0.796118E+01 -0.108365E+04  0.980721E-04  0.416992E-04 -0.311824E-03
   11    0.464609E+02 -0.174382E+02 -0.118906E+04  0.706648E-04  0.496622E-04 -0.335391E-03
   12   -0.119718E+03 -0.596853E+03 -0.143961E+04  0.642463E-04 -0.928149E-04 -0.369871E-03
   13    0.174921E+03 -0.108206E+02 -0.108997E+04  0.101701E-03  0.406550E-04 -0.314006E-03
   14    0.618247E+02 -0.502954E+01 -0.119244E+04  0.745498E-04  0.525755E-04 -0.337668E-03
   15   -0.937821E+02 -0.588987E+03 -0.144149E+04  0.712474E-04 -0.918101E-04 -0.372051E-03
   16    0.212859E+03 -0.127280E+02 -0.111717E+04  0.113997E-03  0.396589E-04 -0.323375E-03
   17    0.133886E+03  0.137100E+02 -0.121094E+04  0.947797E-04  0.552814E-04 -0.347198E-03
   18   -0.511111E+02 -0.494904E+03 -0.145440E+04  0.789225E-04 -0.670600E-04 -0.382409E-03
   19    0.181008E+03  0.285205E+01 -0.953732E+03  0.962525E-04  0.376993E-04 -0.276682E-03
   20    0.148254E+03  0.177925E+02 -0.950896E+03  0.862029E-04  0.433248E-04 -0.275034E-03
   21   -0.595657E+02 -0.334656E+03 -0.117030E+04  0.551341E-04 -0.352765E-04 -0.309910E-03
   22    0.188719E+03 -0.313965E+00 -0.961667E+03  0.989485E-04  0.368207E-04 -0.279127E-03
   23    0.155602E+03  0.199370E+02 -0.955924E+03  0.884048E-04  0.438164E-04 -0.276900E-03
   24   -0.527136E+02 -0.339052E+03 -0.117561E+04  0.575220E-04 -0.365851E-04 -0.311518E-03
```

23-7

```
  25    0.228176E+03 -0.141680E+01 -0.989138E+03  0.111646E-03  0.359797E-04 -0.288684E-03
  26    0.225144E+03  0.293233E+02 -0.975540E+03  0.108529E-03  0.440892E-04 -0.286183E-03
  27   -0.258025E+02 -0.260654E+03 -0.118860E+04  0.619584E-04 -0.152281E-04 -0.320197E-03
0     ELEMENT NO. =    3
   1    0.158715E+02 -0.771695E+01 -0.774164E+03  0.417953E-04  0.340420E-04 -0.217851E-03
   2    0.498285E+02 -0.541199E+00 -0.765317E+03  0.505686E-04  0.340138E-04 -0.217330E-03
   3    0.106008E+03  0.958141E+01 -0.764722E+03  0.658378E-04  0.341458E-04 -0.220329E-03
   4    0.180941E+02 -0.504416E+01 -0.772934E+03  0.422337E-04  0.346309E-04 -0.217739E-03
   5    0.531808E+02 -0.581604E+00 -0.767946E+03  0.516377E-04  0.339679E-04 -0.218227E-03
   6    0.114209E+03  0.733618E+01 -0.771390E+03  0.685671E-04  0.334418E-04 -0.222487E-03
   7    0.197219E+02 -0.269833E+01 -0.772648E+03  0.425649E-04  0.351982E-04 -0.217849E-03
   8    0.597866E+02 -0.318161E+00 -0.771755E+03  0.536627E-04  0.339081E-04 -0.219624E-03
   9    0.130482E+03  0.617584E+01 -0.780606E+03  0.736337E-04  0.327788E-04 -0.225797E-03
  10    0.145017E+02 -0.109963E+02 -0.771692E+03  0.414491E-04  0.330682E-04 -0.216934E-03
  11    0.236078E+02 -0.407230E+01 -0.721422E+03  0.412760E-04  0.321776E-04 -0.203579E-03
  12    0.526573E+02  0.103304E+01 -0.679056E+03  0.471691E-04  0.302014E-04 -0.193310E-03
  13    0.159279E+02 -0.630640E+01 -0.770711E+03  0.415788E-04  0.345543E-04 -0.216951E-03
  14    0.240816E+02 -0.258304E+01 -0.724375E+03  0.414790E-04  0.327145E-04 -0.204503E-03
  15    0.554557E+02 -0.216049E+00 -0.685638E+03  0.483291E-04  0.300311E-04 -0.195233E-03
  16    0.174608E+02 -0.130273E+01 -0.767369E+03  0.416102E-04  0.354442E-04 -0.216325E-03
  17    0.284048E+02 -0.193405E+00 -0.725059E+03  0.426119E-04  0.332119E-04 -0.205015E-03
  18    0.669291E+02  0.400620E+00 -0.691508E+03  0.518029E-04  0.299368E-04 -0.197459E-03
  19    0.981470E+01 -0.173737E+02 -0.784417E+03  0.410450E-04  0.321080E-04 -0.219981E-03
  20   -0.535098E+01 -0.117917E+02 -0.692776E+03  0.321418E-04  0.300247E-04 -0.193781E-03
  21   -0.353900E+01 -0.134405E+02 -0.607357E+03  0.286501E-04  0.253965E-04 -0.169795E-03
  22    0.995801E+01 -0.112447E+02 -0.786448E+03  0.408897E-04  0.340431E-04 -0.220851E-03
  23   -0.758202E+01 -0.989874E+01 -0.698928E+03  0.317178E-04  0.309573E-04 -0.195493E-03
  24   -0.570514E+01 -0.151136E+02 -0.616698E+03  0.285681E-04  0.254755E-04 -0.172236E-03
  25    0.107500E+02 -0.412819E+01 -0.782681E+03  0.405913E-04  0.357032E-04 -0.220170E-03
  26   -0.390622E+01 -0.824406E+01 -0.699083E+03  0.326789E-04  0.312538E-04 -0.195791E-03
  27   -0.163600E+01 -0.114961E+02 -0.621656E+03  0.297751E-04  0.265339E-04 -0.173995E-03
0     ELEMENT NO. =    4
   1    0.128686E+03  0.340228E+01 -0.831957E+03  0.757138E-04  0.345375E-04 -0.240003E-03
   2    0.959741E+01 -0.162941E+02 -0.792950E+03  0.413395E-04  0.328293E-04 -0.222419E-03
   3    0.349294E+02 -0.355950E+02 -0.797947E+03  0.496156E-04  0.264365E-04 -0.224111E-03
   4    0.141241E+03  0.101622E+01 -0.838741E+03  0.796787E-04  0.335915E-04 -0.242394E-03
   5    0.188943E+02 -0.961304E+01 -0.794076E+03  0.436862E-04  0.343156E-04 -0.223498E-03
   6    0.414536E+02 -0.194136E+02 -0.792370E+03  0.504093E-04  0.304039E-04 -0.223628E-03
   7    0.166862E+03 -0.358968E+01 -0.871120E+03  0.886415E-04  0.326205E-04 -0.252493E-03
   8    0.503445E+02 -0.145746E+02 -0.824496E+03  0.542098E-04  0.328727E-04 -0.233308E-03
   9    0.750459E+02 -0.172170E+02 -0.822720E+03  0.611898E-04  0.308661E-04 -0.233863E-03
  10    0.862302E+02  0.194530E+02 -0.581186E+03  0.510467E-04  0.290987E-04 -0.168301E-03
  11    0.391770E+02 -0.117809E+02 -0.409002E+03  0.310985E-04  0.143504E-04 -0.116197E-03
  12    0.843560E+02  0.650528E+01 -0.281338E+03  0.368196E-04  0.112332E-04 -0.833662E-04
  13    0.908322E+02  0.148575E+02 -0.586269E+03  0.528014E-04  0.278308E-04 -0.169729E-03
  14    0.246873E+02 -0.576329E+01 -0.409038E+03  0.267425E-04  0.167344E-04 -0.115802E-03
  15    0.608572E+02  0.123586E+02 -0.273687E+03  0.295739E-04  0.136343E-04 -0.803743E-04
  16    0.109392E+03  0.872375E+01 -0.613067E+03  0.595873E-04  0.265013E-04 -0.177850E-03
  17    0.276534E+02 -0.609258E+01 -0.433538E+03  0.287617E-04  0.176700E-04 -0.122810E-03
  18    0.670305E+02  0.500487E+01 -0.299909E+03  0.329113E-04  0.125260E-04 -0.876838E-04
  19    0.318485E+02  0.183461E+02 -0.403968E+03  0.273607E-04  0.229228E-04 -0.115871E-03
  20    0.641317E+02 -0.150000E+02 -0.109347E+03  0.239525E-04 -0.205459E-05 -0.330615E-04
  21    0.178869E+03  0.130136E+03  0.179793E+02  0.431714E-04  0.271545E-04 -0.970539E-05
  22    0.272996E+02  0.125487E+02 -0.408035E+03  0.265541E-04  0.217055E-04 -0.116519E-03
  23    0.356204E+02 -0.143806E+02 -0.114213E+03  0.161464E-04 -0.286701E-06 -0.330965E-04
```

23-7

24	0.183217E+03	0.793146E+02	0.153137E+02	0.469469E-04	0.127986E-04	-0.823489E-05
25	0.378005E+02	0.545001E+01	-0.429701E+03	0.308774E-04	0.202446E-04	-0.122768E-03
26	0.916634E+01	-0.165424E+02	-0.126260E+03	0.939404E-05	0.944585E-06	-0.351139E-04
27	0.166492E+03	0.418422E+02	0.839252E+01	0.443684E-04	0.340198E-05	-0.759092E-05

23-7

```
0      LOAD FACTOR =    0.40000
0     DAMAGE
0 G.P.          R        DAMAG1        DAMAG2        DAMAG3
0     ELEMENT NO. =     1
    1    0.225550E-01  0.000000E+00  0.000000E+00  0.000000E+00
    2    0.325971E-01  0.000000E+00  0.000000E+00  0.000000E+00
    3    0.496700E-01  0.000000E+00  0.000000E+00  0.000000E+00
    4    0.230928E-01  0.000000E+00  0.000000E+00  0.000000E+00
    5    0.337172E-01  0.000000E+00  0.000000E+00  0.000000E+00
    6    0.530106E-01  0.000000E+00  0.000000E+00  0.000000E+00
    7    0.240475E-01  0.000000E+00  0.000000E+00  0.000000E+00
    8    0.371219E-01  0.000000E+00  0.000000E+00  0.000000E+00
    9    0.634879E-01  0.000000E+00  0.000000E+00  0.000000E+00
   10    0.220301E-01  0.000000E+00  0.000000E+00  0.000000E+00
   11    0.269395E-01  0.000000E+00  0.000000E+00  0.000000E+00
   12    0.351589E-01  0.000000E+00  0.000000E+00  0.000000E+00
   13    0.224997E-01  0.000000E+00  0.000000E+00  0.000000E+00
   14    0.274714E-01  0.000000E+00  0.000000E+00  0.000000E+00
   15    0.368688E-01  0.000000E+00  0.000000E+00  0.000000E+00
   16    0.232728E-01  0.000000E+00  0.000000E+00  0.000000E+00
   17    0.297614E-01  0.000000E+00  0.000000E+00  0.000000E+00
   18    0.436751E-01  0.000000E+00  0.000000E+00  0.000000E+00
   19    0.213530E-01  0.000000E+00  0.000000E+00  0.000000E+00
   20    0.222805E-01  0.000000E+00  0.000000E+00  0.000000E+00
   21    0.249976E-01  0.000000E+00  0.000000E+00  0.000000E+00
   22    0.217028E-01  0.000000E+00  0.000000E+00  0.000000E+00
   23    0.224911E-01  0.000000E+00  0.000000E+00  0.000000E+00
   24    0.256514E-01  0.000000E+00  0.000000E+00  0.000000E+00
   25    0.222996E-01  0.000000E+00  0.000000E+00  0.000000E+00
   26    0.239370E-01  0.000000E+00  0.000000E+00  0.000000E+00
   27    0.296179E-01  0.000000E+00  0.000000E+00  0.000000E+00
0     ELEMENT NO. =     2
    1    0.766303E-01  0.000000E+00  0.000000E+00  0.000000E+00
    2    0.502368E-01  0.000000E+00  0.000000E+00  0.000000E+00
    3    0.149102E+00  0.179884E-02  0.360074E-02  0.701044E-02
    4    0.837947E-01  0.208839E-03  0.662764E-04  0.000000E+00
    5    0.531922E-01  0.000000E+00  0.000000E+00  0.000000E+00
    6    0.140110E+00  0.199054E-02  0.275495E-02  0.552448E-02
    7    0.102685E+00  0.160900E-02  0.433032E-03  0.000000E+00
    8    0.662726E-01  0.000000E+00  0.000000E+00  0.000000E+00
    9    0.117733E+00  0.153010E-02  0.105843E-02  0.269115E-02
   10    0.619736E-01  0.000000E+00  0.000000E+00  0.000000E+00
   11    0.454026E-01  0.000000E+00  0.000000E+00  0.000000E+00
   12    0.104296E+00  0.545530E-03  0.732029E-03  0.157235E-02
   13    0.662251E-01  0.000000E+00  0.000000E+00  0.000000E+00
   14    0.479482E-01  0.000000E+00  0.000000E+00  0.000000E+00
   15    0.101353E+00  0.553092E-03  0.601328E-03  0.131029E-02
   16    0.833579E-01  0.182481E-03  0.616789E-04  0.313009E-05
   17    0.625993E-01  0.000000E+00  0.000000E+00  0.000000E+00
   18    0.859592E-01  0.179597E-03  0.972470E-04  0.290012E-03
   19    0.607964E-01  0.000000E+00  0.000000E+00  0.000000E+00
   20    0.495357E-01  0.000000E+00  0.000000E+00  0.000000E+00
   21    0.490156E-01  0.000000E+00  0.000000E+00  0.000000E+00
   22    0.642431E-01  0.000000E+00  0.000000E+00  0.000000E+00
   23    0.521463E-01  0.000000E+00  0.000000E+00  0.000000E+00
```

123-7

```
   24    0.496058E-01  0.000000E+00  0.000000E+00  0.000000E+00
   25    0.833995E-01  0.188340E-03  0.511359E-04  0.313092E-06
   26    0.814670E-01  0.785259E-04  0.224050E-04  0.000000E+00
   27    0.429435E-01  0.000000E+00  0.000000E+00  0.000000E+00
0     ELEMENT NO. =    3
    1    0.188626E-01  0.000000E+00  0.000000E+00  0.000000E+00
    2    0.206557E-01  0.000000E+00  0.000000E+00  0.000000E+00
    3    0.289727E-01  0.000000E+00  0.000000E+00  0.000000E+00
    4    0.189943E-01  0.000000E+00  0.000000E+00  0.000000E+00
    5    0.210822E-01  0.000000E+00  0.000000E+00  0.000000E+00
    6    0.310800E-01  0.000000E+00  0.000000E+00  0.000000E+00
    7    0.191469E-01  0.000000E+00  0.000000E+00  0.000000E+00
    8    0.219384E-01  0.000000E+00  0.000000E+00  0.000000E+00
    9    0.355812E-01  0.000000E+00  0.000000E+00  0.000000E+00
   10    0.185537E-01  0.000000E+00  0.000000E+00  0.000000E+00
   11    0.167992E-01  0.000000E+00  0.000000E+00  0.000000E+00
   12    0.170014E-01  0.000000E+00  0.000000E+00  0.000000E+00
   13    0.187644E-01  0.000000E+00  0.000000E+00  0.000000E+00
   14    0.170211E-01  0.000000E+00  0.000000E+00  0.000000E+00
   15    0.175455E-01  0.000000E+00  0.000000E+00  0.000000E+00
   16    0.188914E-01  0.000000E+00  0.000000E+00  0.000000E+00
   17    0.173509E-01  0.000000E+00  0.000000E+00  0.000000E+00
   18    0.190904E-01  0.000000E+00  0.000000E+00  0.000000E+00
   19    0.187870E-01  0.000000E+00  0.000000E+00  0.000000E+00
   20    0.144919E-01  0.000000E+00  0.000000E+00  0.000000E+00
   21    0.110744E-01  0.000000E+00  0.000000E+00  0.000000E+00
   22    0.191700E-01  0.000000E+00  0.000000E+00  0.000000E+00
   23    0.147382E-01  0.000000E+00  0.000000E+00  0.000000E+00
   24    0.112851E-01  0.000000E+00  0.000000E+00  0.000000E+00
   25    0.193469E-01  0.000000E+00  0.000000E+00  0.000000E+00
   26    0.149781E-01  0.000000E+00  0.000000E+00  0.000000E+00
   27    0.117629E-01  0.000000E+00  0.000000E+00  0.000000E+00
0     ELEMENT NO. =    4
    1    0.375404E-01  0.000000E+00  0.000000E+00  0.000000E+00
    2    0.192499E-01  0.000000E+00  0.000000E+00  0.000000E+00
    3    0.197077E-01  0.000000E+00  0.000000E+00  0.000000E+00
    4    0.413640E-01  0.000000E+00  0.000000E+00  0.000000E+00
    5    0.198382E-01  0.000000E+00  0.000000E+00  0.000000E+00
    6    0.204803E-01  0.000000E+00  0.000000E+00  0.000000E+00
    7    0.511594E-01  0.000000E+00  0.000000E+00  0.000000E+00
    8    0.230126E-01  0.000000E+00  0.000000E+00  0.000000E+00
    9    0.256523E-01  0.000000E+00  0.000000E+00  0.000000E+00
   10    0.178465E-01  0.000000E+00  0.000000E+00  0.000000E+00
   11    0.641851E-02  0.000000E+00  0.000000E+00  0.000000E+00
   12    0.994324E-02  0.000000E+00  0.000000E+00  0.000000E+00
   13    0.187709E-01  0.000000E+00  0.000000E+00  0.000000E+00
   14    0.568378E-02  0.000000E+00  0.000000E+00  0.000000E+00
   15    0.613186E-02  0.000000E+00  0.000000E+00  0.000000E+00
   16    0.234953E-01  0.000000E+00  0.000000E+00  0.000000E+00
   17    0.645601E-02  0.000000E+00  0.000000E+00  0.000000E+00
   18    0.736070E-02  0.000000E+00  0.000000E+00  0.000000E+00
   19    0.628262E-02  0.000000E+00  0.000000E+00  0.000000E+00
   20    0.489857E-02  0.000000E+00  0.000000E+00  0.000000E+00
   21    0.406756E-01  0.000000E+00  0.000000E+00  0.000000E+00
   22    0.602650E-02  0.000000E+00  0.000000E+00  0.000000E+00
```

23-7

23	0.173548E-02	0.000000E+00	0.000000E+00	0.000000E+00
24	0.383749E-01	0.000000E+00	0.000000E+00	0.000000E+00
25	0.711420E-02	0.000000E+00	0.000000E+00	0.000000E+00
26	0.522560E-03	0.000000E+00	0.000000E+00	0.000000E+00
27	0.312076E-01	0.000000E+00	0.000000E+00	0.000000E+00

Appendix C
DETAILED EXPRESSIONS FOR D MATRICES

$$D_I(1,1) = \frac{(1-\alpha w_1)(1-\nu^2(1-\alpha w_2)(1-\alpha w_3))}{A} E_o = \frac{A_1}{A}$$
$$D_I(1,2) = \frac{\nu(1-\alpha w_1)(1-\alpha w_2)(1+\nu(1-\alpha w_3))}{A} E_o = \frac{A_2}{A}$$
$$D_I(1,3) = \frac{\nu(1-\alpha w_1)(1-\alpha w_3)(1+\nu(1-\alpha w_2))}{A} E_o = \frac{A_3}{A}$$
$$D_I(2,1) = \frac{\nu(1-\alpha w_1)(1-\alpha w_2)(1+\nu(1-\alpha w_3))}{A} E_o = \frac{A_2}{A}$$
$$D_I(2,2) = \frac{(1-\alpha w_2)(1-\nu^2(1-\alpha w_1)(1-\alpha w_3))}{A} E_o = \frac{A_4}{A}$$
$$D_I(2,3) = \frac{\nu(1-\alpha w_2)(1-\alpha w_3)(1+\nu(1-\alpha w_1))}{A} E_o = \frac{A_5}{A}$$
$$D_I(3,1) = \frac{\nu(1-\alpha w_1)(1-\alpha w_3)(1+\nu(1-\alpha w_2))}{A} E_o = \frac{A_3}{A}$$
$$D_I(3,2) = \frac{\nu(1-\alpha w_2)(1-\alpha w_3)(1+\nu(1-\alpha w_1))}{A} E_o = \frac{A_5}{A}$$
$$D_I(3,3) = \frac{(1-\alpha w_3)(1-\nu^2(1-\alpha w_1)(1-\alpha w_2))}{A} E_o = \frac{A_6}{A}$$

$$A = 1-\nu^2((1-\alpha w_2)(1-\alpha w_3)+(1-\alpha w_1)(1-\alpha w_3)+(1-\alpha w_1)(1-\alpha w_2)) - 2\nu^3 \times (1-\alpha w_1)(1-\alpha w_2)(1-\alpha w_3)$$

$$
\begin{aligned}
\frac{\partial A_1}{\partial w_1}dw_1 &= -\alpha dw_1\left(1-\nu^2(1-\alpha w_2)(1-\alpha w_3)\right)\\
&= -\alpha dw_1+\nu^2\alpha dw_1(1-\alpha w_2)(1-\alpha w_3)=DA11\\
\frac{\partial A_1}{\partial w_1}dw_2 &= (1-\alpha w_1)\nu^2\alpha dw_2(1-\alpha w_3)\\
&= \nu^2\alpha dw_2(1-\alpha w_1)(1-\alpha w_3)=DA12\\
\frac{\partial A_1}{\partial w_1}dw_3 &= (1-\alpha w_1)\nu^2\alpha dw_3(1-\alpha w_2)\\
&= \nu^2\alpha dw_3(1-\alpha w_1)(1-\alpha w_2)=DA13\\
\frac{\partial A_2}{\partial w_1}dw_1 &= -\nu\alpha dw_1(1-\alpha w_2)(1+\nu(1-\alpha w_3))=DA21\\
\frac{\partial A_2}{\partial w_1}dw_2 &= -\nu\alpha dw_2(1-\alpha w_1)(1+\nu(1-\alpha w_3))=DA22\\
\frac{\partial A_2}{\partial w_1}dw_3 &= \nu(1-\alpha w_1)(1-\alpha w_2)(-\nu\alpha dw_3)\\
&= -\nu^2\alpha dw_3(1-\alpha w_1)(1-\alpha w_2)=DA23\\
\frac{\partial A_3}{\partial w_1}dw_1 &= -\nu\alpha dw_1(1-\alpha w_3)(1+\nu(1-\alpha w_2))=DA31\\
\frac{\partial A_3}{\partial w_2}dw_2 &= -\nu^2\alpha dw_2(1-\alpha w_1)(1-\alpha w_3)=DA32\\
\frac{\partial A_3}{\partial w_3}dw_3 &= -\nu\alpha dw_3(1-\alpha w_1)(1+\nu(1-\alpha w_2))=DA33\\
\frac{\partial A_4}{\partial w_1}dw_1 &= \nu^2\alpha dw_1(1-\alpha w_2)(1-\alpha w_3)=DA41\\
\frac{\partial A_4}{\partial w_1}dw_2 &= -\alpha dw_2\left(1-\nu^2(1-\alpha w_2)(1-\alpha w_3)\right)\\
&= -\alpha dw_2+\nu^2\alpha dw_2(1-\alpha w_2)(1-\alpha w_3)=DA42\\
\frac{\partial A_4}{\partial w_1}dw_3 &= \nu^2\alpha dw_3(1-\alpha w_1)(1-\alpha w_2)=DA43\\
\frac{\partial A_5}{\partial w_1}dw_1 &= -\nu^2\alpha dw_1(1-\alpha w_2)(1-\alpha w_3)=DA51\\
\frac{\partial A_5}{\partial w_2}dw_2 &= -\nu\alpha dw_2(1-\alpha w_3)(1+\nu(1-\alpha w_1))=DA52\\
\frac{\partial A_5}{\partial w_3}dw_3 &= -\nu\alpha dw_3(1-\alpha w_2)(1+\nu(1-\alpha w_1)=DA53\\
\frac{\partial A_6}{\partial w_1}dw_1 &= \nu^2\alpha dw_1(1-\alpha w_3)(1-\alpha w_2)=DA61\\
\frac{\partial A_6}{\partial w_2}dw_2 &= \nu^2\alpha dw_2(1-\alpha w_3)(1-\alpha w_1)=DA62\\
\frac{\partial A_6}{\partial w_3}dw_3 &= -\alpha dw_3\left(1-\nu^2(1-\alpha w_1)(1-\alpha w_2)\right)\\
&= -\alpha dw_3+\nu^2\alpha dw_3(1-\alpha w_1)(1-\alpha w_2)=DA63
\end{aligned}
$$

$$D_{II}(1,1) = \frac{(1-w_1)^2(1-\beta w_2)(1-\beta w_3)\left((1-w_2)^2(1-w_3)^2 - \nu^2(1-\beta w_1)^2(1-\beta w_2)(1-\beta w_3)\right)}{B} E_o$$
$$= \frac{B_1}{B}$$

$$D_{II}(1,2) = \frac{(1-\beta w_1)(1-\beta w_2)(1-\beta w_3)^2(1-w_1)(1-w_2)\left(\nu(1-w_3)^2 + \nu^2(1-\beta w_1)(1-\beta w_2)\right)}{B} E_o$$
$$= \frac{B_2}{B}$$

$$D_{II}(1,3) = \frac{(1-\beta w_1)(1-\beta w_3)(1-\beta w_2)^2(1-w_1)(1-w_3)\left(\nu(1-w_2)^2 + \nu^2(1-\beta w_1)(1-\beta w_3)\right)}{B} E_o$$
$$= \frac{B_3}{B}$$

$$D_{II}(2,1) = \frac{(1-\beta w_1)(1-\beta w_2)(1-\beta w_3)^2(1-w_1)(1-w_2)\left(\nu(1-w_3)^2 + \nu^2(1-\beta w_1)(1-\beta w_2)\right)}{B} E_o$$
$$= \frac{B_2}{B}$$

$$D_{II}(2,2) = \frac{(1-w_2)^2(1-\beta w_1)(1-\beta w_3)\left((1-w_1)^2(1-w_3)^2 - \nu^2(1-\beta w_1)(1-\beta w_2)^2(1-\beta w_3)\right)}{B} E_o$$
$$= \frac{B_4}{B}$$

$$D_{II}(2,3) = \frac{(1-\beta w_1)^2(1-\beta w_2)(1-\beta w_3)^2(1-w_2)(1-w_3)\left(\nu(1-w_1)^2 + \nu^2(1-\beta w_2)(1-\beta w_3)\right)}{B} E_o$$
$$= \frac{B_5}{B}$$

$$D_{II}(3,1) = \frac{(1-\beta w_1)(1-\beta w_3)(1-\beta w_2)^2(1-w_1)(1-w_3)\left(\nu(1-w_2)^2 + \nu^2(1-\beta w_1)(1-\beta w_3)\right)}{B} E_o$$
$$= \frac{B_3}{B}$$

$$D_{II}(3,2) = \frac{(1-\beta w_1)^2(1-\beta w_2)(1-\beta w_3)^2(1-w_2)(1-w_3)\left(\nu(1-w_1)^2+\nu^2(1-\beta w_2)(1-\beta w_3)\right)}{B}E_o$$
$$= \frac{B_5}{B}$$

$$D_{II}(3,3) = \frac{(1-w_3)^2(1-\beta w_1)(1-\beta w_2)\left((1-w_1)^2(1-w_2)^2-\nu^2(1-\beta w_1)(1-\beta w_2)(1-\beta w_3)^2\right)}{B}E_o$$
$$= \frac{B_6}{B}$$

$$B = \{(1-w_1)^2(1-w_2)^2(1-w_3)^2 - \nu^2((1-\beta w_1)(1-\beta w_2)(1-\beta w_3)^2 + (1-\beta w_1)^2 \times (1-\beta w_2)(1-\beta w_3)(1-w_1)^2 + (1-\beta w_1)(1-\beta w_2)^2(1-\beta w_3)(1-w_2)^2) - 2\nu^3 \times \left((1-\beta w_1)^2(1-\beta w_2)^2(1-\beta w_3)^2\right)\}$$

$$\begin{aligned}
\frac{\partial(1-w_1)^2(1-\beta w_1)^2}{\partial w_1} &= -2(1-w_1)(1-\beta w_1)\{1-\beta w_1+\beta(1-w_1)\} \\
&= -2(1-w_1)(1-\beta w_1)(1+\beta-2\beta w_1) = DBW1 \\
\frac{\partial(1-\beta w_1)^2(1-w_1)^2}{\partial w_1} &= -\beta(1-w_1)^2-2(1-\beta w_1)(1-w_1) \\
&= -(1-w_1)\{\beta-\beta w_1+2-2\beta w_1\} = -(1-w_1)(2+\beta-3\beta w_1) \\
&= DBW2
\end{aligned}$$

$$\begin{aligned}
\frac{\partial(1-w_1)(1-\beta w_1)}{\partial w_1} &= -(1-\beta w_1)-\beta(1-w_1) = -1-\beta+2\beta w_1 = DBW3 \\
\frac{\partial(1-w_1)(1-\beta w_1)^2}{\partial w_1} &= -(1-\beta w_1)^2-2\beta(1-\beta w_1)(1-w_1) = -(1-\beta w_1)\{1-\beta w_1+2\beta-2\beta w_1\} \\
&= -(1-\beta w_1)(1+2\beta-3\beta w_1) = DBW4
\end{aligned}$$

$$\begin{aligned}
\frac{\partial(1-w_2)^2(1-\beta w_2)^2}{\partial w_2} &= -2(1-w_2)(1-\beta w_2)\{1-\beta w_2+\beta(1-w_2)\} \\
&= -2(1-w_2)(1-\beta w_2)(1+\beta-2\beta w_2) = DBW5 \\
\frac{\partial(1-\beta w_2)^2(1-w_2)^2}{\partial w_2} &= -\beta(1-w_2)^2-2(1-\beta w_2)(1-w_2) \\
&= -(1-w_2)\{\beta-\beta w_2+2-2\beta w_2\} = -(1-w_2)(2+\beta-3\beta w_2) \\
&= \mathrm{DBW6}
\end{aligned}$$

$$\begin{aligned}
\frac{\partial(1-w_2)(1-\beta w_2)}{\partial w_2} &= -(1-\beta w_2)-\beta(1-w_2) = -1-\beta+2\beta w_2 = DBW7 \\
\frac{\partial(1-w_2)(1-\beta w_2)^2}{\partial w_2} &= -(1-\beta w_2)^2-2\beta(1-\beta w_2)(1-w_2) = -(1-\beta w_2)\{1-\beta w_2+2\beta-2\beta w_2\} \\
&= -(1-\beta w_2)(1+2\beta-3\beta w_2) = DBW8
\end{aligned}$$

$$\begin{aligned}
\frac{\partial(1-w_3)^2(1-\beta w_3)^2}{\partial w_3} &= -2(1-w_3)(1-\beta w_3)\{1-\beta w_3+\beta(1-w_3)\} \\
&= -2(1-w_3)(1-\beta w_3)(1+\beta-2\beta w_3) = DBW9 \\
\frac{\partial(1-\beta w_3)^2(1-w_3)^2}{\partial w_3} &= -\beta(1-w_3)^2-2(1-\beta w_3)(1-w_3) \\
&= -(1-w_3)\{\beta-\beta w_3+2-2\beta w_3\} = -(1-w_3)(2+\beta-3\beta w_3) \\
&= \mathrm{DBW10}
\end{aligned}$$

$$\begin{aligned}
\frac{\partial(1-w_3)(1-\beta w_3)}{\partial w_3} &= -(1-\beta w_3)-\beta(1-w_3) = -1-\beta+2\beta w_3 = DBW11 \\
\frac{\partial(1-w_3)(1-\beta w_3)^2}{\partial w_3} &= -(1-\beta w_3)^2-2\beta(1-\beta w_3)(1-w_3) = -(1-\beta w_3)\{1-\beta w_3+2\beta-2\beta w_3\} \\
&= -(1-\beta w_3)(1+2\beta-3\beta w_3) = DBW12
\end{aligned}$$

$$\frac{\partial B_1}{\partial w_1}dw_1 = \{-2(1-w_1)(1-\beta w_2)(1-\beta w_3)(1-w_2)^2(1-w_3)^2 + 2\nu^2(1-w_1)(1-\beta w_1) \times (1+\beta-2\beta w_1)(1-\beta w_2)^2(1-\beta w_3)^2\}dw_1 = DB11$$

$$\frac{\partial B_1}{\partial w_2}dw_2 = -(1-w_2)(2+\beta-3\beta w_2)(1-w_1)^2(1-\beta w_3)(1-w_3)^2 + 2\beta\nu^2(1-w_1)^2 \times (1-\beta w_1)^2(1-\beta w_2)(1-\beta w_3)^2 dw_2 = DB12$$

$$\frac{\partial B_1}{\partial w_3}dw_3 = \{-(1-w_3)(2+\beta-3\beta w_3)(1-w_1)^2(1-\beta w_2)(1-w_2)^2 + 2\beta\nu^2(1-w_1)^2 \times (1-\beta w_1)^2(1-\beta w_2)^2(1-\beta w_3)\}dw_3 = DB13$$

$$\frac{\partial B_2}{\partial w_1}dw_1 = \{\nu(-1-\beta+2\beta w_1)(1-\beta w_2)(1-w_2)(1-\beta w_3)^2(1-w_3)^2 - \nu^2(1-\beta w_1) \times (1+2\beta-3\beta w_1)(1-w_2)(1-\beta w_2)^2(1-\beta w_3)^2\}dw_1 = DB21$$

$$\frac{\partial B_2}{\partial w_2}dw_2 = \{\nu(-1-\beta+2\beta w_2)(1-\beta w_1)(1-w_1)(1-\beta w_3)^2(1-w_3)^2 - \nu^2(1-\beta w_2) \times (1+2\beta-3\beta w_2)(1-w_1)(1-\beta w_1)^2(1-\beta w_3)^2\}dw_2 = DB22$$

$$\frac{\partial B_2}{\partial w_3}dw_3 = \{-2\nu(1-w_3)(1-\beta w_3)(1+\beta-2\beta w_3)(1-\beta w_1)(1-w_1)(1-\beta w_2) \times (1-w_2) - 2\beta\nu^2(1-w_1)(1-\beta w_1)^2(1-w_2)(1-\beta w_2)^2(1-\beta w_3)\}dw_3 = DB23$$

$$\frac{\partial B_3}{\partial w_1}dw_1 = \{\nu(-1-\beta+2\beta w_1)(1-\beta w_2)^2(1-w_2)^2(1-\beta w_3)(1-w_3) - \nu^2(1-\beta w_1) \times (1+2\beta-3\beta w_1)(1-w_3)(1-\beta w_2)^2(1-\beta w_3)^2\}dw_1 = DB31$$

$$\frac{\partial B_3}{\partial w_2}dw_2 = \{-2\nu(1-w_2)(1-\beta w_2)(1+\beta-2\beta w_2)(1-\beta w_1)(1-w_1)(1-\beta w_3) \times (1-w_3) - 2\beta\nu^2(1-w_1)(1-\beta w_1)^2(1-w_3)(1-\beta w_3)^2(1-\beta w_2)\}dw_2 = DB32$$

$$\frac{\partial B_3}{\partial w_2}dw_3 = \{\nu(-1-\beta+2\beta w_3)(1-\beta w_2)^2(1-w_2)^2(1-\beta w_1)(1-w_1) - \nu^2(1-\beta w_3) \times (1+2\beta-3\beta w_3)(1-w_1)(1-\beta w_1)^2(1-\beta w_2)^2\}dw_3 = DB33$$

$$\frac{\partial B_4}{\partial w_1}dw_1 = \{-(1-w_1)(2+\beta-3\beta w_1)(1-w_2)^2(1-\beta w_3)(1-w_3)^2 + 2\beta\nu^2(1-\beta w_1) \times (1-w_2)^2(1-\beta w_2)^2(1-\beta w_3)^2\}dw_1 = DB41$$

$$\frac{\partial B_4}{\partial w_2}dw_2 = \{-2(1-w_2)(1-\beta w_1)(1-\beta w_3)(1-w_1)^2(1-w_3)^2 + 2\nu^2(1-w_2)(1-\beta w_2) \times (1+\beta-2\beta w_2)(1-\beta w_1)^2(1-\beta w_3)^2\}dw_2 = DB42$$

23-7

$$\frac{\partial B_4}{\partial w_3}dw_3 = \{-(1-w_3)(2+2\beta-3\beta w_3)(1-w_2)^2(1-\beta w_1)(1-w_1)^2 + 2\beta\nu^2(1-\beta w_3) \times (1-w_2)^2(1-\beta w_2)^2(1-\beta w_1)^2\}dw_3 = DB43$$

$$\frac{\partial B_5}{\partial w_1}dw_1 = \{-2\nu(1-w_1)(1-\beta w_1)(1+\beta-2\beta w_1)(1-\beta w_2)(1-w_2)(1-\beta w_3) \times (1-w_3) - 2\beta\nu^2(1-\beta w_1)(1-\beta w_2)^2(1-\beta w_3)^2(1-w_2)(1-w_3)\}dw_1 = DB51$$

$$\frac{\partial B_5}{\partial w_2}dw_2 = \{\nu(-1-\beta+2\beta w_2)(1-\beta w_1)^2(1-w_1)^2(1-\beta w_3)(1-w_3) - \nu^2(1-\beta w_2) \times (1+2\beta-3\beta w_2)(1-\beta w_1)^2(1-\beta w_3)^2(1-w_3)\}dw_2 = DB52$$

$$\frac{\partial B_5}{\partial w_3}dw_3 = \{\nu(-1-\beta+2\beta w_3)(1-\beta w_1)^2(1-w_1)^2(1-\beta w_2)(1-w_2) - \nu^2(1-\beta w_3) \times (1+2\beta-3\beta w_3)(1-\beta w_1)^2(1-\beta w_2)^2(1-w_2)\}dw_3 = DB53$$

$$\frac{\partial B_6}{\partial w_1}dw_1 = \{-(1-w_1)(2+\beta-3\beta w_1)(1-\beta w_2)(1-w_2)^2(1-w_3)^2 + 2\beta\nu^2(1-\beta w_1) \times (1-\beta w_2)^2(1-\beta w_3)^2(1-w_3)^2\}dw_1 = DB61$$

$$\frac{\partial B_6}{\partial w_2}dw_2 = \{-(1-w_2)(2+\beta-3\beta w_2)(1-\beta w_1)(1-w_1)^2(1-w_3)^2 + 2\beta\nu^2(1-\beta w_2) \times (1-\beta w_1)^2(1-\beta w_3)^2(1-w_3)^2\}dw_2 = DB62$$

$$\frac{\partial B_6}{\partial w_3}dw_3 = \{-2(1-w_3)(1-\beta w_1)(1-w_1)^2(1-\beta w_2)(1-w_2)^2 + 2\nu^2(1-w_3) \times (1-\beta w_3)(1+\beta-2\beta w_3)(1-\beta w_1)^2(1-\beta w_2)^2\}dw_3 = DB63$$

$$\frac{\partial A}{\partial w_1}dw_1 = \left\{\nu^2\alpha\left((1-\alpha w_3)+(1-\alpha w_2)\right) + 2\nu^3\alpha(1-\alpha w_2)(1-\alpha w_3)\right\}dw_1 = DA1$$

$$\frac{\partial A}{\partial w_2}dw_2 = \left\{\nu^2\alpha\left((1-\alpha w_1)+(1-\alpha w_3)\right) + 2\nu^3\alpha(1-\alpha w_1)(1-\alpha w_3)\right\}dw_2 = DA2$$

$$\frac{\partial A}{\partial w_3}dw_3 = \left\{\nu^2\alpha\left((1-\alpha w_1)+(1-\alpha w_2)\right) + 2\nu^3\alpha(1-\alpha w_1)(1-\alpha w_2)\right\}dw_3 = DA3$$

$$\frac{\partial B}{\partial w_1}dw_1 = \{-2(1-w_1)(1-w_2)^2(1-w_3)^2 + \nu^2(\beta(1-\beta w_2)(1-\beta w_3)^2(1-w_3)^2 + 2(1-w_1) \times (1-\beta w_1)(1+\beta-2\beta w_1)(1-\beta w_2)(1-\beta w_3) + \beta(1-\beta w_2)^2(1-w_2)^2(1-\beta w_3)) + 2\nu^3\beta(1-\beta w_1)(1-\beta w_2)^2(1-\beta w_3)^2\}dw_1 = DB1$$

$$\frac{\partial B}{\partial w_2}dw_2 = \{-2(1-w_1)^2(1-w_2)(1-w_3)^2 + \nu^2(\beta(1-\beta w_1)(1-\beta w_3)^2(1-w_3)^2 + \beta(1-\beta w_1)^2 \times (1-w_1)^2(1-\beta w_3) + 2(1-\beta w_2)(1-w_2)(1+\beta-2\beta w_2)(1-\beta w_1)(1-\beta w_3)) + 2\nu^3\beta \times (1-\beta w_1)^2(1-\beta w_2)(1-\beta w_3)^2\}dw_2 = DB2$$

23-7

$$\frac{\partial B}{\partial w_3}dw_3 = \{-2(1-w_1)^2(1-w_2)^2(1-w_3) + \nu^2(2(1-\beta w_1)(1-\beta w_2)(1-\beta w_3)(1-w_3) \times (1+\beta-2\beta w_3) + \beta(1-\beta w_1)^2(1-w_1)^2(1-\beta w_2) + \beta(1-\beta w_1)(1-\beta w_2)^2 \times (1-w_2)^2) + 2\nu^3\beta(1-\beta w_1)^2(1-\beta w_2)^2(1-\beta w_3)\}dw_3 = DB3$$

$$DTMAT1(1,1) = \frac{DA11 \times A - A1 \times DA1}{A^2} E_o$$

$$DTMAT1(1,2) = \frac{DA21 \times A - A2 \times DA1}{A^2} E_o$$

$$DTMAT1(1,3) = \frac{DA31 \times A - A3 \times DA1}{A^2} E_o$$

$$DTMAT1(2,2) = \frac{DA41 \times A - A4 \times DA1}{A^2} E_o$$

$$DTMAT1(2,3) = \frac{DA51 \times A - A5 \times DA1}{A^2} E_o$$

$$DTMAT1(3,3) = \frac{DA61 \times A - A6 \times DA1}{A^2} E_o$$

$$DTMAT2(1,1) = \frac{DA12 \times A - A1 \times DA2}{A^2} E_o$$

$$DTMAT2(1,2) = \frac{DA22 \times A - A2 \times DA2}{A^2} E_o$$

$$DTMAT2(1,3) = \frac{DA32 \times A - A3 \times DA2}{A^2} E_o$$

$$DTMAT2(2,2) = \frac{DA42 \times A - A4 \times DA2}{A^2} E_o$$

$$DTMAT2(2,3) = \frac{DA52 \times A - A5 \times DA2}{A^2} E_o$$

$$DTMAT2(3,3) = \frac{DA62 \times A - A6 \times DA2}{A^2} E_o$$

$$DTMAT3(1,1) = \frac{DA13 \times A - A1 \times DA3}{A^2} E_o$$

$$DTMAT3(1,2) = \frac{DA23 \times A - A2 \times DA3}{A^2} E_o$$

$$DTMAT3(1,3) = \frac{DA33 \times A - A3 \times DA3}{A^2} E_o$$

$$DTMAT3(2,2) = \frac{DA43 \times A - A4 \times DA3}{A^2} E_o$$

$$DTMAT3(2,3) = \frac{DA53 \times A - A5 \times DA3}{A^2} E_o$$

$$DCMAT1(1,1) = \frac{DB11 \times B - B1 \times DB1}{B^2} E_o$$

$$DCMAT1(1,2) = \frac{DB21 \times B - B2 \times DB1}{B^2} E_o$$

$$DCMAT1(1,3) = \frac{DB31 \times B - B3 \times DB1}{B^2} E_o$$

$$DCMAT1(2,2) = \frac{DB41 \times B - B4 \times DB1}{B^2} E_o$$

$$DCMAT1(2,3) = \frac{DB51 \times B - B5 \times DB1}{B^2} E_o$$

$$DCMAT1(3,3) = \frac{DB61 \times B - B6 \times DB1}{B^2} E_o$$

$$DCMAT2(1,1) = \frac{DB12 \times B - B1 \times DB2}{B^2} E_o$$

$$DCMAT2(1,2) = \frac{DB22 \times B - B2 \times DB2}{B^2} E_o$$

$$DCMAT2(1,3) = \frac{DB32 \times B - B3 \times DB2}{B^2} E_o$$

$$DCMAT2(2,2) = \frac{DB42 \times B - B4 \times DB2}{B^2} E_o$$

$$DCMAT2(2,3) = \frac{DB52 \times B - B5 \times DB2}{B^2} E_o$$

$$DCMAT2(3,3) = \frac{DB62 \times B - B6 \times DB2}{B^2} E_o$$

$$DCMAT3(1,1) = \frac{DB13 \times B - B1 \times DB3}{B^2} E_o$$

$$DCMAT3(1,2) = \frac{DB23 \times B - B2 \times DB3}{B^2} E_o$$

$$DCMAT3(1,3) = \frac{DB33 \times B - B3 \times DB3}{B^2} E_o$$

$$DCMAT3(2,2) = \frac{DB43 \times B - B4 \times DB3}{B^2} E_o$$

$$DCMAT3(2,3) = \frac{DB53 \times B - B5 \times DB3}{B^2} E_o$$

$$DCMAT3(3,3) = \frac{DB63 \times B - B6 \times DB3}{B^2} E_o$$

REFERENCES

1. Bazant,Z.P., and Shieh,C.L.., 1980, *Hysteric Fracturing Endochronic Theory for Concrete, J.Engg.Mech.,ASCE,106, 929-949*

2. Bazant,Z.P., Xi,Y., and Reid,S.G., 1991, *Statistical Size Effect in Quasi-Brittle structures: I. Is Weibull theory applicable?, J.Engg.Mech.,ASCE,117,No.11, pp2609-2622*

3. Brebbia,C.A., Connors,J.J., *Fundamentals of Finite Element Techniques. Butterworth and Co.(Publishers) Ltd., pp 160-162*

4. Caboche,J.L., 1987, *Fracture Mechanics and Damage Mechanics: Complementarity of Approaches, 309-321*

5. Chen,E.,and Buyukozturk,O., 1984, *Constitutive Model for Concrete in Cyclic Compression, J.Engg.Mech.,ASCE,111(6), 797-813.*

6. Chou,J.H.,Lee,J.D,and Erdman,A.G., 1990, *Development of a Three-Dimensional Finite Element Program for Large Strain Elastic-plastic Solids,Comp.Struct.,36(4),631-645.*

7. Chow,C.L.,and Wang,J., 1988, *A Finite Element Analysis of Continuum Damage Mechanics for Ductile Fracture,Int.J.Fracture,38,pp.83-102.*

8. Cordebois,J.P., and Sidoroff,F.,1982 *Endomaggment Anisotrope en Elasticite et Plasticite, J.Mec.Thoer.Appl.,No.Special, 45-59*

9. Dafalias,Y.F., 1977a, *Elasto-plastic Coupling within thermodynamic Strain Space Formulation of Plasticity, Int.J.Nonlinear Mech.,12, 327.*

10. Dafalias,Y.F., 1977b, *Hiushin's Postulate and Resulting Thermodynamic Conditions on Elasto-plastic Coupling, Int.J.Solids.Structures,13,239*

11. Dafalias,Y.F., 1978, *Restrictions on Continuum Description of Elasto-plastic Coupling for Concrete within Thermodynamics,Eds.,Chang,T.Y.,and Krempl,E.,Inelastic Behavior of Pressure Vessels and Piping Components, Series PVP-PB-028,ASME,29*

12. De wolf,J.T.,and Kou,J., 1987, *Three-Dimensional Finite Element Analysis Of Concrete, Publication SP-ACI 98,pp.95-115.*

13. Dragon,A., 1985, *Plasticity and Ductile Fracture Damage: Study of Void Growth in Metals, Engg.Fract.Mech.,21, 875-885*

14. Dragon,A., and Chihab,A., 1985, *On Finite Damage: Ductile Fracture-Damage Evolution, Mech.Mater.,4, 95-106*

15. Francois,D., 1984 *Fracture and Damage Mechanics of Concrete, Advances in Fracture Mechanics to Cementitious Composites, NATO Advanced Research Workshop, Shah,S.P.,Ed.,97-110. 1507-1514*

16. Gardener.N., 1969, *Triaxial Behavior of Concrete Procs.,ACI, 66, No:2,136*

17. Gonzalez,V.F.,Kotsovos,M.D.,and Pavlovic,M.N., 1990, *Three-dimensional Finite Element Analysis of Structural Concrete, Computer Aided Analysis and Design of Concrete Structures(Edited by N.Bicanic and H.Mang) Vol.2,pp.1029-1040.*

18. Gonzalez,V.F.,Kotsovos,M.D.,and Pavlovic,M.N., 1991, *Nonlinear Finite Element Analysis of Concrete Structures:Performance of a Three-Dimensional Brittle Model,Comp.Struct.,40(5),pp.1287-1306.*

19. Hinton,E.,and Owen,D.R.J., 1979, *An Introduction to Finite Element Computations, Pineridge Press,London,U.K.*

20. Hinton,E.,and Owen,D.R.J., 1980, *Finite Elements in Plasticity,Theory and Practice,Pineridge Press, Swansea,U.K.,pp.227-228.*

21. Hsu,T.C., Slate,F.O., Sturman,G.M., and Winter,G., 1963 *Microcracking of Plain Concrete and the Shape of Stress-Strain Curve, J.ACI,60,No.2,209*

22. Hueckel,T., 1975 *On Plastic Flow of Granular Rocklike Materials with Variable Elastic Moduli,Bull.Polish Acad.Sci.,23,No.8,405*

23. Hueckel,T., 1976, *Coupling of Elastic and Plastic Deformations of Bulk Solids, Mechanics,11,227*

24. Hueckel,T.,and Mair,G., 1977 *Incremental Boundary Value Problems in the Presence of Coupling of Elastic and Plastic Deformations: A Rock Mechanics Oriented Theory, Int.J.Solids.Structures,13,1*

25. Hult,J., 1974, *Creep in Continua and Structures, Topics in Applied Continuum Mechanics,Springer-Verlag, Vienna.*

26. Irons,B.M., 1970, *A Frontal Solution Program, Int.J.Num.Meth.Eng.,Vol2.,pp.5-32. J.Engg.Mech.,ASCE,106, 929-949.*

27. Ju,J.W., Monteiro,P.J.M., Rashed,A.I., 1989, *On Continuum Damage of Cement Paste and Mortaras Affected by Porosity and Sand Concentration, J.Engg.Mech.,ASCE,115, 105-130*

28. Kachanov,L.M., 1958, *Time of the Rupture Process Under Creep Conditions, Isv.Akad.Nauk S.S.R.Otd. Tekh., 8*

29. Kachanov,L.M., 1972, *Deformation of Medium with Cracks, Izvestia VNIIG, Leningrad, USSR, 99,195-210*

30. Kachanov,L.M., 1980, *Continuum Model of Medium with Cracks, J.Engg.Mech.,ASCE,106,No.Em5,Oct.1039-1051*

31. Kachanov,L.M., 1984 *On a Continuum Modelling of Damage, in Application of Fracture Mechanics to Cementitious Composites, NATO-ARW, Sept.4-7, Northwestern Univ., U.S.A., Shah,S.P.,Ed.*

32. Kachanov,L.M., 1987, *On Modelling of Anisotropic Damage in Elastic-Brittle Materials- A Brief Review, Proc.ASME Winter Annual Meeting*

33. Karsan,D., Jirsa,J.O., 1969, *Behavior of Concrete under Compressive Loading, J.Struct.Div.,95,2543*

34. Khan,A.S.,and Yuan,S.I., 1988, *A Three-Dimensional Finite Element Program for Brittle Bimodular Rock like Materials,Int.J.Num.Anal.Meth.Geomech.,12,pp.599-609.*

35. Krajcinovic,D., and Fonseka,G.U., 1981, *Continuum Damage Mechanics Theory of Brittle Materials,Parts I, II, J.Appl.Mech.,48,809-824.*

36. Krajcinovic,D., 1983, *Constitutive Equations for Damage Materials, J.Appl.Mech.50, 355-360*

37. Krajcinovic,D., and Selvaraj,S., 1983, *Constitutive Equations for Concrete, Proc.Int.Conf.on Constitutive Laws for Engineering Materials,Desai,C.S., Gallagher,R.H., and Tucson,Az.,Eds.*

38. Krajcinovic,D., 1984a, *Continuum Damage Mechanics, Appl.Mech.,Rev.,37(1)*

39. Krajcinovic,D., 1985, *Mechanics of Solids with a Progressively Deteriorating Structure, Applications of Fracture Mechanics to Cementitious Composites,Shah,S.P., Ed.,Northwestern Univ..*

40. Leckie,F.A., and Hayhurst,D.R., 1974, *Creep Rupture of Structure, Proc.R.Soc.A340,323-347*

41. Lemaitre,J.,and Chaboche, 1974, *A Nonlinear Model of Creep-fatigue Damage Accumulation and Interaction, Proc.IUTAM Symp.on Mechanics of Viscoelastic Media and Bodies, Springr-Verlag, Vienna.*

42. Lemaitre,J., and Dufailly,J., 1977, *Modelisation e Identification de l'endommagement Plastique de Metaux, 3eme Congress Francis de Mecanique,Grenoble,France.*

43. Lemaitre,J., 1979, *Damage Modelling for Prediction of Creep Fatigue Failure in Structures, 5th Conf. on structural Mechanics in Reactor Technology,SMIRT 5.*

44. Lemaitre,J.,and Plumtree,A., 1979, *Application of Damage Concepts to Predict Creep-fatigue Failures, J.Engg.Mater.Tech.,101,.284-292*

45. Lemaitre,J., 1984, *Coupled Elasto-plasticity and Damage Constitutive Equations, Invited Lecture at FENOMECH 84, Stuttgart (RFA), also in Comp.Meth. Appl.Mech.Engg.J.*

46. Lemaitre,J., 1985, *A Continuous Damage Mechanics Model for Ductile Fracture, Trans.ASME,J.Engg.Mater.Technol.,107,1.*

47. Lemaitre,J., 1986, *Local Approach of Fracture , Engg.Fract.Mech.,25,523-537*

48. Linse,D., 1973, *Versuchsanlage zur Ermttlung der Dreiachsigen Festigkeit von Beton mit Ersten Versuchsergebnissen,Cem.Conc.Res.,3,No.4,445*

49. Mazars,J., 1984, *Application of the Damage Mechanics in Nonlinear Response and Rupture of Concrete Structures,(Application de la Mecanique de L'Endommagement au Comportement Non Lineare te a la Rupture du Beton De Structure), These de Doctorat d'Etat,universite Pierre et Marie Curie, Paris 6.*

50. Mazars,J.,and Lemaitre,J., 1984, *Application of Continuous Damage Mechanics to Strain Fracture Behavior of Concrete, Proc.NATO Adv.Res. Workshop on Applications of Fracture Mech. on Cementitious Composites,Evanstons,Illinois.*

51. Mazars,J.,and Legendre,D., 1984, *Damage and Fracture Mechanics for Concrete-A Combined Approach, ICF6,New Delhi.*

52. Mazars,J.,and Pijaudier-Cabot,G., 1989, *Continuum Damage Theory:Application to Concrete, J.Engg.Mech.,ASCE,115,No.2,pp.345-365.*

53. Mazars,J., 1986, *Description of the Behavior of Composites Concretes under Complex Loading Through Continuum Damage Mechanics,Proc. Tenth U.S. National Congr.of Applied Mech,Edited by J.P.Lamb,pp.135-139,16-20 June 1986, Austin,TX,ASME.*

54. Mazars,J.,and La Borderie,C., 1987, *Comportement Oligocyclique des Beton Composites,Int.Report No.80- L.M.T.,Cachan*

55. Mills,L.L.,and Zimmerman,R.M., 1970, *Compressive Strength of Plain Concrete under Multiaxial Loading Conditions,Proc.ACI,67,802.*

56. Mills,L.L.,and Zimmerman,R.M., 1971, *Discussion of paper, Compressive Strength of Plain Concrete under Multiaxial Loading Conditions,author's closure,Proc.ACI,67,802.*

57. Murakami,S., 1981, *Effects of Cavity Distribution in Constitutive Equations of Creep and Creep Damage, EUROMECH Colloquium 147 on Damage Mechanics, Lemaitre,J.,Ed.,Cachan,France.*

58. Niyogi,S.,K., 1974, *Concrete Bearing Strength - Support,Mix,Size Effect. J.Struct.Div. ASCE 105, 1685-1702*

59. Ortiz,M., 1984, *A constitutive Theory for the Inelastic Behavior of Concrete,Report, Division of Engineering,Brown Univ., Providence,Rhode Island 02912, Nov.28*

60. Ortiz,M., 1985, *A Constitutive Theory for the Inelastic Behavior of Concrete, Mech.of Mat.,4,67-93.*

61. Ottosen,N.S., 1977, *A Failure Criterion for Concrete, J.Engg.Mech.,ASCE,103(4), 527-535.*

62. Palaniswamy,R.,and Shah,S.P., 1974, *Fracture and Stress-Strain Relationship of Concrete under Triaxial Compression, J.Struct. Div.,ASCE,100,ST5,901.*

63. Resende,L.,and Martin,J.B., 1984, *Damage Constitutive Model for Granular Materials,Comp.Meth.Appl. Mech.Engg.,42,pp.1-18.*

64. Resende,L., 1987, *A Damage Mechanics Constitutive Theory for the Inelastic Behavior of Concrete,Comp.Meth.Appl.Mech.Engg.,60,pp.57-93*

65. Seraj,S.M.,Kotsovos,M.D.,and Pavlovic,M.N., 1992, *Three-Dimensional Finite Element Modelling of Normal and High-Strength Reinforced Concrete Members, with Special Reference to T-Beams, Comp.Struct.,44(4),pp.699-716.*

66. Simo,J.C.,and Ju,J.W., 1986, *On Continuum Damage-Elastoplasticity at Finite Strain: A Computational Framework,Comput.Mech.,23,7,pp.821-840.*

67. Simo,J.C.,and Ju,J.W., 1987a, *Strain- and Stress-Based Continuum Damage Models,II.COmputational Aspects,J.Solids.Struct.,23,7,pp.841-869.*

68. Siriwardne,H.R.,and Desai,C.S., 1983, *Computational Procedures for Nonlinear Three-Dimensional Analysis with some Advanced Constitutive Laws,Int.J.Num.Anal.Meth.Geomech,7,pp.143-171*

69. Suaris,W.,Ouyang,C.,and Viraj,M.F., 1990, *Damage Model for Cyclic Loading of Concrete, J.Engg.Mech.,ASCE,116, 1020-1035.*

70. Taher,S.E.-D.F.,Baluch,M.H.,Al-Gadhib,A.H., 1994, *Towards a Canonical Elastoplastic Damage Model, Engg.Fract.Mech.,48, 151-166*

71. Voyiadjis,G.,Z.,and Taher,M.A., 1993, *Damage Model for Concrete using Bounding Surface Concept, J.Engg.Mech.,ASCE,1196, 1865-1885.*

72. Wastiels,J., 1979, *Behavior of Concrete under Multiaxial Stresses-A Review, Cem.Conc.Res.,9,35.*

73. Wu,C.H., 1985, *Tension-Compression Test of a Concrete Specimen via a Structure Damage Theory,In Damage Mechanics and Continuum Modelling,Stubbs,N., and Krajcinovic,D.,Eds.,1-12,ASCE.*